Impurity-induced states in conventional and unconventional superconductors

A. V. Balatsky*

Theoretical Division, Los Alamos National Laboratory, Los Alamos, New Mexico 87545

I. Vekhter†

Department of Physics and Astronomy, Louisiana State University, Baton Rouge, Louisiana 70803

Jian-Xin Zhu‡

Theoretical Division, Los Alamos National Laboratory, Los Alamos, New Mexico 87545

(Dated: March 23, 2022)

We review recent developments in our understanding of how impurities influence the electronic states in the bulk of superconductors. Our focus is on the quasi-localized states in the vicinity of impurity sites in conventional and unconventional superconductors and our goal is to provide a unified framework for their description. The non-magnetic impurity resonances in unconventional superconductors are directly related to the Yu-Shiba-Rusinov states around magnetic impurities in conventional s-wave systems. We review the physics behind these states, including quantum phase transition between screened and unscreened impurity, and emphasize recent work on d-wave superconductors. The bound states are most spectacularly seen in scanning tunneling spectroscopy measurements on high- T_c cuprates, which we describe in detail. We also discuss very recent progress on the states coupled to impurity sites which have their own dynamics, and impurity resonances in the presence of an order competing with superconductivity. Last part of the review is devoted to influence of local deviations of the impurity concentration from its average value on the density of states in s-wave superconductors. We review how these fluctuations affect the density of states and show that s-wave superconductors are, strictly speaking, gapless in the presence of an arbitrarily small concentration of magnetic impurities.

Contents

I.	Introduction	2	
	A. Aim and scope of this article	2	
	B. Unconventional superconductivity	3	
	C. Outline	4	
	D. Other related work	5	
II.	A BCS theory primer	6	
	A. Bogoliubov transformation	7	VII
	B. BCS variational wave function	7	VIII
	C. Green's functions	8	
			IX
III.	Impurities in superconductors	8	
	A. Single impurity potential	8	
	B. Many impurities	9	
	C. The self-energy and the T -matrix approximation	10	
	D. Static and dynamic impurities	10	
IV.	Non-magnetic impurities and Anderson's theorem	em11	Х
v.	Single impurity bound state in two-dimensiona	l metal	ls12
VI.	Low-energy states in s-wave superconductors	13	
	A. Potential scattering	13	37
	B. Classical spins	13	\mathbf{X}

A.	Single potential impurity problem	15
В.	Single magnetic impurity problem	17
C.	Self-consistent gap solution near impurity	18
D.	Spin-orbit scattering impurities	18
\mathbf{E} .	Effect of doppler shift and magnetic field	18
F.	Sensitivity of impurity state to details of band	structure19

III. Single impurity bound state in a pseudogap state of two-dimensional

IX. Quantum phase transition in S-wave superconductor with mag

	A. IntroductionB. Quantum phase transition as a level crossingC. Particle and hole component of impurity bound sta	23 24 .te25
	D. Intrinsic π phase shift for $J_0 > J_{crit}$ coupling	26
-	Kondo impurity	26

ĸ.	Kondo impurity	26
	A. Kondo effect in fully gapped superconductors	26
	1. Ferromagnetic exchange	27
	2. Antiferromagnetic coupling	27
	3. Anisotropic exchange and orbital effects	28

B. Kondo effect in gapless superconductors

XI.	$\mathbf{D}\mathbf{y}$	namical	impurities					30	
	Δ	Inclastic	scattering from	a cingle	cnin	in .	d mono	superconduct	ore?

B. Localized vibrational modes in d-wave superconductors32

VII. Impurity-induced virtual bound states in d-wave superconduct

^{*}Electronic address: avb@viking.lanl.gov, http://theory.lanl.gov

[†]Electronic address: vekhter@phys.lsu.edu

[‡]Electronic address: jxzhu@viking.lanl.gov

XII. Interplay between collective modes and impurities in d-wave su

	Scanning tunneling microscopy results A. STM results around a single impurity B. Spatial distribution of particle and hole components C. Fourier-transformed STM Measurement D. Filter	35 35 37 37 38					
AIV.	Average density of states in superconductors with i						
	 A. s-wave 1. Born approximation and the AG Theory 2. Shiba impurity bands 3. Quantum spins and density of states B. d-wave 	40 40 40 41 42					
XV.	Optimal fluctuation A. Introduction B. Tail states in semiconductors and optimal fluctuation	42 42 143					
	 S-wave superconductors Magnetic and non-magnetic disorder Diffusive limit, weak magnetic scattering Diffusive limit, strong scattering Ballistic limit, weak scattering Ballistic regime, strong scattering Summary 	44 44 45 46 46 48					
XVI.	Summary and outlook	48					
	Acknowledgments	49					
	List of Symbols	50					
	References	50					
	Figures	55					
	Tables	58					

I. INTRODUCTION

A. Aim and scope of this article

Real materials are not pure. Sometimes excessive impurities hinder observations of beautiful physics that would be there in cleaner systems. Magnetic disorder destroys the coherence of the superconducting state. At the very least, in conventional metals, impurities lead to higher resistivity. It is therefore very tempting to treat impurities as unfortunate obstacles to our understanding of the true underlying physics of the systems we study, strive to make cleaner and better materials, and ignore imperfections whenever possible.

Yet sometimes impurities directly lead to the desired physical properties. They are crucial in achieving functionality of doped semiconductors: undoped semiconductors are just band insulators and not useful for applications in electronics. The entire multi-billion dollar semiconducting electronics industry is based on the precise control and manipulation of electronic states due to dopant (impurity) states.

Consequently, sensitivity of a physical system to disorder can be a blessing in disguise. It can lead not only to achieving new applications but also to uncovering the nature of exotic ground states, elucidating properties of

electronic correlations, and producing electronic states that are impossible in the bulk of a clean system. Until recently this idea has not been emphasized enough in the study of correlated electron systems, but in recent years more and more efforts are focused on understand-mpunities@changes produced by disorder in a wide variety of strongly interacting electronic matter. One of the most promising directions is the study of disorder near quantum critical points, where several types of order compete and exist in delicate balance that impurities have the power to tip in favor of one of the orders (Millis, 2003).

This is a review of the impurity effects on the electronic states in superconductors. The main purpose of our article is to give a reader an appreciation of recent developments, review the current understanding and outline further questions on impurity effects in conventional, and especially unconventional superconductors. Superconductors present probably the first example of a nontrivial many-electron system where effects of disorder on the electronic states were studied experimentally and theoretically, and this review focuses on these effects.

The subject of impurity effects in superconductors is well established and well covered, see, for example, excellent textbooks and reviews (Abrikosov et al., 1963; Annett, 1990; Fetter and Walecka, 1971; de Gennes, 1989: Schrieffer, 1964: Sigrist and Ueda, 1991: Tinkham. 1996). The main classical results, such as Abrikosov-Gor'kov theory of pairbreaking by magnetic impurities (Abrikosov and Gorkov, 1960), and Anderson theorem, that explains why non-magnetic impurities do not destroy conventional superconductivity, (Anderson, 1959) are well known from the 60s, and are now taught in graduate school. The need to review the subject arose since a) there are many new results; b) the analyses of the classical papers have been substantially modified in applications to novel materials; c) the emphasis of the study of the impurity effects shifted from macroscopic to microscopic length scales.

From the early days of superconductivity, impurity doping was one of the most important tools to identify the nature of the pairing state and microscopic properties. A classical study of the role of magnetic impurities in conventional superconductors was carried out by Woolf and Reif, 1965, and followed by many detailed investigations. Both magnetic and nonmagnetic impurities are pairbreakers in unconventional superconductors, and often impurity suppression of superconductivity is a strong early hint of the unconventional pairing state. For example, the rapid suppression of the transition temperature, T_c , in Al doped SrRuO₄ superconductor was the first and strong indication that it is a p-wave superconductor (Mackenzie et al., 1998; Mackenzie and Maeno, 2003).

In the past two decades we have witnessed a tremendous growth of the number of novel superconductors. Many of them belong to the general class of strongly correlated electron systems, and, as a result of Coulomb interaction, the superconductivity is unconventional, see

below. Study of the effect of impurities on unconventional superconductors is a still developing field, yet it is mature enough to warrant an overview.

Sometimes superconducting state emerges from competition between different phases, such as magnetically ordered and paramagnetic in high-temperature cuprates, organic materials and heavy fermion systems. Experimentally, superconductivity often is the strongest when the two competing states are nearly degenerate, near quantum critical points. This is the case for example for Ce based heavy fermion materials (Sidorov et al., 2002) and UGe₂ (Saxena et al., 2000). Study of impurity effects in these materials allows (at least, in principle) to determine the nature of the superconducting state and reveal competing electronic correlations.

This has driven in part the study of impurity effects in high- T_c superconductors. At present, despite much progress, there is no complete microscopic description and certainly no consensus in the community on the mechanism of superconductivity. Study of competing orders in the neighborhood of impurity atoms has the potential to reveal the nature and origin of the superconducting state.

The new states and structures that appear due to disorder often are confined to micro- or mesoscopic length scales. They would remain in the realm of academic discussion were it not for the development of new techniques and probes of disorder. At the time of classical work, experimental interest lied solely in macroscopic properties of materials: transition temperature, T_c , specific heat, and the average density of states (obtained from planar junction tunneling measurements) were the experimentally measured quantities. With perfection of more local probes such as nuclear magnetic resonance (NMR), and especially with development of scanning tunneling microscopy and spectroscopy (STM/STS), it became possible to experimentally determine the structures on the atomic scales around the impurity sites. Therefore the emphasis of theoretical work also shifted to the study of these local properties.

It is therefore timely and useful to review new results and ideas about impurity-generated states in superconductors.

We had to be selective about the topics that are included in this article. In the spirit of new approaches, our review primarily discusses the physics of the single impurity bound or quasi-bound states and the local electronic effects in the vicinity of defects. We also discuss the physics on the mesoscopic scales, and the behavior of impurities in the presence of competing orders. In the specific case of high- T_c materials we discuss possible competition between superconducting state and some competing orders in the so called pseudogap state of these superconductors.

In all our discussions we restrict ourselves to the study of the behavior of the density of states. A more comprehensive review of all the effects that were studied experimentally and discussed theoretically is a much more difficult task and would take substantially more space. We do not discuss the behavior of transport coefficients: while this is a subject of intense current interest and many important results have been obtained there, it is beyond the scope of this article.

To keep this review useful and relevant for people entering the field, we start with a simple Bardeen-Copper-Schrieffer (BCS) model for superconductivity, and use a modified version of this model throughout the article. We do not consider the corrections due to strong coupling that appear in the Eliashberg analysis; in the known cases of electron-phonon interaction these corrections are quantitative rather than qualitative (Carbotte, 1990; Schachinger, 1982; Schachinger and Carbotte, 1984; Schachinger et al., 1980). In many unconventional materials dynamical glue in the self-consistent theory is not known. For example, there is an ongoing debate on the very nature of the normal state in the high- T_c cuprate superconductors. Yet most people agree that the superconducting state of cuprates is less anomalous then the normal state, and has the superconducting gap of d-wave symmetry. We take a view that at low energies it could be described for the purposes of our article by BCS with d-wave pairing state.

At the same time, while this is a review of recent work on impurity effects in unconventional superconductors, it is emphatically not a comprehensive review of impurity effects in high- T_c cuprates. Nature of superconducting state, detailed microscopic description and competing orders in the cuprates are still a subject of intense debate at present. There is a number of excellent reviews of physics of cuprates, including scanning tunneling microscopy (STM) (Fischer and et al, 2004), angle-resolved photoemission spectroscopy (ARPES) (Campuzano et al., 2004; Damascelli et al., 2003) and on nature of pseudogap state (Timusk and Statt, 1999). Reader is referred to these reviews for the in depth discussion of the issues specific to high- T_c materials.

B. Unconventional superconductivity

Examples of exotic superconductors discovered in the last two decades include high- T_c , heavy fermion superconductors, organic superconductors, $SrRuO_4$. The common feature of all of them is that they are unconventional, i.e. the pairing symmetry is not s-wave, in contrast to conventional materials, such as lead.

Here any superconductor with the gap function that transforms according to a trivial representation of the point group of the crystal will be called an s-wave superconductor. We call a superconducting order parameter unconventional if it transforms as a nontrivial representation of the symmetry group. To be more precise, superconductivity is characterized by an order parameter, that describes pairing of fermions with time-reversed momenta, \mathbf{k} and $-\mathbf{k}$,

$$\Psi(\mathbf{k})_{\alpha,\beta} = \langle \psi_{\mathbf{k},\alpha} \psi_{-\mathbf{k},\beta} \rangle, \tag{1.1}$$

where α, β are spin indices of the paired fermionic states. We distinguish between the spin singlet pairing (total spin of the pair S=0), for which $\Psi(\mathbf{k})_{\alpha,\beta} = \Psi(\mathbf{k})(i\sigma_{\alpha\beta}^{(y)})$, where $\sigma^{(y)}$ is the Pauli matrix in spin space, and spin triplet state (S = 1), when $\Psi_{\alpha\beta}$ is a symmetric spinor in α, β . Since the order parameter has to be antisymmetric with respect of permutation of fermion operators in Eq. (1.1), the spatial part of $\Psi(\mathbf{k})_{\alpha,\beta}$ is even for spin singlet superconductors and odd in the spin-triplet case. Expanding in eigenfunctions of orbital momentum, it follows that spin singlet pairing corresponds to even orbital function of momentum **k** and hence we call it s- (for l=0), d-wave (for l=2), etc. superconductor in analogy with the notation for the atomic states. For spin triplet superconductor, the orbital part is an odd function of \mathbf{k} , and hence spin triplet superconductor can be p-wave (l=1), f-wave (l=3) etc. More rigorously one would characterize pairing states by the irreducible representation of the symmetry of the crystal lattice, including the spin-orbit interaction (Blount, 1985; Sigrist and Ueda, 1991; Volovik and Gor'kov, 1984). Characterization in terms of orbital moment is an oversimplification, and we will use this terminology with understanding that the correct symmetries are used for a given crystal structure. The above classification is given for BCS-like or even frequency superconductors. This classification is opposite for odd-frequency pairing, where, for example, spin singlet state has odd parity because pairing wave function is odd function of time (Balatsky and Abrahams, 1992; Berezinskii, 1974). We will focus on BCS like or evenfrequency superconductors here.

A reasonable definition of unconventional pairing state, that we adopt here, is that the order parameter average over the Fermi surface vanishes:

$$\sum_{\mathbf{k}} \Psi(\mathbf{k})_{\alpha\beta} = 0. \tag{1.2}$$

Hence superconductors with the constant or nearly constant order parameter on the Fermi surface are s-wave, while p-, d- or higher wave states, where Eq. (1.2) holds, are signatures of an unconventional superconductor. There are several excellent recent reviews that address the unconventional nature of superconducting pairing states in specific compounds, such as p-wave superconductivity in SrRuO₄ (Mackenzie and Maeno, 2003) and d- wave state in high- T_c materials (Annett, 1990; Harlingen, 1995; Tsuei and Kirtley, 2000).

C. Outline

We start with the general overview of BCS-like superconductivity. To review the effects of impurities we need to discuss the properties of superconductors in general. In cuprates, as well as in some heavy fermion systems and other novel superconductors, there is some evidence for the existence of an order competing with superconductivity on all or parts of the Fermi surface. The exact nature of the competing order parameter is only conjectured. A general feature of all such models is the enhancement of the competing order once superconductivity is destroyed, for example in the vicinity of a scattering center. It has been suggested that the reaction of the system to the introduction of impurities can be an important test of the order, or even growing correlations towards such an order, in the superconducting state.

The prerequisite for such a test is the detailed understanding of the behavior of "simple" superconductors with impurities. Work aimed at developing this understanding spans a period of more than 40 years, and some of the very recent results continue to be fresh and unexpected. Therefore we devote a large fraction of this review to the discussion of the properties of superconductors with impurities in the absence of any competing order. In this case, from a theoretical standpoint, before discussing the impurity effects we need to agree upon methods to describe the very phenomenon that makes the impurity effects so interesting: superconductivity. Even in the most exotic compounds investigated so far the superconducting state itself is not anomalous, in that it results from pairing of fermionic quasiparticles, and in that these Cooper pairs may be broken by interaction with impurities or external fields.

Impurity effects in conventional superconductors were subject of the very early studies by Anderson, so called "Anderson theorem", (Anderson, 1959) and by Abrikosov and Gor'kov (Abrikosov and Gorkov, 1960), hereafter AG. This pioneering work laid the foundation for our understanding of impurity effects in conventional and unconventional superconductors, described in terms of electron lifetime due to scattering on an ensemble of impurities. AG predicted the existence of the gapless superconductivity that was subsequently observed in experiments (Woolf and Reif, 1965). The brief summary of the AG theory and its extensions to non-s-wave superconductivity is given Table I where effect of impurities on the superconducting state on average, or globally is listed.

After intense interest in the early days of the BCS theory, the subject was considered "closed" in mid-60s, with most experimentally relevant problems solved. However, as often happens, recently there has been a revival of the interest in the studies of "traditional" low-temperature s-wave superconductors with magnetic and non-magnetic impurities, with many new theoretical and experimental results changing our perspective on this classical problem.

A special place in this review is devoted to the study of impurity induced local bound states or resonances. This is an old subject, going back to the 60's when the bound states near magnetic impurities in s-wave superconductors were predicted in a pioneering work of Yu, Shiba and Rusinov (Rusinov, 1969; Shiba, 1968; Yu, 1965). They considered pairbreaking by a single magnetic impurity in a superconductor, and found that there are quasiparticle states inside the energy gap that are localized in the vicinity of the impurity atom. The corresponding

gap suppression occurs locally and the concept of lifetime broadening is inapplicable. In general, in this situation it is more useful to focus on local quantities, such as local density of states (LDOS), local gap etc., rather than on average impurity effects (which vanish for the single impurity in the thermodynamic limit). Yet it is clear that this local physics at some finite concentration of impurities suppresses superconductivity completely. This connection was discussed in (Rusinov, 1969; Shiba, 1968; Yu, 1965). In particular, formation of the intragap bound state and impurity bands due to magnetic impurity leads to filling of the superconducting gap, and therefore connects to the AG theory (Abrikosov and Gorkov, 1960).

At the time there were no experimental techniques to directly observe single impurity states. As a result the entire subject was largely forgotten until the STM was applied to study the impurity states by Yazdani et al. (Yazdani et al., 1997). This reinvigorated the field and lead to a firm shift in the interest from global to local properties. Soon afterwards STM was used to observe local impurity states near vacancies and impurities in the high- T_c cuprates (Hudson et al., 2001, 1999; Pan et al., 2000b; Yazdani et al., 1999). These discoveries opened a new field of research where impurities open a window into the study of electronic properties of exotic materials with atomic spatial resolution. As a first test of theories this allowed a direct comparison of the local electronic features in tunneling characteristics with the theoretical predictions for the density of states.

We start by briefly reviewing the BCS theory in Sec. II. Our main goal there is to review three approaches that will be used to analyze the impurity effects: direct diagonalization of the hamiltonian via Bogoliubov-Valatin transformation, variational wave function of the original BCS paper, and the Green's function method which is well suited to the analysis of multiple impurity problems. Then we define different types of impurity scattering in Sec. III. We pay special attention to distinguishing between magnetic and non-magnetic impurities, and differentiating between static and dynamic scatterers. The basic features of non-magnetic scattering in s-wave superconductors are outlined in Sec. IV.

To keep in tune with our intention to make the review readable by graduate students and researchers entering the field, we begin the discussion of the localized states by considering an example of an impurity bound state in a two-dimensional (2D) metal in Sec. V. Then we discuss the low-energy bound state in s- and d-wave superconductors in Sec. VI and Sec. VII respectively. Changes in the ground state of a superconductor containing a classical spin as a function of the coupling strength between the spin and conduction electrons are discussed in Sec. IX.

We proceed to consider the situations when the impurities have their own dynamics, so that their effect on the electrons is complicated, see Sec. XI, and the combined influence of the collective modes and impurities, Sec. XII. We briefly touch upon possible existence of

impurity resonances in different models of the pseudogap state of the cuprates in Sec. VIII, and discuss recent STM measurements on both conventional and unconventional superconductors in Sec. XIII. The final two parts of our review are devoted to the discussion of the effects on impurities on meso- and macroscopic scale. For completeness, we briefly review the basics ideas of computing the average density of states for a macroscopic sample in Sec. XIV. For lack of space we cannot do justice to this very rich subject and use it largely to discuss new results on the impurity effect on the scales small compared to the sample size, but large relative to the superconducting coherence length. In that situation there are dramatic consequences of local impurity realizations that may be different from the average, and we overview the results for the density of states in Sec. XV. We conclude with the summary in Sec. XVI.

D. Other related work

In focusing largely on the properties of impurities on atomic or mesoscopic scales, we cannot give due attention within the confines of this review to several other questions that have been important in the studies of impurities. One of these is how exactly does the impurity band grow out of bound states on individual impurity sites, i.e. what is the effect of interference between such sites is in real space. We briefly review some of recent work in Sec. XIV, but do not discuss the subject in depth. The answer to this question is still somewhat unsettled even in general: while the usual finite lifetime approach (Gorkov and Kalugin, 1985; Hirschfeld et al., 1986; Schmitt-Rink et al., 1986) gives a constant density of states at the Fermi level in a d-wave superconductor, and even though the same result has been obtained in field theoretical models of Dirac fermions in two dimensions, mimicking the d-wave superconductor (Ziegler, 1996; Ziegler et al., 1996), it has also been argued that this DOS diverges (Pepin and Lee, 1998, 2001), or vanishes. Vanishing DOS can occur with different power laws in energy depending on the approach one uses to treat disorder (Nersesyan and Tsvelik, 1997; Nersesyan et al., 1995; Senthil and Fisher, 1999) (see also (Bhaseen et al., 2001)). The vanishing itself can be traced to level repulsion when the system is treated within random matrix theory (Altland and Zirnbauer, 1997). Detailed selfconsistent numerical studies indicate, however, the the behavior of the DOS depends on the details of the impurity scattering and electronic structure (Atkinson et al., 2000; Zhu et al., 2000b). In particular, the divergence only occurs in perfectly particle-hole symmetric systems, and generically Atkinson et al. find that there is a nonuniversal suppression of the density of states over a small energy scale close to the Fermi level.

The interference between many impurities have been investigated recently (Atkinson *et al.*, 2003; Zhu *et al.*, 2003, 2004b) with the eye on the importance of these

effects for the interpretation of the features in the STM data on the high- T_c cuprates collected over a large area of the sample. The interference is also responsible for the formation of the impurity bands and therefore is crucial for determining the transport properties, which we do not address in this review. Within the framework of the t-matrix approximation transport properties of unconventional superconductors in general (Arfi et al., 1988; Graf et al., 1996; Hirschfeld et al., 1989, 1986, 1988; Pethick and Pines, 1986a; Schmitt-Rink et al., 1986), and high- T_c cuprates in particular (Duffy et al., 2001; Graf et al., 1995; Hirschfeld and Goldenfeld, 1993; Hirschfeld et al., 1994, 1997; Quinlan *et al.*, 1996, 1994) have been extensively discussed, and the experiments on both microwave, optical, and thermal conductivity are used to extract properties of impurity scattering, see (Timusk and Statt, 1999) for a review as well as very recent results in both experiment (Carr et al., 2000; Chiao et al., 2000; Corson et al., 2000; Hill et al., 2004; Hosseini et al., 1999; Lee et al., 2004; Segre et al., 2002; Tu et al., 2002; Turner et al., 2003) and theory (Berlinsky et al., 2000; Chubukov et al., 2003; Hettler and Hirschfeld, 1999; Howell et al., 2004; Nicol and Carbotte, 2003). The question of localization in both s-wave (Ma and Lee, 1985) and d-wave (Atkinson and Hirschfeld, 2002; Lee, 1993; Senthil and Fisher, 2000; Senthil et al., 1998; Vishveshwara et al., 2000; Yashenkin et al., 2001) continues to be investigated. Some of these results have been summarized in recent reviews on high-T_c systems (Timusk and Statt, 1999). We also do not touch upon the rich phenomena related to the surfaces playing the role of extended impurities that can also lead to the formation of the bound states (Aprili et al., 1998; Blonder et al., 1982; Buchholtz and Zwicknagl, 1981; Covington et al., 1997; Fogelström et al., 1997; Hu, 1994; Kashiwaya and Tanaka, 2000).

By now there are also few reviews available on the subject of impurity states. Joynt (Joynt, 1997) reviewed early work on the impurity states within the t-matrix theory focusing on anomalous transport due to finite lifetime of the quasibound states around impurities. Byers, Flatte and Scalapino, contributed substantially to studies of the detailed electronic structure of the resonance state and interference patterns (Byers et al., 1993; Flatté and Byers, 1997a,b; Flatte and Byers, 1998), and reviewed their and related work (Flatté and Byers, 1999). An excellent review of thermal and transport properties of low-energy quasiparticles in nodal superconductors was recently given by Hussey (Hussey, 2002).

The subject is so rich and well developed that it does not seem possible to do justice to both local quasiparticle properties around a single impurity site and the questions of interference and transport within the confines of a single paper. With this in mind we now are ready for a main discussion.

II. A BCS THEORY PRIMER

We begin by reviewing the Bardeen-Cooper-Schrieffer (BCS) theory. This section only briefly summarizes the results pertinent to our discussion; many excellent textbooks provide an in-depth view on the theory (de Gennes, 1989; Ketterson and Song, 1999; Schrieffer, 1964; Tinkham, 1996). Consider a general hamiltonian $\mathcal{H}_{BCS} = \hat{H}_0(\mathbf{r}) + H_{int}$, where

$$\widehat{H}_0(\mathbf{r}) = \sum_{\alpha} \int d^d \mathbf{r} \psi_{\alpha}^{\dagger}(\mathbf{r}) [\epsilon(-i\nabla_{\mathbf{r}}) - \mu] \psi_{\alpha}(\mathbf{r}) \qquad (2.1)$$

is the band hamiltonian of quasiparticles with dispersion $\epsilon(\mathbf{k})$, μ is the chemical potential, and the interaction part

$$H_{int} = -\frac{1}{2} \sum_{\substack{\alpha,\beta\\\gamma,\delta}} \int d^d \mathbf{r} d^d \mathbf{r}' \psi_{\alpha}^{\dagger}(\mathbf{r}) \psi_{\beta}^{\dagger}(\mathbf{r}') V_{\alpha\beta\gamma\delta}(\mathbf{r}, \mathbf{r}') \psi_{\gamma}(\mathbf{r}') \psi_{\delta}(\mathbf{r}).$$
(2.2)

Here ${\bf r}$ is the real space coordinate, α and β are the spin indices, and ψ^{\dagger} and ψ are the fermionic creation and annihilation operators respectively. The mean field approximation consists of decoupling the four-fermion interaction into a sum of all possible bilinear terms, so that

$$H_{int} = \sum_{\alpha,\beta} \int d^{d}\mathbf{r} d^{d}\mathbf{r}' \bigg\{ \widetilde{V}_{\alpha\beta}(\mathbf{r},\mathbf{r}') \psi_{\alpha}^{\dagger}(\mathbf{r}) \psi_{\beta}(\mathbf{r}')$$
 (2.3)

$$+\Delta_{\alpha\beta}(\mathbf{r},\mathbf{r}')\psi_{\alpha}^{\dagger}(\mathbf{r})\psi_{\beta}^{\dagger}(\mathbf{r}') + \Delta_{\alpha\beta}^{\star}(\mathbf{r},\mathbf{r}')\psi_{\beta}(\mathbf{r})\psi_{\alpha}(\mathbf{r}')\bigg\}.$$

The effective potential, $\widetilde{V}_{\alpha\beta}(\mathbf{r},\mathbf{r}')$ is the sum of the Hartree and Fock (exchange) terms, and the last two terms account for superconducting pairing. The pairing field, Δ , is determined self-consistently from

$$\Delta_{\alpha\beta}(\mathbf{r}, \mathbf{r}') = \frac{1}{2} V_{\alpha\beta\gamma\delta}(\mathbf{r}, \mathbf{r}') \langle \psi_{\gamma}(\mathbf{r}') \psi_{\delta}(\mathbf{r}) \rangle. \tag{2.4}$$

The pairing occurs only below the transition temperature, T_c ; above T_c the average of the two annihilation operators in Eq. (2.4) vanishes, and therefore $\Delta_{\alpha\beta}=0$. In contrast, Hartree and Fock terms are finite at all temperatures, and can be incorporated in the quasiparticle dispersion, $\epsilon(\mathbf{k})$. These terms do change below T_c , upon entering the superconducting state. Their relative change, however, is of the order of the fraction of electrons participating in superconductivity, and therefore is small for weak coupling superconductors ($\sim \Delta/W \ll 1$, where W is the electron bandwidth). Therefore the effective potential, \widetilde{V} , is not explicitly included in the following discussion except where specified.

Therefore we start with a reduced mean field BCS hamiltonian,

$$\mathcal{H}_{BCS} = \sum_{\alpha} \int d^{d}\mathbf{r} \psi_{\alpha}^{\dagger}(\mathbf{r}) \widehat{H}_{0}(\mathbf{r}) \psi_{\alpha}(\mathbf{r})$$

$$+ \sum_{\alpha,\beta} \int d^{d}\mathbf{r} d^{d}\mathbf{r}' \left\{ \Delta_{\alpha\beta}(\mathbf{r}, \mathbf{r}') \psi_{\alpha}^{\dagger}(\mathbf{r}) \psi_{\beta}^{\dagger}(\mathbf{r}') + h.c. \right\}.$$
(2.5)

The spatial and spin structure of $\Delta_{\alpha\beta}(\mathbf{r},\mathbf{r}')$ determines the type of superconducting pairing. In most of this review we consider singlet pairing, when Δ has only the off-diagonal matrix elements in spin space, and it is common to write $\Delta_{\alpha\beta}(\mathbf{r},\mathbf{r}')=(i\sigma^y)_{\alpha\beta}\Delta(\mathbf{r},\mathbf{r}')$, where Δ is now a scalar function, see previous section.

In a uniform superconductor the interaction depends only on the relative position of the electrons, so that $V(\mathbf{r}, \mathbf{r}') = V(\boldsymbol{\rho} \equiv \mathbf{r} - \mathbf{r}')$. Therefore in the absence of impurities, the structure of the order parameter in real space depends on the symmetry properties of $V(\boldsymbol{\rho})$. These are easier to consider in momentum, rather than coordinate, space. In models with local attraction, when $V(\boldsymbol{\rho}) = V_0 \delta(\boldsymbol{\rho})$, the Fourier transform of the interaction is featureless, and $\Delta(\mathbf{k}) = \Delta_0$; an example of an isotropic, or s-wave superconductor.

In the remainder of this section we overview the main methods solving the BCS hamiltonian since the same methods are commonly applied to the studies of impurity effects in superconductors. The approaches that we consider are: a) direct diagonalization via Bogoliubov-Valatin transformation; b) variational determination of the ground state energy from the trial wave function; and c) Green's function formalism.

A. Bogoliubov transformation

Since the effective hamiltonian of Eq. (2.5) is bilinear in fermion operators, ψ and ψ^{\dagger} , it can be diagonalized by a canonical transformation of the form

$$\psi_{\alpha}(\mathbf{r}) = \sum_{n} \left[u_{n\alpha}(\mathbf{r}) \gamma_{n} + v_{n\alpha}(\mathbf{r}) \gamma_{n}^{\dagger} \right], \qquad (2.6)$$

subject to condition $|u_{n\alpha}(\mathbf{r})|^2 + |v_{n\alpha}(\mathbf{r})|^2 = 1$. The resulting equations on the coefficients u and v are

$$Eu_{\alpha}(\mathbf{r}) = H_{0}(\mathbf{r})u_{\alpha}(\mathbf{r}) + \int d^{d}\mathbf{r}' \Delta_{\alpha\beta}(\mathbf{r}, \mathbf{r}')v_{\beta}(\mathbf{r}') (2.7)$$
$$-Ev_{\alpha}(\mathbf{r}) = H_{0}^{\star}(\mathbf{r})v_{\alpha}(\mathbf{r}) + \int d^{d}\mathbf{r}' \Delta_{\alpha\beta}^{\star}(\mathbf{r}, \mathbf{r}')u_{\beta}(\mathbf{r}') (2.8)$$

Here we suppressed the label n for brevity. Clearly, when $\Delta = 0$, coefficients u and v do not couple, and there is no particle-hole mixing.

For each n there are four functions, $u_{\uparrow}(\mathbf{r}), u_{\downarrow}(\mathbf{r}), v_{\uparrow}(\mathbf{r}), u_{\downarrow}(\mathbf{r})$ that need to be determined. However, for a singlet superconductor, for example, the matrix $\Delta_{\alpha\beta}$ is off-diagonal in the spin indices, so that u_{\uparrow} (u_{\downarrow}) couples only to v_{\downarrow} (v_{\uparrow}), so that in practice only two of the equations are coupled. In the presence of the impurity potential, however, in general all four components become interdependent.

Equations (2.7)-(2.8), are coupled integro-differential equations for the functions $u_{n\alpha}(\mathbf{r})$ and $v_{n\alpha}(\mathbf{r})$. They have to be complemented by the self-consistency equations on

 $\Delta_{\alpha\beta}$, which can be obtained directly from Eq. (2.4) to be

$$\Delta_{\alpha\beta}(\mathbf{r}, \mathbf{r}') = -\frac{1}{2} V_{\alpha\beta\gamma\delta}(\mathbf{r}, \mathbf{r}') \sum_{n} \left[u_{n\gamma}(\mathbf{r}') v_{n\delta}^{\star}(\mathbf{r}) f(E_n) + v_{n\gamma}^{\star}(\mathbf{r}') u_{n\delta}(\mathbf{r}) (1 - f(E_n)) \right]. \quad (2.9)$$

Here the Fermi function $f(E) = [\exp(E/T) + 1]^{-1}$.

In a uniform superconductor the Fourier transform of the Bogoliubov equations, Eqs. (2.7)-(2.8), into the momentum space gives

$$(\xi_{\mathbf{k}} - E_{\mathbf{k}})u_{\mathbf{k}\alpha} + \Delta_{\alpha\beta}(\mathbf{k})v_{\mathbf{k}\beta} = 0, \qquad (2.10)$$

$$(\xi_{\mathbf{k}} + E_{\mathbf{k}})v_{\mathbf{k}\alpha} + \Delta_{\alpha\beta}^{*}(-\mathbf{k})u_{\mathbf{k}\beta} = 0, \qquad (2.11)$$

where $\xi_{\mathbf{k}}$ is the bare quasiparticle energy, measured with respect to the chemical potential, $\xi_{\mathbf{k}} = \epsilon(\mathbf{k}) - \mu$. In a singlet superconductor

$$(\xi_{\mathbf{k}} - E_{\mathbf{k}})u_{\mathbf{k}\uparrow} + \Delta(\mathbf{k})v_{\mathbf{k}\downarrow} = 0, \qquad (2.12)$$

$$(\xi_{\mathbf{k}} + E_{\mathbf{k}})v_{\mathbf{k}\downarrow} - \Delta^{*}(\mathbf{k})u_{\mathbf{k}\uparrow} = 0, \qquad (2.13)$$

and recover the familiar energy spectrum $E_{\mathbf{k}} = \sqrt{\xi_{\mathbf{k}}^2 + |\Delta(\mathbf{k})|^2}$, with the coefficients u and v given by

$$\begin{pmatrix} u_{\mathbf{k}}^2 \\ v_{\mathbf{k}}^2 \end{pmatrix} = \frac{1}{2} \left[1 \pm \frac{\xi_{\mathbf{k}}}{E_{\mathbf{k}}} \right]. \tag{2.14}$$

B. BCS variational wave function

Superconductivity originates from the instability of the Fermi sea towards pairing of time-reversed quasiparticle states. Therefore a variational wave function approach, originating with the classic BCS paper, is to restrict the trial wave function to the subspace of either empty or doubly occupied states,

$$|\Psi(\mathbf{r})\rangle = \prod_{n} (a_n + b_n c_{n\uparrow}^{\dagger} c_{\bar{n}\downarrow}^{\dagger})|0\rangle,$$
 (2.15)

and to minimize the energy, $E_{BCS} = \langle \Psi | H | \Psi \rangle$. This is a legitimate approximation at T=0, and is a very good approach at low temperatures. In Eq. (2.15) the vacuum state $|0\rangle$ denotes the filled Fermi sea, and $c_{n\uparrow}^{\dagger}$ ($c_{\bar{n}\downarrow}^{\dagger}$) creates a quasiparticle with spin up (down) and with the wave function $\phi_n(\mathbf{r})$ ($\phi_n^{\star}(\mathbf{r})$) that is the eigenfunction of the single particle Hamiltonian. Normalization requires that $|a_n|^2 + |b_n|^2 = 1$.

In the absence of impurities these eigenfunctions can be labeled by the same indices, \mathbf{k} and α , as in the previous section. Consequently, the variational approach is completely equivalent to the Bogoliubov analysis with the choice $u_n(\mathbf{r}) = a_n \phi_n(\mathbf{r})$, and $v_n(\mathbf{r}) = b_n \phi_n(\mathbf{r})$. In general, however, interaction with impurities may lead to the appearance of the single particle states in the ground state wave function, see Sec. IX. Moreover, it is worth remembering that energy of the state described by the BCS wave function is greater or equal to that of the exact ground state obtained by solving the Bogoliubov equations.

C. Green's functions

The third approach that we will use in this work is the Green's function method, which originates with the work of Gor'kov. Following Nambu we introduce a 4vector that is a spinor representation of the particle and hole states,

$$\Psi^{\dagger}(\mathbf{r}) = (\psi_{\uparrow}^{\dagger}, \psi_{\downarrow}^{\dagger}, \psi_{\uparrow}, \psi_{\downarrow}). \tag{2.16}$$

The matrix Green's function is defined as the imaginarytime ordered average

$$\widehat{G}(x, x') = -\langle T_{\tau} \Psi(x) \Psi^{\dagger}(x') \rangle, \qquad (2.17)$$

where the four-vector $x=(\mathbf{r},\tau)$ combines the real space coordinate, \mathbf{r} , and the imaginary time, τ . The time evolution of the creation and annihilation operators in the Heisenberg approach is given by $\partial \psi/\partial \tau = [\mathcal{H}_{BCS} - \mu N, \psi]$.

For a singlet homogeneous superconductor the Hamiltonian of Eq. (2.5) in the Nambu notation takes the form,

$$H_{BCS} = \int d\mathbf{r} \Psi^{\dagger}(\mathbf{r})(\xi(-i\nabla)\tau_3 + \Delta\tau_1\sigma_2)\Psi(\mathbf{r}), \quad (2.18)$$

and we find (Maki, 1969)

$$\widehat{G}_0^{-1}(\mathbf{k},\omega) = i\omega_n - \varepsilon(\mathbf{k})\tau_3 - \Delta(\mathbf{k})\sigma_2\tau_1.$$
 (2.19)

Here $\omega_n = \pi T(2n+1)$ is the Matsubara frequency, σ_i are the Pauli matrices acting in spin space, τ_i are the Pauli matrices in the particle-hole space, and $\tau_i \sigma_j$ denotes a direct product of the matrices operating in the 4-dimensional Nambu space. The self-consistency equation for a single superconductor takes the form

$$\Delta(\mathbf{k}) = -T \sum_{\omega_n} \int d\mathbf{k}' V(\mathbf{k}, \mathbf{k}') \operatorname{Tr} \left[\tau_1 \sigma_2 G_0 \right].$$
 (2.20)

In BCS the interaction is restricted to a thin shell of electrons near the Fermi surface, and therefore

$$\Delta(\widehat{\Omega}) = -TN_0 \sum_{\omega_n} \int d\widehat{\Omega}' V(\widehat{\Omega}, \widehat{\Omega}') \operatorname{Tr} \left[\tau_1 \sigma_2 \int d\xi_{\mathbf{k}} G_0 \right],$$
(2.21)

where $\widehat{\Omega}$ denotes a direction on the Fermi surface, and N_0 is the normal state density of states.

The off-diagonal component of \widehat{G}_0 , is often called the Gor'kov's anomalous F, (Gor'kov) Green's functions since it describes the pairing average

$$F_{\alpha\beta}(x, x') = -\langle T_{\tau} \psi_{\alpha}(x) \psi_{\beta}(x') \rangle. \tag{2.22}$$

In general $F_{\alpha\beta}(x,x') = g_{\alpha\beta}F(x,x')$, where g is the matrix describing the spin structure of the superconducting order. For the singlet pairing $g=i\sigma^{(y)}$, where $\sigma^{(y)}$ is the Pauli matrix. Therefore in a singlet spatially uniform superconductor normal and anomalous components of \hat{G}_0 are

$$G(\omega_n, \mathbf{k}) = \frac{i\omega_n + \xi_{\mathbf{k}}}{(i\omega_n)^2 - \xi_{\mathbf{k}}^2 - |\Delta(\mathbf{k})|^2}, \qquad (2.23)$$

$$F(\omega_n, \mathbf{k}) = \frac{\Delta(\mathbf{k})}{(i\omega_n)^2 - \xi_{\mathbf{k}}^2 - |\Delta(\mathbf{k})|^2}.$$
 (2.24)

The connection with the Bogoliubov's transformation is provided by rewriting the Green's functions as

$$G(\omega_n, \mathbf{k}) = \frac{u_{\mathbf{k}}^2}{i\omega_n - E_{\mathbf{k}}} + \frac{v_{\mathbf{k}}^2}{i\omega_n + E_{\mathbf{k}}}, \qquad (2.25)$$

$$F(\omega_n, \mathbf{k}) = u_{\mathbf{k}} v_{\mathbf{k}}^{\star} \left(\frac{1}{i\omega_n - E_{\mathbf{k}}} - \frac{1}{i\omega_n + E_{\mathbf{k}}} \right), (2.26)$$

where $u_{\mathbf{k}}$ and $v_{\mathbf{k}}$ are given by Eq. (2.14).

The three approaches discussed above are complementary and equivalent in the case of homogeneous superconductors. However, some of them are better suited for addressing specific questions in the presence of impurities. In particular, we will see that the Green's function method is sometimes advantageous for determining the thermodynamic properties of a material and averaging over many impurity configurations. For inhomogeneous problems, where we are interested in the spatial variations of the superconducting order and electron density, both Bogoliubov equations and Green's functions are often used. In general, the choice of a specific methods depends on the type of question asked in the presence of impurities, and we briefly describe the basic models and issues related to impurity scattering in superconductors below.

III. IMPURITIES IN SUPERCONDUCTORS

A. Single impurity potential

If we are to address theoretically the question of what defects do to superconductivity, we must describe the defects and superconductivity in the same framework. Grain and surface boundaries, twinning planes, and other structural inhomogeneities scatter conduction electrons and therefore affect the resulting order parameters. However, here we focus on only one type of imperfection: impurity atoms.

a. Potential scattering. First and foremost an impurity atom has a different electronic configuration than the host solid, and therefore interacts with the density of conduction electrons via a Coulomb potential.

$$H_{imp} = \sum_{\alpha} \int d\mathbf{r} \psi_{\alpha}^{\dagger}(\mathbf{r}) U_{pot}(\mathbf{r}) \psi_{\alpha}(\mathbf{r}).$$
 (3.1)

In good metals the Coulomb interaction is screened at the length scales comparable to the lattice spacing, and therefore the resulting scattering potential is often assumed to be completely local, $U_{pot}(\mathbf{r}) = U_0 \delta(\mathbf{r} - \mathbf{r}_0)$, with the impurity at \mathbf{r}_0 . The resulting scattering occurs only in the isotropic, s-wave, angular momentum channel. If finite range of the interaction is relevant, scattering in $l \neq 0$ channels needs to be considered. In that case the treatment is similar to that of magnetic scattering in conventional superconductors, see Sec. VI, and was applied to unconventional superconductors in, for example (Balatsky et al., 1994; Kampf and Devereaux, 1997).

In the 4-vector notation of the previous section the potential scattering has to have the same matrix structure as the chemical potential, or $\varepsilon(\mathbf{k})$ in Eq. (2.19), so that

$$H_{imp} = \int d\mathbf{r} \Psi^{\dagger}(\mathbf{r}) U_{pot}(\mathbf{r}) \tau_3 \Psi(\mathbf{r}), \qquad (3.2)$$

or, in Nambu notation,

$$\widehat{U}_{pot} = U_0 \tau_3 \delta(\mathbf{r} - \mathbf{r}_0) \tag{3.3}$$

b. Magnetic scattering. In addition to the electrostatic interactions, if the impurity atom has a magnetic moment, there is an exchange interaction between the local spin on the impurity site and the conduction electrons,

$$H_{imp} = \sum_{\alpha\beta} \int d\mathbf{r} J(\mathbf{r}) \psi_{\alpha}^{\dagger}(\mathbf{r}) \mathbf{S} \cdot \boldsymbol{\sigma}_{\alpha\beta} \psi_{\beta}(\mathbf{r}). \tag{3.4}$$

The range of interaction here is determined by the quantum mechanical structure of the electron cloud associated with the localized spin. Again, in reality we often consider a simplified exchange hamiltonian with $J(\mathbf{r}) = J_0 \delta(\mathbf{r} - \mathbf{r}_0)$, which captures the essential physics of the problem. In the 4-vector notations of the previous section the electron spin operator becomes

$$\alpha = \frac{1}{2} \left[(1 + \tau_3) \boldsymbol{\sigma} + (1 - \tau_3) \sigma_3 \boldsymbol{\sigma} \sigma_3 \right].$$
 (3.5)

Therefore

$$H_{imp} = \int d\mathbf{r} \Psi^{\dagger}(\mathbf{r}) J(\mathbf{r}) \mathbf{S} \cdot \boldsymbol{\alpha} \Psi(\mathbf{r}), \qquad (3.6)$$

or, in Nambu notation,

$$\widehat{U}_{mag} = J(\mathbf{r})\mathbf{S} \cdot \boldsymbol{\alpha}. \tag{3.7}$$

c. Anderson impurity. However, even if the ground state of an isolated impurity has an electron spin, the result of putting such an impurity into a host matrix may modify the spin configuration as the impurity electrons couple to the conduction band. Therefore a realistic model for an

impurity site is based on the Anderson model, with the Hamiltonian

$$H_A = \sum_{\alpha} E_0 d_{\alpha}^{\dagger} d_{\alpha} + U n_{d\uparrow} n_{d\downarrow} + H_{sd}, \qquad (3.8)$$

$$H_{sd} = \sum_{\mathbf{k},\alpha} V_{sd} c_{\mathbf{k},\alpha}^{\dagger} d_{\alpha} + h.c. \tag{3.9}$$

Here E_0 is the position of the impurity level relative to the Fermi energy, d^{\dagger} and d operate on the impurity site, U is the Coulomb repulsion for the electrons localized on the impurity site, and $c_{\mathbf{k}}^{\dagger}, c_{\mathbf{k}}$ create and annihilate the conduction electrons. This Hamiltonian allows the electrons to hop on and off the impurity site, resulting in a finite width of the impurity level, $\Gamma = \pi |V_{sd}|^2 N_0$. The model describes the potential scattering, when $U \ll \Gamma$. On the other hand, when $E_0 \ll E_F$, $E_0 + U \gg E_F$, and $U \gg \Gamma$, we expect the local levels to remain split, so that the impurity state is singly occupied and has a local spin. Therefore it allows a natural interpolation between potential and magnetic scattering, as well as the study of the mixed valence regime. The price to pay for such a rich behavior of the Anderson impurities is the difficulty of studying them analytically, and therefore in practice many results have been obtained in the simplified models above, although a number of very thorough numerical renormalization group studies of Anderson impurities in superconductors exist. We will review some of them for completeness, but will not focus on those extensively.

B. Many impurities

In all of our discussions we assume noninteracting impurities, so that the net impurity potential is simply

$$\widehat{U}_{imp}(\mathbf{r}) = \sum_{i} \widehat{U}_{imp}(\mathbf{r} - \mathbf{r}_i)$$
 (3.10)

$$= \int d\mathbf{r}' \rho_{imp}(\mathbf{r}') \widehat{U}_{imp}(\mathbf{r} - \mathbf{r}'). \quad (3.11)$$

Here \widehat{U} denotes the matrix structure of the potential in both spin and particle-hole space, and we introduced the impurity density,

$$\rho(\mathbf{r}) = \sum_{i} \delta(\mathbf{r} - \mathbf{r}_{i}). \tag{3.12}$$

We also assume the dilute impurity limit of the average impurity concentration $n_i \ll 1$, where

$$n_i = \int \frac{d\mathbf{r}}{V} \rho(\mathbf{r}). \tag{3.13}$$

For magnetic scatterers it was explicitly shown that the effect of the RKKY interaction between scattering centers on the superconducting properties is small (Galitskii and Larkin, 2002; Larkin *et al.*, 1971).

If we now compute a local physical quantity, such as the density of states measured at the position \mathbf{r} by the STM, it will depend on the distance from the nearby impurities, and therefore will be different for different realization of impurity distributions. In contrast, thermodynamic quantities, such as the density of states measured in planar junctions, or the specific heat, average the density of states over many random local configurations of impurities. Therefore in computing their values we average over *all* impurity configurations (Abrikosov *et al.*, 1963), so that, for example,

$$\bar{G}(\omega_n, \mathbf{k}) = \prod_{i=1}^{N_i} \left[\frac{1}{V} \int d\mathbf{r}_i G(\omega_n, \mathbf{k}, \mathbf{r}_1, \dots, \mathbf{r}_{N_i}) \right]. \quad (3.14)$$

Here a bar denotes such an impurity average.

By definition $\bar{\rho}_{imp} = n_i$. We also assume an *uncorrelated*, or random, impurity distribution, which means

$$\overline{\rho(\mathbf{r})\rho(\mathbf{r}')} \equiv \prod_{i=1}^{N_i} \left[\frac{1}{V} \int d\mathbf{r}_i \rho(\mathbf{r}, \mathbf{r}_1, \dots, \mathbf{r}_{N_i}) \rho(\mathbf{r}', \mathbf{r}_1, \dots, \mathbf{r}_{N_i}) \right]
= n_i \delta(\mathbf{r} - \mathbf{r}') + n_i^2.$$
(3.15)

Since the impurities are dilute, $n_i^2 \ll n_i$, and we neglect the second term compared to the first. In Sec. XIV we implement this impurity averaging procedure to determine the average density of states.

C. The self-energy and the T-matrix approximation

In practice to compute the Green's function in the presence of impurities we will often employ the *T*-matrix approximation. This method is described in detail in many original articles and reviews (Hirschfeld and Goldenfeld, 1993; Hirschfeld *et al.*, 1986, 1988; Hotta, 1993; Hussey, 2002; Mahan, 2000), and we only briefly summarize it.

For a single impurity with the scattering potential $\widehat{U}_{\mathbf{k},\mathbf{k}'}$ in the momentum space (given by one of the models discussed at the beginning of this chapter), the T-matrix accounts exactly for multiple scattering off of one impurity. In the language of Feynman diagrams, the corresponding process is shown in Fig. 1. Here, and throughout the review, the hat over a letter means that it denotes a matrix in Nambu space. Therefore the full Green's function is

$$\widehat{G}(\mathbf{k}, \mathbf{k}') = \widehat{G}_0(\mathbf{k}) + \widehat{G}_0(\mathbf{k})\widehat{U}_{\mathbf{k}, \mathbf{k}'}\widehat{G}_0(\mathbf{k}')$$

$$+ \sum_{\mathbf{k}''} \widehat{G}_0(\mathbf{k})\widehat{U}_{\mathbf{k}, \mathbf{k}''}\widehat{G}_0(\mathbf{k}'')\widehat{U}_{\mathbf{k}'', \mathbf{k}'}\widehat{G}_0(\mathbf{k}') + \dots$$
(3.16)

Here we suppressed the frequency index in the Green's function as the scattering is elastic. The series can be summed to write (see Fig. 1)

$$\widehat{G}(\mathbf{k}, \mathbf{k}') = \widehat{G}_0(\mathbf{k}) + \widehat{G}_0(\mathbf{k})\widehat{T}_{\mathbf{k}, \mathbf{k}'}\widehat{G}_0(\mathbf{k}'), \tag{3.17}$$

where the T-matrix is given by

$$\widehat{T}_{\mathbf{k},\mathbf{k}'} = \widehat{U}_{\mathbf{k},\mathbf{k}'} + \sum_{\mathbf{k}''} \widehat{U}_{\mathbf{k},\mathbf{k}''} \widehat{G}_0(\mathbf{k}'') \widehat{U}_{\mathbf{k}'',\mathbf{k}'} + \dots (3.18)$$

$$= \widehat{U}_{\mathbf{k},\mathbf{k}'} + \sum_{\mathbf{k}''} \widehat{U}_{\mathbf{k},\mathbf{k}''} \widehat{G}_0(\mathbf{k}'') \widehat{T}_{\mathbf{k}'',\mathbf{k}'}. \qquad (3.19)$$

This equation needs to be solved for \widehat{T} . If the impurity scattering is purely local, $\widehat{U}(\mathbf{r} - \mathbf{r}')$, the scattering is isotropic, $\widehat{U}_{\mathbf{k},\mathbf{k}'} = \widehat{U}$, greatly simplifying the process of solving the equation for the T-matrix, as \widehat{T} depends only on frequency.

Notice that we could draw the set of diagrams in Fig. 1 in real space, and write the corresponding set of equations for the T-matrix and Green's function $\widehat{G}(\mathbf{r},\mathbf{r}')$ in complete analogy with Eq. (3.19). The main observation here is that, in the vicinity of the impurity, the translational invariance is broken, and the Green's function depends on two momenta, \mathbf{k} and \mathbf{k}' .

$$\widehat{G}(\mathbf{r}, \mathbf{r}'; \omega) = \widehat{G}_0(\mathbf{r}, \mathbf{r}'; \omega) + \widehat{G}_0(\mathbf{r}, \mathbf{r}_0; \omega) \widehat{T}(\omega) \widehat{G}_0(\mathbf{r}_0, \mathbf{r}'; \omega)$$
(3.20)

The T-matrix lends itself easily to describe the effect of an ensemble of impurities. The so called self-consistent T-matrix approach (SCTM) considers multiple scattering on a single site of an electron that has already been scattered on all other impurity sites (Hirschfeld et~al., 1986, 1988). This results in replacing the bare Green's function in Eq. (3.19) by its impurity-averaged counterpart, $\widehat{G}(\mathbf{k},\omega)$. Notice that after averaging over the random impurity distribution the translational invariance is restored, so that the Green's function depends on a single momentum \mathbf{k} . The combined effect of impurities is given by the self energy, $\widehat{\Sigma}(\mathbf{k},\omega) = n_{imp}\widehat{T}_{\mathbf{k},\mathbf{k}}$, so that

$$\widehat{G}^{-1}(\mathbf{k},\omega) = \widehat{G}_0^{-1}(\mathbf{k},\omega) - \widehat{\Sigma}(\mathbf{k},\omega). \tag{3.21}$$

In contrast to the single impurity case where Eq. (3.17) with the T-matrix given by Eq. (3.19) is the exact solution of the problem, the Green's function given above is an approximation, and much recent research is motivated by questions about how accurately it describes the properties of nodal superconductors with impurities.

D. Static and dynamic impurities

So far we only discussed the *static* impurities, and most of our review addressed such a situation. However, even for purely potential scattering a situation is possible when a vibrational mode leads to a time-dependent modulation of the charge on an impurity site, and, as a result, U_{pot} acquires a characteristic frequency. Such a mode can be extended, as a phonon, or local. Influence of the dynamical impurity on the local properties of a superconductor is a relatively new subject of research and we summarize recent results in Sec. XI

For magnetic scattering the situation is more complex even in a normal metal. The degeneracy between the spin-up and spin-down states on the impurity site and the non-trivial commutation relations between different spin components ensure that quantum dynamics of the impurity is generated even if the exchange constant is purely static. In simple words, if the scattering process, which flips both the spin of the conduction electron and the impurity spin, is relevant, the dynamics of the local spin flips becomes essential. This dynamics leads to Kondo screening of the impurity spin in a metal, and in Sec. XI we briefly discuss the current status of the yet not fully understood problem of Kondo effect in a superconductor.

In the limit of large impurity spin, however, the change of the impurity spin by 1 during the spin flip scattering is not relevant, and its dynamics does not play a major role. In this limit of *classical* spin the static local and global density of states is discussed in Sec. VI and Sec. XIV respectively. Such a spin acquires dynamics only when placed in an external magnetic field, which also affects the superconducting state.

IV. NON-MAGNETIC IMPURITIES AND ANDERSON'S THEOREM

One of the most important early results was the robustness of the conventional superconductivity to small concentrations of non-magnetic impurities. Theoretical underpinning of this result is known as Anderson's theorem (Anderson, 1959). Anderson's observation was that, since superconductivity is due to the instability of the Fermi surface to pairing of time-reversed quasiparticle states, any perturbation that does not lift the Kramers degeneracy of these states does not affect the mean field superconducting transition temperature.

This is most clearly seen from the BCS analysis, which we carry out following Ma and Lee, 1985. We consider an isotropic pairing potential, $V_{\alpha\beta\gamma\delta}(\mathbf{r},\mathbf{r}') = V\delta(\mathbf{r} - \mathbf{r}')$. In the absence of a magnetic field the coefficients $a_n = \sin \theta_n$ and $b_n = \cos \theta_n$ can be taken real without loss of generality, so that the self-consistency condition, Eq. (2.9) reads

$$\Delta_n = V \sum_{m \neq n} \frac{\Delta_m}{(\xi_m^2 + \Delta_m^2)} \int d^d \mathbf{r} \phi_n^2(\mathbf{r}) \phi_m^2(\mathbf{r}).$$
 (4.1)

Here

$$\Delta_n = \int d^d \mathbf{r} \Delta(\mathbf{r}) \phi_n^2(\mathbf{r}). \tag{4.2}$$

As noted above, in the BCS approach ϕ 's are the eigenfunctions of the single particle hamiltonian. In the absence of impurities the system is translationally invariant, so that $\Delta(\mathbf{r}) = \Delta_n = \Delta_0$. The most important assumption underlying Anderson's theorem is that the superconducting order parameter can be taken to be uniform, $\Delta(\mathbf{r}) = \Delta_1$, even in the presence of impurities. In that case the individual eigenfunctions of the single particle hamiltonian including impurities are rather complicated. However, the gap equation, Eq. (4.1), takes the form

$$\frac{1}{V} = \int d\epsilon \frac{N(\epsilon, \mathbf{r})}{\sqrt{\epsilon^2 + \Delta_1^2}},\tag{4.3}$$

equivalent to that of a pure superconductor provided the density of states

$$N(\epsilon, \mathbf{r}) = \sum_{n} \phi_m^2(\mathbf{r}) \delta(\epsilon - \epsilon_m), \tag{4.4}$$

is unchanged compared to the pure metal, $N(\epsilon, \mathbf{r}) \approx \rho_0$. If this condition is satisfied, the solution Δ_1 of the gap equation Eq. (4.3) must be identical to that of the BCS equation in the absence of impurities, and therefore the transition temperature and the gap are insensitive to the impurity scattering at the mean field level.

Anderson's theorem helped explain why superconductivity was robust to impurities in many early experiments. It is important to realize however that it is an approximate statement about the thermodynamic averages of the system. Beginning with the next section we will analyze in more detail the changes that impurities create in superconductors in their immediate surrounding as well as on average. We will see that even purely potential scattering does induce changes in the local properties of superconductors, albeit the corresponding change in the transition temperature remains minimal. Anderson's theorem brings to the fore the need to separate the study of impurity effects on different lengths scales, from lattice spacing to the coherence length, to sample size.

Before we proceed to study the local properties we discuss the extensions of the Anderson's treatment of impurities. In weakly disordered systems the density of states remains nearly constant as a function of disorder. Ma and Lee (Ma and Lee, 1985) argued that Anderson's theorem remains valid in the form above even in a strongly disordered system provided the localization length, $L \gg (\rho_0 \Delta_0)^{1/d}$. In that case there is a large number of states localized within energy Δ_0 of the Fermi surface, and these state form a local superconducting patch. The Josephson interaction between the patches then leads to global phase coherence at T=0. Moreover, they argued that the theorem holds all the way to the limit of site localization.

It is important to note that the superfluid stiffness, i.e. the ability of the superconductor to screen out the magnetic field, is affected by disorder. In particular, when the quasiparticle lifetime, τ , becomes sufficiently short, $\Delta_0 \tau \ll 1$, the superfluid density $\rho_s \approx \Delta_0 \tau$. Consequently the superconductor is sensitive to the local phase fluctuations of the order parameter, and the experimentally observed transition temperature may be severely suppressed compared to the mean field T_c , as it is, for example, in granular superconductors. Approaches extending beyond the mean field picture are largely outside the scope of this review.

Therefore for dilute impurities Anderson's theorem is valid provided the superconducting order parameter can be taken to be nearly uniform. Since the "healing length" of $\Delta(\mathbf{r})$ over which it can change appreciably is the coherence length, $\xi_0 \simeq \hbar v_F/\Delta_0$, where v_F is the Fermi velocity, while the Coulomb screening length for the charged impurities in metals is of the order of

the lattice spacing, a, for $\xi_0 \gg a$ the order parameter remains essentially uniform, and Anderson's theorem holds. Much work has been done recently on the effect of the ultrashort coherence length on the impurity scattering in superconductors. In particular, it has been shown that when the superconducting pairing is of the order of the electron bandwidth, Anderson's theorem is violated (Ghosal *et al.*, 1998; Moradian *et al.*, 2001; Tanaka and Marsiglio, 2000).

Ghosal et al. (Ghosal $et\ al.$, 1998), and Xiang and Wheatley (Xiang and Wheatley, 1995) have explored in detail the discrepancy between the single particle excitation gap and the superconducting order parameter as a function of disorder in these circumstances. Beyond Anderson's regime of the constant density of states, both quantities decrease at first, since the disorder depletes the density of states. Then, however, the spectral gap persists while the superconducting order vanishes. As pointed out by Ma and Lee (Ma and Lee, 1985) in the limit of strong disorder the models with on-site pairing, such as those studied by Tanaka and Marsiglio, and Ghosal et al., show the on-site spectral gap (so-called Anderson negative-U glass) without the off-diagonal long range order and without symmetry breaking.

In most experimentally relevant situations, however, the corrections to the main statement of Anderson's theorem are quantitative rather than qualitative. This is generally true of most results pertaining to the impurity scattering in superconductors, and therefore it is very instructive to consider this problem in BCS-like systems.

V. SINGLE IMPURITY BOUND STATE IN TWO-DIMENSIONAL METALS

Before we proceed to calculate the effect of impurity in a d-wave superconductor it is instructive to review a simpler problem of a single impurity in a metal. We show here a T-matrix calculation for finding the bound states due to a single impurity in d dimensions with an attractive potential $U_0 \leq 0$. The Hamiltonian for the problem is

$$H = \sum_{\mathbf{k}} [\epsilon(\mathbf{k}) - \mu] c_{\mathbf{k},\sigma}^{\dagger} c_{\mathbf{k},\sigma} + \sum_{\mathbf{k},\mathbf{k}'} U_0 c_{\mathbf{k},\sigma}^{\dagger} c_{\mathbf{k}',\sigma}$$
 (5.1)

the U_0 term describes the on-site energy change of electron density $n(\mathbf{r})$ in external potential $U(\mathbf{r}) = U_0 \delta(\mathbf{r})$. We consider a single particle $(\mu = 0)$, although the calculation for the normal metal with a finite density of states follows simply by replacing $\epsilon(\mathbf{k}) \to \xi(|bfk|)$ in the following.

The bare Green's function for a free particle is

$$G_0(\omega, \mathbf{k}) = [\omega - \epsilon(\mathbf{k})]^{-1}.$$
 (5.2)

Since the vertex of the impurity interaction, U_0 is momentum independent, the equation for the T-matrix is

particularly simple and follows from Eq. (3.19),

$$T(\omega) = U_0 + U_0 \sum_{\mathbf{k}} G_0(\omega, \mathbf{k}) T(\omega)$$
$$T(\omega) = \frac{U_0}{1 - U_0 \sum_{\mathbf{k}} G_0(\omega, \mathbf{k})}$$
(5.3)

Summation over momentum in $\sum_{\mathbf{k}}$ is easily performed using the density of states

$$N(\epsilon) = \sum_{\mathbf{k}} \delta(\epsilon - \epsilon(\mathbf{k})) = \Gamma_d \epsilon^{\frac{d}{2} - 1}, \tag{5.4}$$

where Γ_d is a constant dependent on dimension. Therefore

$$g_0(\omega) = \sum_{\mathbf{k}} G_0(\omega, \mathbf{k}) = \int_0^W \frac{d\epsilon N(\epsilon)}{\omega - \epsilon} \simeq -\Gamma_d \omega^{\frac{d-2}{2}}, (5.5)$$

for $d \neq 2$, where W is the electron half bandwidth. In two dimensions $g_0 \simeq -\Gamma_2 \ln(W/|\omega|)$. Consequently, the T-matrix for $d \neq 2$ is given by

$$T = \frac{U_0}{1 - q_d \omega^{\frac{d-2}{2}}} \tag{5.6}$$

where $g_d = -U_0\Gamma_d$ is the effective coupling constant, and by the same expression with the obvious substitution of $\ln(W/\omega)$ for d=2.

Since the Green's functions in the presence of impurity scattering is $G = G_0 + G_0 T G_0$, see Eq. (3.17), poles of the T-matrix are the new poles of G that are not poles of G_0 , signifying the appearance of new states. We can find this pole, ω_0 , from Eq. (5.6) for different dimension d. The bound state ($\omega_0 < 0$, see Fig. 2) is formed for an arbitrarily small potential $|U_0|$ in d = 1, 2, but requires a critical coupling for d = 3. The energy of this state is given by

$$\omega_0 \sim (g_1)^2,$$
 if $d = 1;$ (5.7)

$$\omega_0 = W \exp(-\frac{1}{a_2}), \quad \text{if } d = 2; \quad (5.8)$$

$$\omega_0 \sim [g_3^{\frac{1}{2}} - g_{3c}^{\frac{1}{2}}], \ g_3 \ge g_{3c}, \quad \text{if } d = 3, \quad (5.9)$$

where the d=3 critical coupling $g_{3c} \sim W^{-1/2}$.

We focus in more detail on the two-dimensional case, when $g_2 = \Gamma_2 |U_0|$ and $\Gamma_2 = \frac{m}{2\pi}$ is the electron density of states. The bandwidth, $W \simeq \frac{\hbar^2}{2ma^2}$ is the ultraviolet cutoff corresponding to the lattice parameter a for free particle. This result can be compared to the solution of the Schrödinger's equation for the particle in the 2D attractive potential U_0 (Landau and Lifshitz, 2000), Ch. 45. For an arbitrary potential $U(\mathbf{r})$ the solution obtained using the T-matrix is asymptotically correct if the scattering length is greater than a. For shallow potential the bound state energy $-\omega_0$ is small, and the characteristic extent of the bound state wave function is $l_0 = (\frac{\hbar^2}{2m\omega_0})^{1/2} \gg a$ Therefore in this limit we can safely approximate $U(\mathbf{r}) = U_0 \delta(\mathbf{r})$, where $U_0 = \int U(\mathbf{r}) d\mathbf{r}$.

Finding the energy of the bound state, Eq. (5.8), is only one part to the solution. We also want to determine the corrections to the *local Density of States* due to bound state. We write the equation for the Green's function in real space, Eq. (3.20),

$$G(\mathbf{r}, \mathbf{r}'; \omega) = G_0(\mathbf{r}, \mathbf{r}'; \omega) + G_0(\mathbf{r}, 0; \omega)T(\omega)G_0(0, \mathbf{r}'; \omega)$$

and read off the position dependent Density of states (DOS)

$$N(\mathbf{r}, \omega) = -\frac{1}{\pi} Im G(\mathbf{r}, \mathbf{r}; \omega)$$
$$= N_0(\mathbf{r}, \omega) + \delta N(\mathbf{r}, \omega). \tag{5.10}$$

Here the first term is the DOS of a clean system, and the second is the correction due to the bound state. We focus on the energy range close to the bound state energy, $\omega \simeq \omega_0$. Since the bound state is below the bottom of the band, the unperturbed Green's function G^0 has no imaginary part in this range $(N_0 = -\text{Im}g_0(\omega = 0)/\pi)$. Therefore the only contribution to the imaginary part of the full Green's function, Eq. (5.10) comes from the T-matrix:

$$\operatorname{Im} T(\omega) = \operatorname{Im} \frac{1}{1/g_2 - \log[W/(-\omega)]}$$

$$= \operatorname{Im} \ln^{-1} \left[\frac{\omega + i\delta}{\omega_0}\right]$$

$$= \pi \delta(\omega - \omega_0), \qquad (5.11)$$

and the correction to the DOS of a clean system is:

$$\delta N(\mathbf{r}, \omega) = |G_0(\mathbf{r}, \omega_0)|^2 \delta(\omega - \omega_0)$$
 (5.12)

with $G_0(\mathbf{r},\omega) = N_0 J_0(k_F r) \ln[\frac{W}{\omega}]$ is the real part of Green's finction in 2D systems. Equations (5.9) and (5.12) are the main results of this section. They establish the logic we will adhere to in finding impurity induced bound states: a) find the poles of the T matrix in the and the poles of the dressed Green's function Eq. (5.9), b) find the inhomogeneous DOS due to impurity induced state, Eq. (5.12). One should keep in mind that this approach is just one of many one can implement in a search for scattering induced bound states. Alternatively one can use for example the exact numerical solution of a finite system. As we will argue for superconducting case the self-consistency condition can not be implemented analytically and the numerical solution remains the only method available.

VI. LOW-ENERGY STATES IN s-WAVE SUPERCONDUCTORS

A. Potential scattering

Even though the potential scattering does not change the bulk properties of isotropic superconductors, it does affect the local density of states (Machida and Shibata, 1972; Shiba, 1973). Let us consider the Anderson impurity model, Eqs. (3.8)-(3.9) in the limit U=0 (resonance scattering). As discussed above the localized state acquires a finite width, $\Gamma=\pi|V_{sd}|^2N_0$, due to hybridization with the conduction band. The Green's function of the conduction electrons can be evaluated in the T-matrix approach, with the result at real frequencies (Machida and Shibata, 1972; Shiba, 1973)

$$\widehat{T}(\omega) = |V_{sd}|^2 \tau_3 \left[\omega - E_0 \tau_3 - |V_{sd}|^2 \tau_3 \sum_{\mathbf{k}} \widehat{G}_0(\mathbf{k}, \omega) \tau_3 \right]^{-1} \tau_3.$$
(6.1)

The poles of the T-matrix determine the location of the bound states

$$\omega^{2} \left[1 + \frac{2\Gamma}{\sqrt{\Delta^{2} - \omega^{2}}} \right] = E_{0}^{2} + \Gamma^{2}. \tag{6.2}$$

In most physical situations $\Gamma \gg \Delta$, so that the bound states are located at

$$\omega_0 = \pm \Delta (1 - 2\pi^2 (\Delta N_d(0))^2), \tag{6.3}$$

where $N_d(0) = \pi^{-1}\Gamma/(\Gamma^2 + E_0^2)$ is the density of states of the resonant impurity level. For typical densities of states $\Delta N_d(0) \sim 10^{-3}$, so that the bound states lies essentially at the gap edge. Shiba considered a finite but small value of the Coulomb repulsion and allowed for the induced pairing on the impurity site (Shiba, 1973). He concluded that, even though there may be a shift of the bound state to lower energies, it still lies within $10^{-3}\Delta$ of the mean field gap edge, and therefore can be neglected in the discussions of physical properties.

B. Classical spins

If the substitution atoms have a magnetic moment, the time-reversal symmetry is violated, and therefore superconductivity will be suppressed. We consider the magnetic scattering, Eq. (3.6), which we rewrite in the momentum space as

$$H_{ex} = \frac{1}{2N} \sum_{\substack{\mathbf{k}, \mathbf{k}' \\ \alpha\beta}} J(\mathbf{k} - \mathbf{k}') c_{\mathbf{k}, \alpha}^{\dagger} \boldsymbol{\sigma}_{\alpha\beta} \cdot \mathbf{S} c_{\mathbf{k}'\beta}.$$
(6.4)

We first review a simplified version of this problem, where we do not need to consider Kondo screening. We review scattering on classical spins first studied independently at about the same time by Shiba, Rusinov, and Yu (Rusinov, 1968, 1969; Shiba, 1968; Yu, 1965). Quantum mechanical properties of spin can be neglected when $S \to \infty$, and we simultaneously take $J \to 0$ so that the product JS = const. In this limit the localized spin acts as a local magnetic field.

Therefore we study the effect of the impurity with the potential $U(\mathbf{r}) = U_0 + U_{ex}$, or $H_{imp} = H_{imp} + H_{ex}$, on a

BCS s-wave superconductor with the unperturbed hamiltonian of the form

$$H_0 = \sum_{\mathbf{k}\alpha} \varepsilon_{\mathbf{k}} c_{\mathbf{k},\alpha}^{\dagger} c_{\mathbf{k}\alpha} + \Delta_0 \sum_{\mathbf{k}} \{ c_{\mathbf{k}\uparrow}^{\dagger} c_{-\mathbf{k}\downarrow}^{\dagger} + c_{-\mathbf{k}\downarrow} c_{\mathbf{k}\uparrow} \}. \quad (6.5)$$

This problem serves as a starting point for all subsequent analysis of the resonance states in superconductors.

To find a localized state with energy $0 < E < \Delta_0$ near a single paramagnetic impurity we perform a Bogoliubov transformation (Rusinov, 1968; Yu, 1965) to find

$$Eu_{\alpha}(\mathbf{r}) = \varepsilon(\mathbf{k})u_{\alpha}(\mathbf{r}) + i\Delta\sigma_{\alpha\beta}^{y}v_{\beta}(\mathbf{r}) + U_{\alpha\beta}(\mathbf{r})u_{\beta}(\mathbf{r})(6.6)$$

$$Ev_{\alpha}(\mathbf{r}) = -\varepsilon(\mathbf{k})v_{\alpha}(\mathbf{r}) - i\Delta\sigma_{\alpha\beta}^{y}u_{\beta}(\mathbf{r}) - U_{\alpha\beta}(\mathbf{r})v_{\beta}(\mathbf{r})(6.7)$$

This system is solved by Fourier transforming the equations and expanding the impurity potential in spherical harmonics, and has solutions with energies

$$\frac{E_l}{\Delta_0} = \frac{1 + (\pi N_0 V_l)^2 - (\pi N_0 J_l S/2)^2}{\sqrt{[1 + (\pi N_0 V_l)^2 - (\pi N_0 J_l S/2)^2]^2 + 4(\pi N_0 J_l S/2)^2}},$$
(6.8)

where N_0 is, again, the density of states at the Fermi energy in the normal state. This result can be written in a more elegant form if we introduce the phase shifts, δ_l , of scattering for up (+) and down (-) electrons, in each angular channel,

$$\tan \delta_l^{\pm} = (\pi N_0)(V_l \pm J_l S/2). \tag{6.9}$$

Then the energies of the states in the gap become

$$\epsilon_l = \frac{E_l}{\Delta_0} = \cos(\delta_l^+ - \delta_l^-). \tag{6.10}$$

Clearly, for purely potential scattering $(\delta_l^+ = \delta_l^-)$ the spectrum begins at the gap edge, and there are no intragap states. However, as the magnetic scattering increases, a series of low-energy states below the gap edge appear. Purely magnetic scattering corresponds to $\delta_l^+ = -\delta_l^-$, and strong scattering (large phase shift) yields a localized state deep in the gap, while weak scattering (small phase shift) results in the bound state very close to the gap edge.

The same result can be obtained using the Green's function formulation (Rusinov, 1969; Shiba, 1968) and solving the single impurity problem using the T-matrix method described above. With the impurity hamiltonian of Eq. (3.6) in the Nambu notations the matrix Green's function for the system is

$$\widehat{G}(\mathbf{k}, \mathbf{k}'; \omega) = \widehat{G}_0(\mathbf{k}, \omega)\delta(\mathbf{k} - \mathbf{k}') + \widehat{G}_0(\mathbf{k}, \omega)\widehat{T}(\mathbf{k}, \mathbf{k}')\widehat{G}_0(\mathbf{k}', \omega).$$
(6.11)

Here the T-matrix is computed as in Sec. III, and we sum over the indices of the matrix α in each vertex. The l-th angular component of the T-matrix satisfies the matrix equation (for a spherical Fermi surface and isotropic gap)

$$\widehat{T}_l(\omega) = \widehat{U}_l + \widehat{U}_l \int d\varepsilon \widehat{G}_0(\mathbf{k}, \omega) \widehat{T}_l(\omega). \tag{6.12}$$

The full expressions for the T-matrix for both potential and magnetic scattering in all angular channels is straightforward to obtain (Rusinov, 1969) but is rather cumbersome, so that we don't give it here. Even the case of only spherically symmetric scattering (l=0) with both $U_0 \neq 0$ and $J \neq 0$ the T-matrix is simple yet lengthy (Okabe and Nagi, 1983). The main results for the energy of the Shiba states remains the same, of course as Eq. (6.10).

In the particular case of purely magnetic spherically symmetric exchange, $J(\mathbf{k} - \mathbf{k}') = J$, only l = 0 components are non-vanishing and the T-matrix has a particularly simple form (Shiba, 1968). The diagonal in spin indices component is,

$$T^{(1)}(\omega) = \frac{1}{N} \frac{(JS/2)^2 \widehat{g}_0(\omega)}{I - (JS\widehat{g}_0(\omega)/2)^2}.$$
 (6.13)

Here \hat{g}_0 is the local matrix Green's function.

$$\widehat{g}_0(\omega) = \frac{1}{N} \sum_{\mathbf{k}} \widehat{G}_0(\mathbf{k}, \omega) = -\pi N_0 \frac{\omega + \Delta_0 \sigma_2 \tau_2}{\sqrt{\Delta_0^2 - \omega^2}}.$$
 (6.14)

The bound state energy

$$\epsilon_0 = \frac{E_0}{\Delta_0} = \frac{1 - (JS\pi N_0/2)^2}{1 + (JS\pi N_0/2)^2}.$$
 (6.15)

The wave functions of the bound states at E_l can be computed using the Bogoliubov equations above. In the simplest case of isotropic scattering at distances $r \gg p_F^{-1}$, both $u(\mathbf{r})$ and $v(\mathbf{r})$ vary as (Fetter, 1965; Rusinov, 1969)

$$\frac{\sin(p_F r - \delta_0^{\pm})}{p_F r} \exp(-r/\xi_0 |\sin(\delta_0^+ - \delta_0^-)|, \qquad (6.16)$$

that is, the state is localized near the impurity site at distances

$$r_0 \sim \frac{\xi_0}{|\sin(\delta_0^+ - \delta_0^-)|} = \frac{\xi_0}{\sqrt{1 - \epsilon_0^2}}.$$
 (6.17)

The square of these coefficients gives the spatial dependence of the amplitude of the particle and hole components of the density of states at a given position **r** (Yazdani *et al.*, 1997).

The analysis above was carried out under the assumption that the variation of the superconducting order parameter, Δ , around the impurity site does not change the position of the resonance low energy state. There are several characteristic length scales for this variation, $\delta\Delta(\mathbf{r})$. Far away from the impurity, $r \gg \xi_0$, at temperatures close to T_c , where this variation can be determined perturbatively, $\delta\Delta(\mathbf{r})/\Delta_0 \simeq 1/(p_F r)$ (Heinrichs, 1968; Rusinov, 1968). This power law is insensitive to the phase shifts of scattering on the impurity. At low temperatures a fully self-consistent treatment is required, which leads to $\delta\Delta(\mathbf{r})$ decaying as $(p_F r)^{-3}$ and oscillating on the scale of $\xi_0\Delta_0/\omega_D$, where the Debye temperature ω_D sets the

scale for the interaction between electrons (Schlottmann, 1976).

In the immediate vicinity of impurity, $v_F/\omega_D \ll r \ll \xi_0$, the variation of the order parameter is $\delta\Delta(\mathbf{r})/\Delta_0 \simeq 1/(p_F r)^2$ in the linear response approximation (Rusinov, 1968). In the fully self-consistent treatment at distances $r \ll \xi_0 \omega_D/E_F$, this dependence was found to acquire an oscillating factor $\sin^2 p_F r$ (Schlottmann, 1976).

In all these cases, since the suppression of the order parameter is determined by the Fermi wavelength, the effect is negligible in determination of the position of the bound state.

VII. IMPURITY-INDUCED VIRTUAL BOUND STATES IN d-WAVE SUPERCONDUCTORS

We are now ready to extend our discussion to impurity induced states in d-wave superconductors. Scalar (non-magnetic) impurities are pair-breakers for "higher-orbital-momentum" states, such as a d-wave pairing state. This occurs because change of the momentum of particles in the Cooper pair upon scattering disrupts the phase assignment for particular momenta in a nontrivial pairing (Anderson, 1959; Markowitz and Kadanoff, 1963; Tsuneto, 1962). More rigorously this follows from the analysis of the normal and anomalous self-energies due to scattering within the Abrikosov-Gorkov theory (Abrikosov et al., 1963). We also note that one of the first arguments about pairbreaking effects of potential scattering was given by Larkin (Larkin, 1965).

As we have emphasized, for pairbreaking impurities the local properties of the superconductor near an impurity site, such as the local density of states and the gap amplitude, will be modified dramatically. To capture these modifications, we use a variation of the Yu-Shiba-Rusinov approach (Rusinov, 1968; Shiba, 1968; Yu, 1965), which treats magnetic impurities in the strong scattering limit, see Sec. VI. We restrict our consideration to the s-wave scatterers with the phase shift close to the unitarity limit, $\delta_0 \simeq \pi/2$, when the bound state has energy away from the gap edge. In contrast to the s-wave superconductors, in d-wave systems the density of states below the gap maximum is non-zero, and varies linearly with energy in a pure system. Consequently, the overlap with the particle-hole continuum only allows the formation of virtual bound states with a finite lifetime.

We focus in this section on point-like defects, and use the T-matrix approach. A closely related method uses quasiclassical approximation and picture of Andreev scattering ideas to reproduce the results of T-matrix calculation (Chen $et\ al.$, 1999; Choi and Muzikar, 1990; Shnirman $et\ al.$, 1999). Even more interesting results are obtained within the quasiclassical formalism for extended defects. For example, it has been shown that index theorem dictates the existence of the low energy quasi-bound state (Adagideli $et\ al.$, 1999).

Zn substitutions in cuprates are one example of non-

magnetic atoms that are predominantly potential scatterers in high- T_c superconductors. Although Zn ions are nominally non-magnetic, T_c is strongly suppressed by Zn substitution of Cu in the planes (Hotta, 1993; Ishida *et al.*, 1991). Therefore, it is reasonable to assume that Zn ions are non-magnetic unitary scatterers, see below.

We analyze virtual impurity-bound states in a d-wave superconductor and, within this framework, explore possible implications of the assumption that the pairing in cuprates is in the $d_{x^2-y^2}$ channel. We model cuprates as a 2D d-wave superconductor, based on strong anisotropy of electronic transport. Our results, can be easily extended for any nontrivial pairing state and may be relevant, e.g. for heavy-fermion superconductors with impurities. Here we closely follow the references (Balatsky $et\ al.$, 1995; Buchholtz and Zwicknagl, 1981; Salkola $et\ al.$, 1996, 1997; Stamp, 1987).

Main results of this section are as follows: (i) A strongly-scattering scalar impurity is a requirement for a localized, virtual or virtually bound state (or resonance) to exist in a d-wave superconductor. It is intuitively obvious that any strong enough pair-breaking impurity — magnetic or non-magnetic — will induce such a state. Indeed, the low-lying quasiparticle states close to the nodes in the energy gap will be strongly influenced even by a non-magnetic impurity potential, resulting in a virtual bound state in the unitary limit. (ii) This should be compared to the fact that, in s-wave superconductors, both magnetic and resonant non-magnetic impurities produce bound states inside the energy gap (Machida and Shibata, 1972). The energy Ω' and the decay rate Ω'' of this state are given by

$$\Omega \equiv \Omega' + i\Omega'' = -\Delta_0 \frac{\pi c/2}{\log(8/\pi c)} \left[1 + \frac{i\pi}{2} \frac{1}{\log(8/\pi c)} \right] (7.1)$$

where $c=\cot\delta_0$. These results are computed assuming logarithmic accuracy is sufficient, with $\log(8/\pi c)\gg 1$. In the unitary limit, defined as $\delta_0\to\pi/2$ ($c\to0$), the virtual bound state becomes a resonance at $\Omega\to0$ with $\Omega''/\Omega'\to0$. In the opposite case of weak scattering with $c\lesssim1$, the energy of the virtual bound state formally approaches $\Omega'\sim\Delta_0$ and the state is ill-defined because $\Omega''\sim\Omega'$ (see Fig. 10. The wave function of the bound state is found to decay as a power law: $\Psi(r)\sim1/r$ and is not normalizable. This is consistent with the virtually bound state being not really a bound state. Wave function is localized along the directions of the vanishing gap, so called nodal directions.

A. Single potential impurity problem

Consider the single scalar impurity problem with

$$H_{\rm int} = \sum_{\mathbf{k}\mathbf{k}'\sigma} U_0 c_{\mathbf{k}\sigma}^{\dagger} c_{\mathbf{k}'\sigma} \tag{7.2}$$

where U_0 is the strength of the scalar impurity potential at $\mathbf{r} = 0$, resulting in s-wave phase shift δ_0 .

The scattering is described by a T-matrix, $\hat{T}(\omega)$, which is independent of wavevector. The Green's function in the presence of an impurity is

$$\widehat{G}(\mathbf{k}, \mathbf{k}'; \omega) = \widehat{G}_0(\mathbf{k}, \omega) \delta_{\mathbf{k}\mathbf{k}'} + \widehat{G}_0(\mathbf{k}, \omega) \widehat{T}(\omega) \widehat{G}_0(\mathbf{k}', \omega) (7.3)$$

where $\Delta_{\mathbf{k}} = \Delta_0 \cos 2\varphi$ is the gap function of $d_{x^2-y^2}$ -symmetry,

¿From the previous analyses (Balatsky et al., 1994; Hirschfeld and Goldenfeld, 1993; Hirschfeld et al., 1988; Lee, 1993; Pethick and Pines, 1986b; Schmitt-Rink et al., 1986; Shiba, 1968; Stamp, 1987), it is known that $\hat{T} = T_0\hat{\tau}_0 + T_3\hat{\tau}_3$ for s-wave scattering. The T-matrix takes the form

$$T(\omega)_{11} = 1/[c - g_{11}(\omega)],$$
 (7.4)

where $g_{11}(\omega) = \frac{1}{2\pi N_0} \sum_{\mathbf{k}} \operatorname{Tr} \widehat{G}^{(0)}(\mathbf{k}, \omega) (\widehat{\tau}_0 + \widehat{\tau}_3)_{11}$. The quasi bound states in the single-impurity problem are given by the poles of the T-matrix

$$c = g_{11}(\Omega), \tag{7.5}$$

which is an implicit equation for impurity resonance Ω_0 as a function of c, the strength of impurity scattering. Choosing the gap function at the Fermi surface so that $\Delta(\varphi) = \Delta_0 \cos 2\varphi$, one finds for particle-hole symmetric case $g_{11} = g_0(\omega) = \left\langle \omega/\sqrt{\Delta(\varphi)^2 - \omega^2} \right\rangle_{FS}$, where the angular brackets denote averaging over the Fermi surface; for simplicity, we take $\langle \bullet \rangle_{FS} = \int \bullet \ d\varphi/2\pi^{-1}$. For $|\omega| \ll \Delta_0$, one finds

$$g_0(\omega) = -\frac{2\omega}{\pi \Delta_0} \left(\log \frac{4\Delta_0}{\omega} - \frac{i\pi}{2} \right). \tag{7.6}$$

In Fig. 3 we illustrate a solution of the Eq. (7.5).

In principle, the solution of Eq. (7.5) is complex, indicating a resonant nature of the quasiparticle state, better described as a virtual state. This is easily seen form Eq. (7.1), which solves Eq. (7.5) to logarithmic accuracy. However, as $c \to 0$, the resonance can be made arbitrarily sharp. For c=0, the virtual state becomes a sharp resonance state bound to the impurity (Balatsky et~al., 1995). As $c \to 1^-$, Ω' and Ω'' increase without bound so that $\Omega''/\Omega' \to 1^-$, and the solution becomes unphysical. For c>1, no solution has been found for Ω .

To properly solve a single impurity state one has to retain both components of the T-matrix. Assumptions about particle-hole symmetry alone are not sufficient to leave the T_3 contribution out while computing the density of states around the impurity site. Full solution, Eq. (7.4), leads to the definite sign of the resonance energy depending on the sign of c. Indeed, if we assume that T_3 is zero we find that

$$T_0 = \frac{g_0(\omega)}{c^2 - g_0^2(\omega)} , \quad T_3 = \frac{c}{c^2 - g_0^2(\omega)} , \quad (7.7)$$

and T_0 has now two poles at $c=\pm g_0(\omega)$. This means that there would be two solutions to the "poles" of the T-matrix for each c, one on positive and one on negative frequency. This would clearly contradict the obvious particle hole asymmetry introduced by impurity. One can not get a symmetric density of states if we have only repulsive $(U_0 > 0)$ or attractive $(U_0 < 0)$ impurity potential. This argument shows that one is not allowed to ignore T_3 contributions, because T_3 is not a smooth function of energy near the pole.

Now we turn to the physical implications of these virtual bound states in a d-wave superconductor. Consider the most interesting case of unitary impurities in the dilute limit, separated by a distance greater than the coherence length ξ . Before averaging over impurities, these bound states are nearly localized close to the impurity sites (see below) and can substantially modify the local characteristics of the superconductor: for example, the local density of states, observed in STM and the local NMR relaxation rates of atoms close to the impurities.

Consider a local density of states, defined as

$$N(\mathbf{r},\omega) = -\frac{1}{\pi} \operatorname{Im} g_{11}(\mathbf{r}, \mathbf{r}; \omega + i0^{+})$$
 (7.8)

with the total Green's function in the presence of the impurity

$$\widehat{G}(\mathbf{r}, \mathbf{r}'; \omega) = \widehat{G}_0(\mathbf{r} - \mathbf{r}', \omega) + \widehat{G}_0(\mathbf{r}, \omega) \widehat{T}(\omega) \widehat{G}_0(\mathbf{r}', \omega).$$
(7.9)

We find two terms in the local density of states

$$N(\mathbf{r}, \omega) = N(\omega) + N_{\text{imp}}(\mathbf{r}, \omega) . \qquad (7.10)$$

The first term originates from the bulk quasiparticles, which are described by plane-wave eigenstates with $E_{\bf k} = \sqrt{\xi_{\bf k}^2 + \Delta_{\bf k}^2}, \ g^{(0)}(0,\omega) = \sum_{\bf k} [u_{\bf k}^2/(\omega - E_{\bf k}) + v_{\bf k}^2/(\omega + E_{\bf k})],$ where $u_{\bf k}$ and $v_{\bf k}$ are the standard Bogoliubov factors. The bulk density of states is constant in the system with $N(\omega)/N_0 = \omega/\Delta_0$, for $\omega \ll \Delta_0$. The second term,

$$N_{\rm imp}(\mathbf{r},\omega) = -\frac{1}{\pi} \text{Im} \left[\widehat{G}_0(\mathbf{r},\omega) \widehat{T}(\omega) \widehat{G}_0(\mathbf{r},\omega) \right]_{11} (7.11)$$

originates from the virtual bound state created at the impurity. This impurity state will have a form of a cross with long tails extended along the gap nodes see

We assume that the energy gap has line nodes in three dimensions with weak quasiparticle dispersion along the z axis; an extension to a general three-dimensional case is straightforward.

² The related model of the Anderson impurity in an unconventional superconductor has been considered by L. Borkowskii and P. Hirschfeld, Phys. Rev. B 46, 9274 (1992). The results found here for pure potential scattering require the generalization of the Anderson model to include the impurity potential phase shift, independent of the Kondo temperature. This aspect of impurity scattering has not been addressed previously.

Fig. 4. As an clarifying example, consider the limit of unitary scattering for which the resonant state is formed at $E_{\mathrm{imp},n} \equiv \Omega \to 0$, see also previous Sec. V. Because $\mathrm{Im}\,G^{(0)}(\mathbf{r},\omega=0) = -\pi N(\omega=0) = 0$, only the imaginary part of the T-matrix contributes to N_{imp} and the bound-state probability density is found to decay as the inverse second power of the distance from the impurity, mostly localized along the nodes of the gap function,

$$N_{\text{imp}}(\mathbf{r}, \omega = 0) = \text{Re}\left[\hat{G}^{(0)}(\mathbf{r}, \omega = 0)\right]^2 \propto r^{-2}, (7.12)$$

and similarly, but with smaller amplitude, in the vicinity of the extrema of the gap function,

$$N_{\rm imp}(\vec{r}, \omega = 0) \propto \frac{\Delta_0^2}{E_F^2} r^{-2},$$
 (7.13)

In addition to the power law decaying large distance asymptotics there is also an additional exponentially decaying piece that decays with $\xi(\varphi)$, the angle-dependent coherence length of the superconductor, defined as $\xi(\varphi) = \hbar v_F / |\Delta(\varphi)|$. Exponentially decaying part is important to compare the induced DOS to the observed in STM near impurity site although it does not change asymptotic behavior at large distances. In practice the intensity near impurity is mapped out only within few lattice sites.

Gap nodes lead to the power law decay of the wave function along all directions at large distances $r >> \xi$. This follows from the power counting of the d-wave propagator we estimate: $G(\mathbf{r}, \omega \to 0) \sim \int d^2k \exp(i\mathbf{k} \cdot \mathbf{r}) G(\mathbf{k}, \omega \to 0) \sim \int kdk \exp(i\mathbf{k} \cdot \mathbf{r}) \frac{v_F k}{k^2} \sim 1/r$. The fact that the impurity state is virtually bound is reflected in the logarithmically divergent normalization. This divergence should be cut off at an average distance between impurities at any finite concentration. More generally, for an arbitrary position of the resonance, taking into account that only one state has been produced with $E_{\text{imp},n} = \Omega' + i\Omega''$, we find

$$N_{\text{imp}}(\mathbf{r}, \omega) = \frac{\Omega_i''}{\pi} \sum_{i} \left[\frac{|u(\mathbf{r} - \mathbf{r}_i)|^2}{(\omega - \Omega_i')^2 + \Omega_i''^2} - \frac{|v(\mathbf{r} - \mathbf{r}_i)|^2}{(\omega + \Omega_i')^2 + \Omega_i''^2} \right], \tag{7.14}$$

where we have introduced the sum over different impurities, located at \mathbf{r}_i , and $u(\mathbf{r} - \mathbf{r}_i), v(\mathbf{r} - \mathbf{r}_i)$ are the eigenfunction of the Bogoliubov-de Gennes equation at the impurity level.

The local effects of impurities are best revealed by local probes. NMR experiments on Cu in Zn-doped cuprates are quite useful in this regard. From Eq. (7.12) and below, one concludes immediately that the local NMR signal would show two distinct relaxation rates (or even the hierarchy of rates): one coming from the Cu sites, far away from the impurities, and another from the sites, close to the impurities. The Cu sites near the impurities will be sensitive to the higher local density of states

and will have a higher relaxation rate at low temperatures. At finite impurity concentration ($\sim 2\%$), the volume-averaged density of states will have a finite limit at $\omega \to 0$, as follows from Eq. (7.12). The relaxation rates of Cu atoms close to and away from an impurity will, therefore, have the same temperature dependence $(T_1T)^{-1} = const$, but will be of a different magnitude. Precisely this behavior has been observed experimentally: Ishida et al. (Ishida et al., 1991) have measured two NMR relaxation rates for Cu in Zn-doped YBa₂Cu₃O_{7- δ}. The second NMR signal with higher relaxation was inferred arising from the near-impurity Cu sites. Alloul and collaborators have pointed out that the NMR signal coming from the sites close to impurties shows a distribution of relaxation times and reflect local electronic and magnetic distortions produced by impurities, see (Bobroff et al., 2001) and references therein.

More direct evidence for the impurity induced resonances in high- T_c is coming from STM experiments. Local variations of the density of states can be probed using scanning-tunneling microscopy. These experiments were crucial in establishing the existence of the impurity induced resonances in cuprates and their anisotropic nature (Hudson *et al.*, 1999; Pan *et al.*, 2000b), see section XIII.

We would like to contrast our picture of the dilute limit of strongly scattering centers to the usual approach of averaging over impurities at finite concentration. If one considers averaging over impurities, two NMR relaxation rates, arising from unequivalent sites, cannot be resolved; similarly local inhomogeneous aspect of the localized states will be lost after averaging over impurity positions.

For practical purposes the distinction between the a true bound states and continuum in our case is not well defined, as it is in s-wave superconductors. Any finite temperature will produce a finite lifetime for these bound states, and they will be hybridized with the continuum of low-energy quasiparticles as they are not separated by a well defined gap.

B. Single magnetic impurity problem

The similar analysis for the magnetic impurity is more involved. For a quantum spin s=1/2 in d-wave superconductor one needs to address the Kondo effect. It is discussed in more details in Sec. XI. For a classical spin $S\gg 1$ the analysis within the mean field is similar to the one in the previous section (Salkola *et al.*, 1997).

The main effect is that exchange coupling between the local spin S and electron spin leads to the renormalization of the effective scattering potential. Namely for electrons of two spin polarization the net impurity potential is $U_0 \pm J$, where U_0 is the potential scattering strength and J is the exchange coupling to impurity spin, see Sec. XIII. There are two virtual bound states, one for each electron spin orientation. STM data on Ni-doped Bi2212 are fit well using this simple formula. This mean

field approach does not address the dynamics of the large spin S. More analysis is required to address this problem.

C. Self-consistent gap solution near impurity

Impurity scattering will produce local modifications of the order parameter. We already addressed some of the effects in s-wave superconductors in Sec. IX. Here we will discuss the self-consistently determined gap in d-wave superconductors.

To address these effects at small distances one would need to use an numerically determined exact spectra near impurity and solve self-consistent gap equation. We define:

$$\Delta(i, i + \delta) = \frac{V_{i, i + \delta}}{2} \sum_{n} [u_n(i + \delta)v_n^*(i) + u_n^*(i)v_n(i + \delta)] \times \tanh(\frac{E_n}{2k_BT}).$$

$$(7.15)$$

Numerical solution of this problem was presented in (Franz et al., 1996; Salkola et al., 1997; Tsuchiura et al., 2000; Zhu et al., 2000a). The main result is that impurity scattering suppresses the gap magnitude. Suppression is strongest on the impurity site and quickly gap recovers a bulk value, although there are always oscillating tails at far distance due to $2k_F$ oscillations, Fig. 5.

In practice, the difference between self-consistent and non self-consistent solution is not important at distance beyond few lattice sites away from impurity. Local gap suppression is clearly seen in STM data, see Sec. XIII.

D. Spin-orbit scattering impurities

Spin-orbit coupling in impurity scattering in superconductors is the least discussed among all other kinds of impurity scattering. Standard spin orbit scattering is of the form:

$$H_{SOimp} = \sum_{\mathbf{k}, \mathbf{k}'} \lambda_{SO} c_{\mathbf{k}, \alpha}^{\dagger} \vec{\sigma}_{\alpha\beta} \cdot (\mathbf{k} \times \mathbf{k}') c_{\mathbf{k}'\beta} \qquad (7.16)$$

where λ_{SO} is the strength of Spin Orbit scattering. This kind of SO scattering would be present even for non-magnetic impurities, it will be a pairbreaker and it will produce the the quasi-bound states inside the gap, although the detailed calculation has not been done to our knowledge.

Another kind of SO scattering impurities scattering in d-wave from the magnetic impurity can be considered as well. It was initially motivated by experiments on Ni doped Bi2212 (Movshovich et al., 1998; Neils and Harlingen, 2002). In this approach impurity spin is coupled to the orbital motion of the conduction electrons (Balatsky, 1998; Barash et al., 1997; Graf et al., 2000; Grimaldi, 1999):

$$H_{SO,imp} = \sum_{\mathbf{k},\mathbf{k}'} \gamma_{SO} c_{\mathbf{k},\sigma}^{\dagger} \mathbf{S} \cdot (\mathbf{k} \times \mathbf{k}') c_{\mathbf{k}'\sigma}$$
 (7.17)

where γ_{SO} is the strength of coupling and **S** is the impurity spin. This term is the SO coupling $H_{SO,imp} =$ $\gamma_{SO}\hat{\mathbf{L}}\cdot\mathbf{S}$ written in second quantized notation. Predominantly in plane motion of electrons as is the case in Bi2212 will couple L_z to S_z , $\hat{\mathbf{L}}_z = i\hbar\partial_{\phi}$ is the angular momentum operator L_z with respect to the impurity site. The net effect of this term is twofold. This scattering term is a pairbreaker, locally gap is suppressed and resonance is formed. However the more interesting and nontrivial is the distortion of the d-wave order parameter in the vicinity of impurity, which results from the nontrivial orbital structure of the d-wave order. The d-wave state is a linear combination of the state with l=2 and l=-2, $\Delta(\phi) = \Delta_0 \cos(2\phi) \propto \exp(2i\phi) + \exp(-2i\phi) \sim x^2 - y^2.$ The orbital angular momentum components will be affected differently as a result of scattering. In the first order perturbation theory in H_{SOimp} one generates the correction to the order parameter $\Delta' = i\Delta_0 \gamma_{SO} \sin(2\phi) \sim$ xy. There is a finite amplitude for incoming d-wave pair $|in\rangle \propto |x^2 - y^2\rangle$ to scatter into $|out\rangle \propto i|xy\rangle$ channel:

$$|out\rangle = i\gamma_{SO}\Delta_0\hat{\mathbf{L}}\cdot\mathbf{S}|in\rangle = i\hbar\gamma_{SO}\Delta_0\sin(2\phi)$$
. (7.18)

Therefore as is the case for SO scattering, sometimes impurity scattering can produce nontrivial distortions of the initial order parameter, aside from trivial suppression. For more details, see (Balatsky, 1998; Graf et~al., 2000; Zhu and Balatsky, 2002). Similarly, magnetic field, that acts similarly to the S_z term in Eq. (7.18), not only suppresses the d-wave order parameter but also produces the secondary d_{xy} component, see (Balatsky, 2000; Franz and Tešanović, 1998; Kuboki and Sigrist, 1998; Laughlin, 1998; Tanuma et~al., 1998).

E. Effect of doppler shift and magnetic field

Here we are focusing on the orbital effect of magnetic field and thus the problem is closely related to the effect of Doppler shift on impurity resonance.

In the presence of a superflow with velocity \mathbf{v}_S propagators are modified: $G(\mathbf{k},\omega) \to G(\mathbf{k},\omega-\mathbf{k}\cdot\mathbf{v}_S)$ for a planar wave state at vector \mathbf{k} and similar change for F function. Hence the rest of the calculation for the impurity state goes through as before. Since only local propagators enter into solution for impurity resonance Eq. (7.1), the modifications will arise as a result of changes in density of states due to Doppler shift.

Interesting effect of the superflow produced by the screening currents on the impurity state was studied by Samokhin and Walker (Samokhin and Walker, 2001). They pointed out that Doppler shift will result in the broadening of the impurity induced resonance. This is a consequence of the local scattering nature of impurity that means summing over all momenta to obtain local Green's function $G_0(\omega)$. One would need to compare the typical value of the Doppler shift $v_S k_F$ and the energy of the resonance Ω' . In the case when Doppler shift is small

effect is negligible. In the opposite limit of $v_S k_f \gg \Omega'$ superflow produces broadening of the resonance but not the energy shift of the resonance.

F. Sensitivity of impurity state to details of band structure

In the above discussion we were using the single band model with particle-hole symmetric structure as a simplest example to prove the existence of the impurity induced resonance. The effect of asymmetric band about the gap midpoint was considered by Joynt (Joynt, 1997), by assuming a constant DOS with different energy ranges outside the gap edge. To make a comparison with the real experimental data on impurity resonances, see Sec. XIII, one has to understand the details of realistic band structure. Microscopically, relevant bands in Cu-O planes are Cu $d_{x^2-y^2}$ and O $p_{x,y}$ bands. In the above analysis we have assumed that upon the reduction of the complicated band structure of high- T_c to a single band model, one can still describe nonmagnetic impurity by a single parameter, i.e. the on-site potential U_0 . We do not have a proof for this and assume that the major physical effects, such as that the impurity induced resonance will be properly captured in a simplified model.

Within the framework of this simplified one band model one can still investigate some effects beyond the simplest assumptions. One of the most obvious questions is the position of the impurity-induced resonance with respect to the Fermi energy. We find the resonance depends on the sign of the impurity potential, the electron occupation, and the band structure. We have performed numerical exact diagonalization for the t-t'-V model with nearest-neighbor hopping t, next nearest neighbor hopping t', and a negative V, that describes the nearest neighbor attraction to produce effectively a d-wave pairing. The single particle energy dispersion for the normal state is given by:

$$\xi_k = -2t(\cos k_x + \cos k_y) - 4t'\cos k_x \cos k_y - \mu$$
, (7.19)

with μ the chemical potential. Impurity was modeled as an on-site potential U_0 . We have looked at three possibilities: (i) $t=1,t'=0,\mu=0$ (the filling factor n=1.0), with band particle-hole symmetry present, Fig. 6; (ii) $t=1,t'=-0.2,\mu=-0.784(n=0.84)$, with no band particle-hole symmetry, Fig. 7; (iii) $t=1,t'=-0.3,\mu=-1.0(n=0.85)$, again with band particle-hole symmetry absent, Fig. 8. Here we talk about the band particle-hole symmetry because as long as an impurity is introduced, the local particle-hole symmetry is always broken.

As shown in these figures, for the cases (i) and (ii), the band DOS has two coherent peaks. Also for the case (ii), the DOS is asymmetric with respect to the zero energy point. In these two cases, a repulsive potential $U_0 > 0$ leads to a negative energy impurity state $\Omega'_0 < 0$. This position is manifested as a resonance peak appearing below the Fermi energy in the LDOS directly impurity site but appearing above the Fermi energy in the LDOS at its

four nearest neighbors. An attractive impurity potential $U_0 < 0$ induces a positive energy impurity state $\Omega_0' > 0$, as reflected as a resonance peak above the Fermi energy in the LDOS directly on the impurity site but below the Fermi energy in the LDOS at its nearest neighbors.

For the case (iii), in addition to the two coherent peaks, there are also two van Hove singularity peaks (the one on the negative energy side being more pronounced and the other on the positive energy side being faint). Then for a repulsive impurity, the on-site resonance peak does shift from the negative energy side across the zero energy. This phenomenon is absent for the cases of (i) and (ii). For $U_0 < 0$, the result is similar to the cases (i) and (ii). We point that in the STM data, the van Hove singularity peaks are absent. Here we have chosen for (ii) and (iii) only in the optimal doping regime. In other doping regime, all possibilities uncovered above could appear. More detailed analysis, especially realistic band structure calculations will allow us better address the details of impurity states in high- T_c materials.

As for the sign of the impurity potential from the Zn and Ni atoms in cuprates, it is still an unsettled issue. It is believed that these atoms substitute Cu in the Cu-O plane, and do not change the hole doping. In case of Zn that has $3d^{10}4s^2$ electrons, Zn⁺⁺ is in d^{10} configuration. The third ionization energy should be a rough measure of the energy level for d-orbital of Cu and Zn/Ni ions though the electrons from the d-orbital of Cu form a band. By comparing the energies of Cu atom $E_{Cu^{++}} = -36.83eV$, and Zn atom $E_{Zn^{++}} = -39.722eV$, we estimate energy to be on the order of $U_0 \simeq -2.89eV$. Therefore, Zn atom plays the role of a strong attractive potential.

In case of Ni doping, Ni⁺⁺ has a $3d^8$ configuration and a spin S=1 ground state is formed. Therefore, Ni impurity will produce both potential scattering U_0 and magnetic scattering J. We can estimate the energy U_0 again by taking the difference between atomic energies for $E_{Cu^{++}} = -36.83eV$ and $E_{Ni^{++}} = -35.17eV$. We estimate $U_0 \simeq 1.66eV$ for Ni. It provides a weaker repulsive potential for the non-magnetic scattering part.

VIII. SINGLE IMPURITY BOUND STATE IN A PSEUDOGAP STATE OF TWO-DIMENSIONAL METALS

In the high-temperature cuprates, many experiments (Loram et al., 2000; Norman et al., 1998; Renner et al., 1998) show that the electronic density of states near the Fermi surface is suppressed within the range of Δ_{PG} above the superconducting phase transition temperature T_c but below a characteristic temperature T^* . So far, the mechanism for the PG state is still hotly debated. For a review see (Timusk, 2003; Timusk and Statt, 1999). The typical competing scenarios for this anomalous phenomenon, including mainly the pre-formed pair with phase-fluctuation model (Emery and Kivelson, 1995), the Bose-Einstein condensation of Cooper pairs (Chen et al., 1998), the

time-reversal-symmetry-breaking circulating current model (Varma, 1999), and the d-density-wave model (DDW) (Chakravarty et al., 2001), which is typical kind of staggered flux state (Affleck and Marston, 1988; Hsu et al., 1991; Marston and Affleck, 1989). In the first scenario, the normal state contains preformed Cooper pairs, and the phase fluctuation of the pairing field destroys the long range order, that is, the superconductivity. Since the pairing field has at the onset a d-wave symmetry in the momentum space for the relative motion degrees of freedom, a d-wave-like pesudogap follows naturally. In the second category of scenarios, it is speculated that the PG state comes as a result of a new order not inheriting from the superconducting pairing.

In this Section, we are not going to discuss the origin for the PG. Instead we are particularly interested in the consequences of the electronic property around a single impurity in the PG state. One can consider the temperature evolution of the impurity state as the temperature increases and eventually becomes larger than T_c . Then there are two possibilities for the evolution of impurity resonance at $T > T_c$: a) the impurity resonance gradually broadens until the superconducting gap vanishes, at which point the impurity resonance totally disappears and b) the resonance gets broader but survives above T_c . Which of the possibilities is realized depends on the normal state phase the superconductor evolves into. It has been argued (Krasnov et al., 2000; Loram et al., 2000) that in the underdoped regime the superconducting gap opens up in addition to the PG present well above T_c . Hence, we find that the impurity resonance survives above T_c in the PG state of high- T_c materials. The position and the width of the resonance are determined by the impurity scattering strength and PG scale. In the absence of PG above T_c the impurity state disappears.

Specifically we calculate the resonant state generated by the substitution of one Cu atom with a Zn atom using the T-matrix approach. We rely on the fact that the density of states (DOS) is depleted at the Fermi energy in the PG regime. We argue that the mere fact that the DOS is depleted at the Fermi energy is sufficient to produce a resonance near the nonmagnetic impurity, such as Zn. Before we consider the impurity effect within specific scenarios, we give a general analysis, which is valid in the PG state with no superconducting phase or amplitude fluctuations above T_c , as long as there are interactions that lead to the PG state. The approach we take is similar to the previous analysis of the nonmagnetic impurity in the superconducting state (Balatsky et al., 1995). See also Fig. 9. The states generated by the impurity are still given by the poles of the T matrix:

$$G_0(\Omega) = \frac{1}{U_0} \ . \tag{8.1}$$

This is an implicit equation for Ω as a function of U_0 . This solution can be complex, indicating the resonant nature of the virtual state. To solve this equation, we need to know the form of nonperturbed Green's function on the impurity site, $g_0(E)$. To do so, we split g_0 into its imaginary and real part $g_0 = g_0' + ig_0''$ with $G_0''(\omega) = -\pi N_0(\omega)$, where $N_0(\omega)$ is the density of states.

Measurements on the electronic specific heat by Loram et al. (Loram et al., 2000) show that the normal state pseudo gap opens abruptly in the underdoped region below a hole doping equal to $p_{crit} \sim 0.19 \text{ holes/CuO}_2$. Inspired by these data, we will assume that around the pseudogap region, states are partly depleted and the density of states is linear, that is $N_0(\omega) = N_0|\omega|/\Delta_{PG}$ for $|\omega| \leq \Delta_{PG}$ and $N_0(\omega) = N_0$ for $\Delta_{PG} < |\omega| < W/2$ with W the bandwidth. This density of states is depicted in Fig. 10(a). As it is obvious from the solution of Eq. (8.1), the precise position and the width of the resonance will depend on the specific form of the PG. We will use this linearly vanishing PG DOS. Results for other forms of $N(\omega)$ like a fully gapped DOS or a DOS with a quadratic dependent gap, can be obtained in the same way and lead essentially to similar expressions.³

Using this DOS for g_0'' and invoking the Kramer-Kronig relation (Mahan, 2000)

$$g_0'(\omega) = \frac{1}{\pi} \int_{-\infty}^{\infty} d\omega' g_0''(\omega') P\left(\frac{1}{\omega' - \omega}\right), \tag{8.2}$$

with P the Cauchy's principle value, one can obtain the real part g'_0 as

$$g_0'(\omega) = -N_0 \ln \left| \frac{\frac{W}{2} - \omega}{\frac{W}{2} + \omega} \right| + N_0 \ln \left| \frac{\Delta_{PG} - \omega}{\Delta_{PG} + \omega} \right| - N_0 \frac{\omega}{\Delta_{PG}} \ln \left| \frac{\Delta_{PG}^2 - \omega^2}{\omega^2} \right|. \tag{8.3}$$

This function is plotted in Fig. 10(b) together with $1/U_0$. If $2U_0N_0 > 1$, one can see from this figure that equation (8.1) has four solutions. Since the width of a resonance state is proportional to $|\Omega|$, the only state with sharp width is the solution with $|\Omega|$ close to zero and we will only consider this solution. After expansion in ω of equation (8.3) we arrive at an expression for this solution Ω of Eq. (8.1):

$$g_0(\Omega) = -\frac{2\Omega N_0}{\Delta_{PG}} \left[\ln \left| \frac{\Delta_{PG}}{\Omega} \right| + 1 - \frac{i\pi \operatorname{sgn}(U_0)}{2} \right] = \frac{1}{U_0},$$
(8.4)

³ We argue that the appearance of the intragap impurity state is a robust feature of any depleted DOS around the Fermi surface. We also considered the model DOS with $N_0(\omega) = N_0[a + (1-a)\omega^2/\Delta_{PG}^2]$ which leads essentially to similar results as a function of the impurity strength with a resonant state at $\Omega = -\Delta_{PG}(1+i\pi aN_0U_0)/(4N_0U_0(1-a-\Delta_{PG}/W))$ $\approx -\Delta_{PG}(1+i\pi aN_0U_0)/(4N_0U_0(1-a))$ when Δ_{PG}/W is small. But also a fully gapped DOS equal to $N(\omega) = N_0$ for $|\omega| \in [\Delta_{PG}, W/2]$ and zero otherwise gives rise to a comparable expression with a resonant state at $\Omega = -\Delta_{PG}/(2U_0N_0)$.

This equation can be solved exactly in terms of LambertW functions, ⁴ which, to logarithmic accuracy with $\ln |2U_0N_0| > 1$, gives: ⁵

$$\begin{split} \Omega &= \Omega' + i\Omega'' \\ &= -\frac{\Delta_{PG}}{2U_0N_0} \frac{1}{\ln|2U_0N_0|} \\ &\times \left[1 - \frac{1}{\ln|2U_0N_0|} + \frac{i\pi \operatorname{sign}(U_0)}{2\ln|2U_0N_0|} \right], \quad (8.5) \end{split}$$

where Ω' is the energy position and Ω'' the decay rate.

Using formula (8.5), and taking $N_0=1$ state/eV, $\Delta_{PG}\sim 300 {\rm K}\sim 30 {\rm meV}$ and the scattering potential $U_0\approx \pm 2 {\rm eV}$, we estimate $\Omega\sim \pm 2 {\rm meV}\sim \pm 20 {\rm K}$ as was found by Loram et al. (Loram et al., 2000). This energy is close to the Zn resonance energy $\omega_0=-16 K$, seen in the superconducting state (Pan et al., 2000b). By combining these results with the band-structure arguments (Martin et al., 2002), we come to conclusion that the Zn impurity in Bi2212 is strongly attractive, with $U_0\sim -2 {\rm eV}$. This result, as we will now see, may be modified due to the particle-hole asymmetry characteristic of doped cuprates.

In the absence of particle-hole symmetry, a similar calculation can be done. The simplest way to introduce the asymmetry is by making the upper and lower cutoffs in the DOS unequal. This situation corresponds to a chemical potential μ , located away from the center of the band. Keeping the DOS otherwise unchanged, with the pseudogap centered at the chemical potential, results only in the following change in the first logarithmic term of Eq. (8.3):

$$-N_0 \ln \left| \frac{\frac{W}{2} - \mu - \omega}{\frac{W}{2} + \mu + \omega} \right| \tag{8.6}$$

Neglecting the frequency ω relative to chemical potential μ and assuming that μ is small relative to the bandwidth, we obtain that the results for the asymmetric case can be obtained from the symmetric ones by the substitution

$$\frac{1}{U_0} \to \frac{1}{U_0} - \frac{4N_0\mu}{W}. \tag{8.7}$$

The effect of the asymmetry term can be estimated for the superconducting cuprates. For 20% hole doping, $\mu \sim -(1/5)W/2 = -W/10$. Hence, the modified value for the Zn impurity strength in Bi2212 can be obtained

⁴ The exact solution in terms of a LambertW function, Lw(-1, x), is $\Omega = -\Delta_{PG} \operatorname{sgn}(U_0) \exp\{Lw(-1, -\operatorname{sgn}(U_0) \exp(i\pi/2 - 1)/(2N_0U_0)) + 1 - i\pi/2\}$, where Lw(x) is such that $Lw(x) \exp[Lw(x)] = x$.

from the symmetric result, $1/U^* = 1/U_0 + 4N_0\mu/W$. The new value is $U^* \sim -1~eV$, which is a strongly attractive potential, as is expected from the band structure arguments.

The solution of the impurity state deep in the superconducting regime involves two aspects: the energy position and the width of the resonance and secondly, the real space shape of the impurity state. We have discussed the energy of the impurity state above. Great advantage of the on-site impurity solution for the local potential U_0 is that only on-site propagator $g_0(\omega)$ enters into calculation. Hence the knowledge of the DOS was sufficient to calculate the impurity state. On the other hand, to calculate the real space image of impurity induced resonance, one would require more detailed knowledge of the Green's functions in the PG regime. Quite generally, one would expect for a d-wave-like PG with nearly nodal points along the $(\pm \pi/2, \pm \pi/2)$ directions, that the impurity resonance in the pseudogap regime would be four-fold symmetric, similar to superconducting solutions (Balatsky et al., 1995). This calculation would require a specific model for the PG state, some of which are considered below.

Impurity state in a DDW system. The model Hamiltonian for a clean DDW system is written as:

$$H_0 = \sum_{ij,\sigma} [-t_{ij} + (-1)^i i W_{ij}] c_{i\sigma}^{\dagger} c_{j\sigma} - \mu \sum_{i,\sigma} c_{i\sigma}^{\dagger} c_{i\sigma} . \quad (8.8)$$

Here $c_{i\sigma}^{\dagger}$ $(c_{i\sigma})$ is the creation and annihilation of an electron with spin projection σ at the ith site. The DDW order parameter W_{ij} has the value $W_{i,i\pm\hat{x}}=W_{\pm\hat{x}}=\frac{W_0}{4}$ and $W_{i,i\pm\hat{y}}=W_{\pm\hat{y}}=-\frac{W_0}{4}$, while is zero otherwise. Notice that the prefactor $i=\sqrt{-1}$ before W_{ij} . It indicates that the DDW state breaks the time reversal symmetry. The quantity μ is the chemical potential. Without loss of generality, we have assumed that the impurity is located at the origin. In the momentum space, the Hamiltonian is given by:

$$H_0 = \sum_{k,\sigma} \xi_k c_{k\sigma}^{\dagger} c_{k\sigma} + \sum_{k,\sigma} iW_k [c_{k\sigma}^{\dagger} c_{k+Q,\sigma} - c_{k+Q,\sigma}^{\dagger} c_{k\sigma}] .$$

$$(8.9)$$

Here $c_{k\sigma}^{\dagger}$ ($c_{k\sigma}$) are the creation and (annihilation) operators of an electron at the wave vetor k and with spin projection σ . The single particle energy dispersion for the normal state is given by Eq. (7.19). The DDW gap is given by:

$$W_k = \frac{W_0}{2} (\cos k_x - \cos k_y) . (8.10)$$

Here the wave vector k_x and k_y are defined in the first Brillouin zone.

In view of the fact that the DDW state breaks the translational symmetry with lattice constant but conserves that by $\sqrt{2}a$ along the diagonals of the square lattice, it is convenient to rewrite the Hamiltonian in the

⁵ The simplest model for thermal broadening is to assign the temperature dependent width: Thermal broadening at high temperatures $T > T_c$ substantially broadens the impurity resonance peak $\Omega''(T) = \sqrt{(\Omega''(T=0))^2 + T^2}$.

reduced Brillouin zone with its area one half of the original by introducing a two-component electron operator $\Psi_{k\sigma}^{\dagger} = (c_{k\sigma}^{\dagger}, c_{k+Q,\sigma}^{\dagger})$ with $\mathbf{Q} = (\pi, \pi)$:

$$H_0 = \sum_{k \in rBZ, \sigma} \Psi_{k\sigma}^{\dagger} \begin{pmatrix} \xi_k & i2W_k \\ -2iW_k & \xi_{k+Q} \end{pmatrix} \Psi_{k\sigma} , \qquad (8.11)$$

where rBZ represents the reduced Brillouin zone.

Accordingly, we can introduce the following Green functions in the clean limit:

$$\hat{\mathcal{G}}^{(0)}(k;\tau) = \begin{pmatrix} \mathcal{G}_{11}^{(0)} & \mathcal{G}_{12}^{(0)} \\ \mathcal{G}_{21}^{(0)} & \mathcal{G}_{22}^{(0)} \end{pmatrix} . \tag{8.12}$$

with

$$\mathcal{G}_{11}^{(0)}(k;\tau) = -\langle T_{\tau}[c_{k\sigma}(\tau)c_{k\sigma}^{\dagger}(0)]\rangle, \qquad (8.13a)$$

$$\mathcal{G}_{12}^{(0)}(k;\tau) = -\langle T_{\tau}[c_{k\sigma}(\tau)c_{k+Q,\sigma}^{\dagger}(0)]\rangle, \quad (8.13b)$$

$$\mathcal{G}_{21}^{(0)}(k;\tau) = -\langle T_{\tau}[c_{k+Q,\sigma}(\tau)c_{k\sigma}^{\dagger}(0)]\rangle , \quad (8.13c)$$

$$\mathcal{G}_{22}^{(0)}(k;\tau) = -\langle T_{\tau}[c_{k+Q,\sigma}(\tau)c_{k+Q,\sigma}^{\dagger}(0)]\rangle . (8.13d)$$

Here the factor T_{τ} is a τ -ordering operator as usual, and $c_{k\sigma}(\tau) = e^{H\tau}c_{k\sigma}e^{-H\tau}$ is the operator in the Heisenberg representation. Given the Hamiltonian Eq. (8.11), with aid of the equation of motion for the field operator $c_{k\sigma}(\tau)$ and $c_{k\sigma}^{\dagger}(\tau)$, and by performing a Fourier transform with respect to τ ,

$$\hat{\mathcal{G}}(k;\tau) = k_B T \sum_{\omega_n} \hat{\mathcal{G}}(k;i\omega_n) e^{-i\omega_n \tau}$$
 (8.14)

with $\omega_n = (2n+1)\pi k_B T$, one can arrive at:

$$\hat{\mathcal{G}}^{(0)}(k; i\omega_n) = \begin{pmatrix} i\omega_n - \xi_k & -2iW_k \\ 2iW_k & i\omega_n - \xi_{k+Q} \end{pmatrix}^{-1} . \quad (8.15)$$

As will be obvious immediately, we also need to calculate the Green function in real space, which through the Fourier transform is given by

$$\mathcal{G}^{(0)}(i,j;i\omega_n) = \frac{1}{N} \sum_{k \in rBZ} e^{i\mathbf{k} \cdot \mathbf{R}_{ij}} [\mathcal{G}_{11}^{(0)}(k;i\omega_n) + \mathcal{G}_{22}^{(0)}(k;i\omega_n) + e^{-i\mathbf{Q} \cdot \mathbf{R}_j} \mathcal{G}_{12}^{(0)}(k;i\omega_n) + e^{i\mathbf{Q} \cdot \mathbf{R}_i} \mathcal{G}_{21}^{(0)}(k;i\omega_n)]$$

where \mathbf{R}_i are the lattice vectors and $\mathbf{R}_{ij} = \mathbf{R}_i - \mathbf{R}_j$. Specially, from Eqs. (8.15) and (8.16), one can obtain:

$$\mathcal{G}^{(0)} = \frac{1}{N} \sum_{k \in rBZ} \frac{2i\omega_n - \xi_{k+Q} - \xi_k}{(i\omega_n - \xi_k)(i\omega_n - \xi_{k+Q}) - 4W_k^2}.$$
(8.17)

In the presence of a single non-magnetic impurity in the DDW state, the T-matrix analysis just shows again that the resonance state is determined by the poles of $T(i\omega_n \to \omega + i0^+)$, i.e., the following equation

$$\mathcal{G}^{(0)}(0,0;\omega+i0^+) = \frac{1}{U_0} \ . \tag{8.18}$$

The existence of the resonant states will directly manifest in the local density of states:

$$N_i(\omega) = -\frac{2}{\pi} \operatorname{Im} \mathcal{G}(i, i; \omega + i\delta) . \tag{8.19}$$

The results are displayed in Figs. 11 and 12. shown in these figures, the electronic excitation spectrum around the impurity in the DDW state is very sensitive to the parameter values, which control the band structure. For t'=0 and at the half filling $(\mu=0)$, the electron density of states in the clean limit is vanishingly small around the Fermi energy, which leads to resonance states near the Fermi energy. With t'=0 but the system doped away from the half filling, the resonant peak in the LDOS is shifted away from the Fermi energy. This is because the energy at which the band DOS vanishes no longer coincides with the Fermi energy. For a set of more realistic parameter values, the density of states in the clean limit shows negligible reduction at low energies, which makes the local density of states near the impurity not exhibit any signature of a resonance state. These results were independently obtained by Zhu et al. (Zhu et al., 2001), Wang (Wang, 2002), and Morr (Morr, 2002). The quasiparticle states in the DDW state with a finite concentration of non-magnetic impurities was investigated by Ghosal and Kee (Ghosal and Kee, 2004).

Phase-fluctuation scenario: We now devote to a discussion on the impurity state in a phase-fluctuating pairing field. For more details, see Wang, 2002. The effective mean field Hamiltonian in a two-dimensional square lattice for a d-wave superconductor can be written as:

$$H = \sum_{ij} \Psi_i^{\dagger} \begin{pmatrix} -t_{ij} - \mu \delta_{ij} & -\Delta_{ij} \\ -\Delta_{ij}^* & -(-t_{ji} - \mu \delta_{ij}) \end{pmatrix} \Psi_j , \quad (8.20)$$

where $\Psi_i^{\dagger}=(c_{i\uparrow}^{\dagger},c_{i\downarrow})$ is the two-component spinor operator in the Nambu space, the other notations are the standard except the pairing field Δ_{ij} is fluctuating. In the phase fluctuation scenario, the amplitude of the superconducting order parameter is fixed while its phase fluctuating. For d-wave superconductivity, one can write the pairing field as:

$$\Delta_{ij} = \frac{\Delta_0 \eta_{ij}}{4} e^{i\varphi_{ij}} = \tilde{\Delta}_{ij} e^{i\varphi_{ij}} , \qquad (8.21)$$

with $\eta_{ij} = 1$ (-1) for x (y) direction bonds and the phase $\varphi_{ij} = (\varphi_i + \varphi_j)/2$. The spatial variation of the phase will give rise to a superfluid flow associated with the Cooper pairs. By performing a gauge transformation,

$$\tilde{\Psi}_i = e^{-i\varphi_i \sigma_3/2} \Psi_i \tag{8.22}$$

with σ_3 the third component of the Pauli matrix, one can remove the phase factor on the pairing field such that

$$\tilde{H} = \sum_{ij} \tilde{\Psi}_{i}^{\dagger} \begin{pmatrix} -\tilde{t}_{ij} - \mu \delta_{ij} & -\tilde{\Delta}_{ij} \\ -\tilde{\Delta}_{ij}^{*} & -(-\tilde{t}_{ji} - \mu \delta_{ij}) \end{pmatrix} \tilde{\Psi}_{j} , \quad (8.23)$$

where $\tilde{t}_{ij} = t_{ij}e^{-i(\varphi_i - \varphi_j)/2}$. In type-II superconductors, the length scale of the phase variation (the London penetration depth) is much larger than the Fermi wavelength. Hence one can specify the phase for the Cooper pair $\varphi_i = 2\mathbf{q}_s \cdot \mathbf{R}_i$, where \mathbf{q}_s is the average momentum per electron in the superfluid state. This ansatz leads to the Green function in the clean limit:

$$\hat{\mathcal{G}}^{(0)}(k;q_s;i\omega_n) = \begin{pmatrix} i\omega_n - \xi_{k+q_s} & -\Delta_k \\ -\Delta_k^* & i\omega_n + \xi_{k-q_s} \end{pmatrix}^{-1},$$
(8.24)

where $\Delta_k = \frac{\Delta_0}{2}(\cos k_x - \cos k_y)$ and the energy dispersion is still given by Eq. (7.19).

In the presence of a non-magnetic single-site impurity at site i = (0,0) in the 2D system, the Green function for the impurity system can be obtained, within the T-matrix approximation,

$$\hat{\mathcal{G}}(i,j;q_s;i\omega_n) = \hat{\mathcal{G}}^{(0)}(i,j;q_s;i\omega_n) + \hat{\mathcal{G}}^{(0)}(i,0;q_s;i\omega_n)
\times \hat{T}(q_s;i\omega_n)\hat{\mathcal{G}}^{(0)}(0,j;q_s;i\omega_n) , (8.25)$$

with the T-matrix given by

$$\hat{T}^{-1}(i\omega_n; \mathbf{q}_s) = \tau_3/U_0 - \hat{\mathcal{G}}^{(0)}(0, 0; q_s; i\omega_n) . \tag{8.26}$$

With a fixed \mathbf{q}_s , the local density of states (LDOS) at site i is given by:

$$N(i; q_s; \omega) = -(2/\pi) \text{Im} \mathcal{G}_{11}(i, i; q_s; \omega + i0^+)$$
. (8.27)

For the fluctuating phase, one needs to take average over \mathbf{q}_s . If the fluctuation is thermal, the statistical distribution is Gaussian, as governed by the Kosterlitz-Thouless (KT) theory (Kosterlitz and Thouless, 1973, 1974; Sheehy et al., 2001), that is $\rho(q_s) = e^{-q_s^2/2n_v}/\sum_{q_s} e^{-q_s^2/2n_v}$, where $n_v = \exp[-\sqrt{aT_c/(T-T_c)}]$ within the KT theory. In the continuum limit, $\sqrt{\langle q_s^2 \rangle} = \sqrt{n_v}$. The averaged LDOS is caculated as $N(i;\omega) = \langle N(i;q_s;\omega) \rangle$.

The results for various values of n_v are shown in Fig. 13. For small n_v , the resonance peak is very sharp and similar to that in the superconducting state $(n_v = 0)$. When n_v is increased, the peak is broadened with decreasing peak height. Finally, the spectrum at low energies becomes featureless.

Finally, in the phase fluctuation scenario of the PG state, the electron excitation spectrum around the impurity is very sensitive to how far the temperature is away from the superconducting transition temperature T_c . However, in the normal-state ordering scenario, the resonance states are not sensitive to the temperature up to the PG critical temperature. Another piece of difference of the electronic states around the impurity between two scenarios is the energy position of the resonance state in the phase fluctuation state is not sensitive to the doping while that in the state with a normal ordering shifts with the doping. More generally, if the superconducting fluctuations are present, then an additional satellite peak

should appear at the opposite bias due to the particle-hole nature of the Bogoliubov quasiparticles. The relative magnitude of the particle and the hole parts of the impurity spectrum can be used to determine the extent to which the PG is governed by the superconducting fluctuations. In the case of fully non-superconducting PG (e.g., the DDW state), there should be no observable counterpart state. Combined with other experimental proposals (Janko et al., 1999; Martin and Balatsky, 2000), the impurity state can help to better understand the mysterious PG state.

IX. QUANTUM PHASE TRANSITION IN S-WAVE SUPERCONDUCTOR WITH MAGNETIC IMPURITY

A. Introduction

In this Chapter we revisit the problem of a localized classical magnetic moment in a superconductor. A remarkable aspect of this interaction we will focus on here is the first-order zero temperature transition which takes place in an s-wave superconductor as a function of the magnetic moment, J_0S , where S is the local impurity spin and J_0 is the exchange coupling. In this transition, the spin quantum number s of the electronic ground state of the superconductor $|\Psi_0\rangle$ changes from zero for a subcritical moment $J_0 < J_{crit}$ to 1/2 for $J_0 > J_{crit}$. The total spin becomes $S \pm 1/2$ depending on the sign of the exchange interaction J_0 . The first to point out the phase transition was Sakurai(Sakurai, 1970) it corresponds to a level crossing between two ground states as a function of the exchange coupling J_0 . In a singlet superconductor level crossing occurs between states where the impurity spin is either unscreened or partially screened. The states have different spin quantum numbers and level crossings are generally allowed. These quantum phase transitions are of the first order and hence do not have divergent time or length scale associated with them.

We address the above problem at zero temperature by using the mean-field approximation within the T-matrix formulation and the self-consistent approach, which takes into account a local gap-function relaxation. Local Coulomb interaction U which breaks particle-hole symmetry and leads to an asymmetric spectral density for the impurity-induced quasiparticle states. Figure 14 illustrates the local effect of a magnetic moment on the low-energy spectral density in an s-wave superconductor. Since we limit our considerations to a classical spin, $S \gg 1$, the impurity moment cannot be screened completely by the quasiparticles. We show that the gross features of the impurity-induced quasiparticle states in s-and d-wave superconductors can be qualitatively understood within the non-self-consistent T-matrix formalism.

The transition is not unique to the classical spin. Similar effect is found in a Kondo model of a quantum spin, see Sec. X.

B. Quantum phase transition as a level crossing

The physical picture of the quantum transition follows from the behavior of the impurity-induced bound state. This transition is a consequence of the instability of the spin unpolarized ground state, because, for a large enough J_0 , the energy of the impurity-induced quasiparticle excitation would fall below the chemical potential.

As we have discussed it in the context of Yu-Shiba-Rusinov solution for a classical spin, see Sec. VI, impurity state has energy that is always below the gap threshold:

$$\Omega_0/\Delta_0 = \frac{1 - (\pi J_0 S N_0)^2}{1 + (\pi J_0 S N_0)^2} \tag{9.1}$$

and has particle (u_{-1}) and hole (v_{-1}) amplitudes at positive and negative energies. One can see the level crossing and change of the ground state already from this result. Ignoring the self-consistency, and using Eq. (9.1), we find that the singularity occurs at

$$J_0 = J_{crit} = 1/\pi N_0 S (9.2)$$

For a weak coupling $J_0 < J_{crit}$, the ground state of the superconductor is a paired state of time-reversed single-particle states in the presence of the impurity scattering, with ground state wave function being the BCS like:

$$|\Psi_0\rangle_{J_0 < J_{crit}} \sim \Pi_n[u_n + v_n \psi_n^{\dagger} \psi_{-n}^{\dagger}]|0\rangle = |\Psi_0\rangle \quad (9.3)$$

Here, since the translational symmetry is broken by impurity, and we consider the eigen-states of the scattering problem in the presence of impurity, states are labeled by a discrete index $n=1,...\infty$ corresponding to a discrete scattering states that are the basis of the Bogoliubov Hamiltonian with impurity. The n=1 state would correspond to an impurity bound state, localized on impurity site. Index -n correspond to a time reversal state, i.e. the localized state with opposite spin. The first excited state at $J_0 < J_{crit}$ would correspond to a single quasiparticle state where one excitation is present. The lowest excited state corresponds to a intragap Yu-Shiba-Rusinov state at energy Ω_0 , see Fig. 15.

The excited state can be written as:

$$\begin{split} |\Psi_{-1}\rangle_{J_0 < J_{crit}} &\sim \gamma_{-1}^{\dagger} |\Psi_0\rangle = |\Phi_{-1}\rangle \\ |\Phi_{-1}\rangle &= \psi_{-1}^{\dagger} \prod_{n>1} [u_n + v_n \psi_n^{\dagger} \psi_{-n}^{\dagger}] |0\rangle \end{split} \tag{9.4}$$

with standard quasiparticle definitions of $\gamma_1=u_1\psi_1-v_1\psi_{-1}^\dagger$, $\gamma_1^\dagger=u_1\psi_1^\dagger-v_1\psi_{-1}$, $\gamma_{-1}^\dagger=u_1\psi_{-1}^\dagger+v_1\psi_1$, etc, with $u_n^2+v_n^2=1$. For future use we introduce

$$|\widetilde{\Psi}_{0}\rangle = \prod_{n>1} [u_{n} + v_{n}\psi_{n}^{\dagger}\psi_{-n}^{\dagger}]|0\rangle$$
 (9.5)

Then $|\Phi_{-1}\rangle = \psi_{-1}^{\dagger} |\Psi_{0}\rangle$. The state $\gamma_{1}^{\dagger} |\Psi_{0}\rangle$ does not appear inside the superconducting gap and hence is not relevant for this discussion. Note that $|\Psi_{0}\rangle$ is a true vacuum

for all quasiparticles: e.g. $\gamma_{\pm 1} \prod_{n>0} [u_n + v_n \psi_n^{\dagger} \psi_{-n}^{\dagger}] \rangle = 0$. ⁶ This state is a true spin singlet $\langle \Psi_0 | \mathbf{S}_{electron} | \Psi_0 \rangle = 0$. To avoid confusion with impurity spin S we explicitly indicate that $\mathbf{S}_{electron}$ is the net spin of conduction electrons. Hence if $|\Psi_0\rangle_{J_0 < J_{crit}} = |\Psi_0\rangle$ is a ground state, the total spin of electrons is zero, and only the spin of impurity counts. The first excited state at energy Ω_0 has a spin 1/2 quasiparticle in it: $\langle \Phi_{-1} | S_{electron}^z | \Phi_{-1} \rangle = -1/2$.

Upon increasing coupling constant J_0 one reaches the regime where these two states cross, Fig. 16. At that point the excited and ground states changes the roles.

$$|\Psi_0\rangle_{J_0>J_{crit}} = |\Psi_{-1}\rangle = |\Phi_{-1}\rangle$$

$$|\Psi_{-1}\rangle_{J_0>J_{crit}} = |\Psi_0\rangle \tag{9.6}$$

Another way to see this quantum phase transition is to examine energy levels as a function of J_0/J_{crit} . For variational wavefunctions $|\Psi_{0,-1}\rangle$ we define the respective energies as expectation vales of the Hamiltonian:

$$E_{0,-1}(J_0/J_{crit}) = \langle \Psi_{0,-1} | H | \Psi_{0,-1} \rangle$$
 (9.7)

Energy of the first excitation, the impurity bound state is then simply

$$\Omega_0(J_0/J_{crit}) = E_{-1} - E_0, J_0 < J_{crit}
\Omega_0(J_0/J_{crit}) = E_0 - E_{-1}, J_0 > J_{crit}$$
(9.8)

There are several implications of this result. Firstly, the ground state of superconductor with a magnetic impurity in the strong coupling limit is a non-BCS state. The ground state is a pair condensate with a single unpaired quasiparticle. Similar result was observed for a Kondo screening in superconductor (Sakai et al., 1993). One can easily understand the result by going to a strong coupling limit $J_0 N_0 \gg 1$. In this case long before any supercondcuting correlation are established the single electron state bound to the impurity site will form. This is the strong coupling limit of a Kondo screening problem. In our case bound electron will partially screen the large impurity spin. In a case of a spin S=1/2 the screening will be complete and the net spin of the state will be singlet (Sakai et al., 1993). Therefore state would evolve to a superconducting state with one unpaired electron that is bound to impurity. Ground state in a strong coupling limit is a non-BCS state with only pairs present. Ultimately this state is formed by the energy balance between superconducting and magnetic energies. Single electron

⁶ Here the spin of the state n=1 is determined by the sign of exchange coupling J_0 . We will assume it to be antiferromagnetic. So the electronic spin of the state n=-1 in Eq. (9.4) is opposite to the local spin S assumed to be up without loss of generality. Case of ferromagnetic coupling is similar. Indeed classical spin solution Eq. (9.1) is symmetric between $J_0 \to -J_0$ as it contains only even powers of exchange.

state bound to a local spin provides a much stronger energy gain $\sim J_0$ compared to the gain due to pairing Δ_0 .

Crossing point and related quantities are shown in the Fig. 17. This crossing point corresponds to a true quantum phase transition.

Secondly, the crossing point occurs exactly at critical point in Eq. (9.1) only in a non-self-consistent treatment where single particle levels provide the only contribution to total energy. In practice the true phase transition occurs slightly earlier. The gap suppression and quasiparticle interaction also contribute to free energy and in self-consistent mean-field approximation, we find that order-parameter relaxation shifts J_{crit} downwards and the energy of the impurity-induced bound state does not reach zero when a first-order transition between the two ground states occurs. In practice the result are qualitatively similar and are typically within 10 percent of the numerical results obtained in a selfconsistent treatment (Salkola et al., 1997). In contrast, a d-wave superconductor has no quantum transition for any value of the magnetic moment when its quasiparticle spectrum in the normal state has particle-hole symmetry. The absence of the transition follows from the behavior of the impurity-induced quasiparticle states which are pinned at the chemical potential for an arbitrarily large magnetic moment, see Sec. VII. However, if particle-hole symmetry is broken or if the pairing state acquires a small s-wave component, the transition is again possible for a large enough moment. The impurity moment induces two virtual-bound states which have four-fold symmetry and extend along the nodal directions of the energy gap.

C. Particle and hole component of impurity bound state

In this section we show that the excited states inside the gap in superconducting state appear in pairs at positive and negative energies. This is a direct consequence of the fact that natural excitations are Bogoliubov excitations. Particle and hole coefficients of the excited state $|\Psi_{-1}\rangle_{J_0 < J_{crit}}$ are given by the u and v components of the quasiparticle operators γ_n , see Sec. II. To be specific we confine subsequent discussion to s-wave case, however the results are applicable to any superconducting state.

Consider two independent processes: a) electron at energy Ω_0 and spin down, n=-1 and b) hole with spin up, n=1 injected in superconductor with the same energy Ω_0 . Hole creation means electron with spin up is extracted from superconductor. This can be achieved by reversing the bias of the STM tip for example and it would correspond to the negative energy axis. Variational wave functions that would describe these processes are

$$\psi_{-1}^{\dagger} |\Psi_{0}\rangle_{J_{0} < Jcrit} = -u_{1} |\Phi_{-1}\rangle$$

$$\psi_{1} |\Psi_{0}\rangle = v_{1} |\Phi_{-1}\rangle$$
 (9.9)

Here, to be specific we consider the case of $J_0 < J_{crit}$. This illustrates the point that in BCS like ground state

the particle excitation with energy Ω_0 and hole excitation with negative energy $-\Omega_0$, aside from irrelevant normalization factors, is the same excited state, namely $|\Phi_{-1}\rangle$. Therefore the poles in the density of states are always coming in pairs at positive and negative energies. The true quasiparticles in superconducting state are Bogoliubov excitations γ_n that have a finite component of particle and hole with amplitudes u_n and v_n . The strength of the electron absorption and emission process is controlled by these coherence factors. This is generally true for BCS superconductor even without impurities. For the case at hand, impurity states are well distinguished from the continuum. The two poles at $\pm\Omega_0$ are part of the same physical excitation. We can write impurity state local spectral function $A_1(\mathbf{r},\omega) = -\text{Im}G_{11}(\mathbf{r},\omega)/\pi$ as

$$A_1(\omega) = Z^+ \delta(\omega - \Omega_0) + Z^- \delta(\omega + \Omega_0) \tag{9.10}$$

and the relative strength is $Z^+ \sim u_{-1}^2$ and $Z^- \sim v_{-1}^2$, so that the net strength of the poles $Z^+ + Z^- >= 1$ as it should for a physical excitation. For more details and references reader is referred to (Salkola *et al.*, 1997).

Analysis for $J_0 > J_{crit}$ is more involved. The ground state wave function is now $|\Phi_{-1}\rangle$. Injection of the electron with spin opposite to the spin of the bound state and extraction of electron with spin down will produce respectively

$$\psi_1^\dagger |\Phi_{-1}\rangle = \psi_1^\dagger \psi_{-1}^\dagger |\widetilde{\Psi_0}\rangle \; , \; \; \psi_{-1} |\Phi_{-1}\rangle = |\widetilde{\Psi_0}\rangle \qquad (9.11)$$

with complementary annihilated states $\psi_1^{\dagger}|\Phi_{-1}\rangle=0$ and $\psi_{-1}^{\dagger}|\Phi_{-1}\rangle=0$. Although the two states written in Eq. (9.11) are different, the only difference is that the number of Cooper pairs in these two states differ by one. For a macroscopically large system with number of Cooper pairs $N\gg 1$ this produces negligible difference in the energies and matrix elements. Therefore, again, the injection of electron with spin up (in our convention) and extraction of electron of spin down physically will produce the same state. This state will have a particle and hole projection just as we discussed in case of $J_0 < J_{crit}$.

Similar quantum phase transition occurs in a d-wave superconductor even for a nonmagnetic impurity. In the case of particle-hole symmetric band the unitary scattering produces a zero energy state, see Sec. VII, Eq. (7.1). However for the particle hole asymmetric band impurity state will reach zero energy and eventually will change the sign as a function of impurity strength. This transition occurs at $U_0 > U_{crit} \sim \mu$, μ being the chemical potential that leads to a particle-hole nonsymmetric band. It is known that single quasiparticle bound state will form at $U_0 > U_{crit}$ and the ground state wavefunction will have unpaired single quasiparticle, apart from the BCS pairs, see (Salkola et al., 1996, 1997).

D. Intrinsic π phase shift for $J_0 > J_{crit}$ coupling

Here we would like to point a little noticed by important fact about the impurity induced modifications of the order parameter at the impurity site, namely a π phase shift of the order parameter near impurity.

¿From the above Fig. 17, it follows that at $J_0 > J_{crit}$ the self-consistent solution indicates that the phase of the order parameter on the impurity site is shifted by π with respect to the phase in the bulk, see Fig. 18.

Spatial extent of the π shifted region in numerical calculation was found to be few atomic sites. Such a sharp change in the phase of the order parameter would cost a superconducting condensate energy and would not be preferential under normal circumstances. In the case at hand however, condensate energy is secondary to the magnetic exchange at strong coupling limit near impurity site. Physics is driven by magnetic interactions in a strong coupling limit. Even thought eh phase difference is π the phase shift does not lead to any time reversal violating observable effects. One can see that for the phase difference π there are no superconducting currents near the impurity: $I = I_c \sin \phi = 0$. These results were obtained in the self-consistent treatment within a negative U model that allows for the on-site pairing (Salkola et al., 1997).

We are not aware of a simple explanation of this effect. It appears to be general and not related to a particular model. It is connected to the π junctions discussed in the context of tunneling barrier. The π phase shift is preferential in the junction in the presence of magnetic impurity or ferromagnetic layer. This subject is covered extensively, see e.g. recent review and other papers (Bulaevskii et al., 1977; Buzdin et al., 1982; Buzdin, 2004; Glazman and Matveev, 1989; Spivak and Kivelson, 1991).

X. KONDO IMPURITY

In all of previous discussions, we have concentrated on static impurities. The next two Sections are devoted to the examples when impurity atoms have their own internal degrees of freedom, the dynamics of which is coupled to the scattering of conduction electrons. This dynamical behavior often leads to qualitatively new results. Quantum dynamics is particularly important for study of magnetic impurities as the earliest and the best known example of non-trivial consequences of this dynamics is the Kondo effect (Kondo, 1964).

Dilute magnetic impurities doped into an otherwise nonmagnetic metallic host have dramatic effects on the low temperature resistivity, susceptibility, and specific heat. These anomalies are associated with screening of the impurity spin by conduction electrons. For $S=\frac{1}{2}$ a global singlet is formed by coupling an electron state to the impurity site; dynamics of spin flips is crucial for the formation of the singlet. For a single magnetic

impurity in the metallic host, this is manifested as a crossover from the Curie susceptibility at high temperatures, $\chi = C/T$ with $C = 4\mu_B^2 S(S+1)/3k_B$, where S the magnitude of the spin and μ the Bohr magneton, to singlet behavior below a characteristic Kondo temperature $T_K \simeq W \exp(-1/2JN_0)$, where W is the electron half band width and J is the exchange constant. Two important notes are that a) Kondo screening occurs only for antiferromagnetic exchange constant J > 0; and b) the process is non-perturbative, as is clear from the non-analytic dependence of the Kondo temperature on the exchange constant. Understanding of the single impurity Kondo proble in a metal required concerted use of the renormalization group (Anderson, 1970; Anderson et al., 1970), numerical renormalization group (NRG) (Wilson, 1975), exact solutions via the Bethe ansatz (Andrei, 1980; Wiegmann, 1980), and large-N expansions (Coleman, 1984, 1985; Read, 1985; Read and Newns, 1983a,b). Many important results are summarized in recent reviews (Cox and Zawadowski, 1998; Hewson, 1993).

Kondo effect depends on the existence of the host electronic excitations at the Fermi energy. In metals, the density of states is constant, which simplifies the analysis. If the density of states varies in the immediate vicinity of the Fermi surface, the effect is realized rather differently (or not at all). Kondo effect in an insulator, with a hard band gap, was investigated in Ogura and Saso, 1993. In superconductors, however, the gap in the single particle spectrum only arises below the transition temperature for the Cooper instability driven by the finite DOS. Consequently, the two effects compete.

Studies of magnetic impurities in superconductors began, and largely continued, with the investigations of the properties of classical spin, $S \to \infty$, for which no reduction in magnitude due to Kondo screening is possible (Rusinov, 1968; Shiba, 1968; Yu, 1965). The question of which conclusion of their analysis are robust for small spin values and in gapless superconductors remains of intense current interest.

A. Kondo effect in fully gapped superconductors

In Shiba-Rusinov analysis the sign of the exchange interaction between the conduction electrons and localized impurity spins is irrelevant. As discussed above in real metals antiferromagnetic exchange leads to a complete screening of the impurity below Kondo temperature T_K , while ferromagnetic exchange does not produce resonance states. Consequently, treatment of quantum impurity spins has to bring out the differences between two signs of J.

For J > 0 opening of the superconducting gap competes with Kondo screening as both instabilities are driven by a finite DOS at zero energy. Qualitatively, it is clear that if $T_K \gg T_c$, the impurity is completely screened by the time of the onset of superconductivity.

In contrast, for $T_K \ll T_c$ Kondo screening is suppressed by a decreased density of states upon opening of the superconducting gap.

Kondo screening can be viewed as growth and divergence of the *effective* exchange coupling as we look at the properties of the system at lower and lower energies. This is the essence of the the NRG method, and the underlying principle of successful analytical work. Therefore the effective exchange constant, and, with it, the phase shift of scattering on the impurity depends on the energy of the incoming electron. Consequently, the effect of scattering varies with temperature.

We immediately conjecture that, while a localized Shiba-like state exists in the gap of a superconductor, its energy in the Kondo limit changes upon lowering the temperature. Therefore the "final", T=0, position of the impurity resonance is a complex function of T_c and T_K . Moreover, as results of the previous section imply, the nature of the ground state, i.e. its spin and degeneracy, depend on the relation between T_c and T_K . As a result, there has been increased interest in determining the properties of the ground state, and the localized excited (Shiba-Rusinov) state of a BCS superconductor with a quantum impurity spin.

1. Ferromagnetic exchange

Early analytical attempts were carried out (Müller-Hartmann, 1973; Zittartz and Müller-Hartmann, 1970) in the framework of Nagaoka decoupling scheme (Hamann, 1967; Nagaoka, 1965, 1967). For J < 0 the bound state splits off the band edge and was found to move towards an asymptotic value

$$\epsilon \equiv \frac{E_0}{\Delta} = \left[1 + g^2 \pi^2 S(S+1) \right]^{-1/2},$$
(10.1)

where $g=\lambda N_0$, and λ is the superconducting coupling in the BCS weak coupling theory. Since $g\ll 1$ the bound state remains close to the gap edge for all values of J<0. This qualitative result was later confirmed by NRG calculations (Sakai *et al.*, 1993; Satori *et al.*, 1992), which showed that the binding energy is well approximated by $\epsilon\approx 1-\pi^2J_{eff}^2/8$, where the renormalized exchange constant

$$J_{eff} = \frac{2|J|/W}{1 + (2|J|W)\ln(W/\Delta)}.$$
 (10.2)

Therefore the ferromagnetic case corresponds to weak coupling and small phase shift of scattering at low temperatures.

The ground state of this system was argued to be a doublet (Sakai et al., 1993; Satori et al., 1992; Soda et al., 1967), since the ferromagnetic interaction renormalizes to weak coupling and the impurity spin remains essentially free. Recently it was suggested that,

since superconducting interaction is relevant in this system, and therefore above a critical coupling, J_C that depends on Δ (J_C is larger for smaller Δ), the ground state of the coupled superconductor-impurity system is a triplet ($m_z=0,\pm 1$) (Yoshioka and Ohashi, 1998). This suggestion is worth exploring further.

2. Antiferromagnetic coupling

If the coupling is antiferromagnetic, in a normal metal Kondo screening corresponds to $J \to \infty$ and to phase shift of scattering, $\delta \to \pi/2$. The Hartree-Fock analysis (Shiba, 1973) is insufficient to fully describe this effect.

The limit $T_K \ll \Delta$ was considered following the work of Shiba (Müller-Hartmann, 1973; Soda et al., 1967; Zittartz and Müller-Hartmann, 1970), and the position of the localized excited state was found with various degrees of accuracy. Notice that in this regime the localized state lies close to the gap edge as it does for ferromagnetic coupling. In the opposite limit, $T_K \gg \Delta$ approximate solution for the position and the residue of the bound state was obtained in Refs. (Müller-Hartmann, 1973; Zittartz and Müller-Hartmann, 1970), however, the results were inexact due to the nature of their approximation. Later, within the local Fermi liquid appraoch, the energy of the bound state in this limit was found to be (Matsuura, 1977)

$$\epsilon = \frac{1 - \alpha^2}{1 + \alpha^2},\tag{10.3}$$

where

$$\alpha \approx \frac{\pi \Delta}{4T_K} \ln \frac{4eT_K}{\pi \Delta}.$$
 (10.4)

This result clearly shows that the phase shift of scattering depends on the ratio T_c/T_K .

The properties of the bound state, including its position and spectral weight, for arbitrary values of T_K/T_c were obtained with the help of NRG (Sakai et al., 1993; Satori et al., 1992). They found level crossing similar to the quantum phase transition of the previous section at $T_K/\Delta \sim 0.3$. For $T_K/\Delta > 0.3$ the impurity moment is largely quenched by the time the depletion of states caused by superconductivity affects screening. In that case the ground state is a Kondo-screened singlet, while the excited intra-gap state is a doublet with the spectral weight $\alpha \approx 2$ for $T_K\Delta \gg 1$, corresponding to a single-particle state. Here α is defined from

$$-\frac{1}{\pi} \operatorname{Im} G(\omega + i\delta) / \pi = \frac{\alpha}{2} \left[\delta(\omega - E_0) + \delta(\omega + E_0) \right]. (10.5)$$

On the other hand, for $T_K \Delta < 0.3$ the Kondo effect is suppressed by the opening of the superconducting gap, the ground state is a doublet corresponding to a free spin state, while the bound excited state is a Kondo singlet. The spectral weight, $\alpha \approx 0.5$ for $T_K \ll \Delta$, and changes discontinuously at the phase transition point.

Level crossing means that the bound state is at zero energy for $T_K/\Delta \approx 0.3$, while it is close to the gap edge for both $T_K \gg \Delta$ and $T_K \ll \Delta$. Numerical results show that the energy of the bound state is not symmetric with respect to the crossing point: $E_0/\Delta < 0.5$ for $0.03 \lesssim T_K/\Delta \lesssim 1$ (Satori *et al.*, 1992).

3. Anisotropic exchange and orbital effects

Several more complicated aspects of Kondo screening in superconductors attracted attention in recent years, and we review them briefly, referring the reader to the original papers for further information. Anisotropic exchange interaction, $J_z \neq J_{\pm}$, allows the investigation of the crossover between the Ising regime, $J_{\pm} = 0$, when the spin-flip is disallowed and there is no Kondo screening, and the isotropic exchange considered so far. The main features of the phase diagram are discussed by Yoshioka and Ohashi, 1998, and new phases occur on the ferromagnetic side. In particular, these authors find an extended regime of Ising-dominated ground state even for $J_{\pm} \neq 0$. In addition, they find small regions of the phase diagram around isotropic ferromagnetic and Ising antiferromagnetic lines, where there exist two localized intra-gap states. They also obtain a perturbative analytic expression for the shift of the bound state energy due to anisotropy of the interaction.

Using the numerical RG approach to analyse Anderson's model allows to interpolate between asymmetric magnetic scattering, Kondo problem, and non-magnetic scattering, including resonance U=0 limit (Yoshioka and Ohashi, 2000). In particular, the crossover from magnetically induced bound state to the resonance non-magnetic scattering regime(Machida and Shibata, 1972) was studied.

Finally, so far we only discussed purely s-wave superconductors. Fully gapped systems include also materials with a complex order parameter combining two (or more) out of phase unconventional gaps, such as $d_{x^2-y^2} + id_{xy}$, or $p_x + ip_y$. In both of these cases Cooper pairs have orbital degrees of freedom that also couple to the impurity spins, leading to multichannel Kondo effect. In addition, for p-wave pairing, the total spin of Cooper pairs is s=1, so that non-trivial changes in screening occur depending on whether the impurity spin S=1/2 or S=1. The NRG analysis of the Kondo problem in this system was carried out very recently (Koga and Matsumoto, 2002a; Matsumoto and Koga, 2002). They found that the two order parameters are indistinguishable when only l=0impurity scattering partial wave is taken into account, i.e. only the depletion of the density of states due to the gap, rather the spin structure of the Cooper pair dictated the Kondo screening. In that case the moment of the ground state is determined by the orbital structure of the Cooper pair. However, inclusion of higher harmonics with $l \neq 0$ for scattering (extended impurity potential), leads to some novel dependencies of the screening and

ground states on the exchange couplings.

B. Kondo effect in gapless superconductors

Gapless systems like d-wave superconductors with the low-energy quasiparticle density of states following the power law, $N(E) \propto |E|^r$ with the exponent r > 0, constitute a marginal situation. The Kondo effect in these systems where the host single particle density of states follows a power law, has been studied (Borkowski and Hirschfeld, 1992, 1994; intensively Bulla et al., 2000. 1997; Cassanello and Fradkin, 1996, 1997; Chen and Jayaprakash, 1995; Gonzalez-Buxton and Ingersent, 1998: Han et al., 2002, 2004; Ingersent, 1996; Ingersent and Si, 1998; Itoh, 1993; Logan and Glossop, 2000; Polkovnikov, 2002; Polkovnikov et al., 2001; Vojta, 2001; Vojta and Bulla, Withoff and Fradkin, 1990: 2001: Zhang et al., 2001; Zhu and Ting, 2001a,b). Fradkin and co-workers (Cassanello and Fradkin. 1996. Withoff and Fradkin, 1990) first employed a combination of the poor man's scaling argument and the large-N approach to the case of spin- $\frac{1}{2}$ (impurity degeneracy N = 2) for $0 < r \le 1$, an showed that a Kondo effect takes place only when the electron-impurity exchange J exceeds a critical value. Otherwise the impurity decouples from the band. However, the study based on a nonperturbative renormalization group approach (Chen and Jayaprakash, 1995; Ingersent, 1996) to a spin- $\frac{1}{2}$ identified particle-asymmetry as a key factor in determining the low-temperature physics. At small asymmetry, the critical coupling J_c above which the impurity moment is screened becomes so large for all $r > \frac{1}{2}$ that the Kondo effect is suppressed. Away from the particle-hole symmetry, any quenching of the impurity moment is accompanied by a low-temperature decrease in the impurity resistivity, rather than the increase found in metals. The discrepancy between the two categories of work may stem from the mean-field nature of the large-N method, or from the symmetry breaking that is implicit, for all N > 2, in the restriction that the impurity level be singly occupied. In real systems, the power-law variation of $N(\epsilon)$ is restricted to an energy range $|\epsilon| \leq \Delta_0$, with $N(\epsilon) \approx N(\Delta)$ for $\Delta_0 < |\epsilon| \le W$. The NRG approach gave results entirely consistent with those known for gapped systems (The gap $2\Delta_0$ is for $r=\infty$ limit). At the particle-hole

⁷ There have also been discussion about local moment formation in high-temperature cuprates (Khaluillin et al., 1997; Kilian et al., 1999; Nagaosa and Lee, 1997; Simon and Varma, 1999). Discussion on Kondo problem in s-wave superconductors, in unconventional superconductors with time-reversal-symmetry-broken pairing state and in insulators can be found in the literatures (Koga and Matsumoto, 2002b; Matsumoto and Koga, 2001; Ogura and Saso, 1993; Sakai et al., 1993; Satori et al., 1992; Yoshioka and Ohashi, 1998, 2000).

symmetric case, an impurity in an insulator retains its moment, no matter how large J is; away from this symmetry, the spin is screened provided that $J > J_c \approx 2W/\ln(W/\Delta_0)$ (Takegahara *et al.*, 1992).

Notice that considering the Kondo effect in a system with the power law dependence of the DOS is not the same as analysing the competition between superconducting and Kondo correlations. Within the Kondo exchange model, the Hamiltonian of the single magnetic impurity in a medium other than a superconductor, can be written as:

$$H = \sum_{\sigma} \int_{-\infty}^{\infty} d\epsilon N(\epsilon) \epsilon c_{\epsilon\sigma}^{\dagger} c_{\epsilon\sigma} + \frac{1}{N_L} \sum_{k,k'} [(U_0 + \frac{J}{2}) c_{k\uparrow}^{\dagger} c_{k'\uparrow} + (U_0 - \frac{J}{2}) c_{k\downarrow}^{\dagger} c_{k'\downarrow}] + \frac{J}{2} \sum_{k,k'} [c_{k\uparrow}^{\dagger} c_{k'\downarrow} S_{-} + c_{k\downarrow}^{\dagger} c_{k'\uparrow} S_{+}],$$

$$(10.6)$$

where $N(\epsilon)$ is the electron density of states, N_L is the lattice size, and all operators are for electrons. In contrast, for a superconductor, we need to rewrite the interaction via the Bogoliubov quasiparticles, and enforce the self-consistency condition on the gap. The resulting hamiltonian is rather lengthy, and follows straightforwardly from symmetric Anderson or Kondo hamiltonian, so that we do not give it here. We note that the formation and screening of the local moments in d-wave superconductors has been investigated using the variational wave function approach (Simon and Varma, 1999).

The interest in the Kondo impurities in the hightemperature cuprates is motivated by the recent STM and NMR experiments around single impurities. Unlike most dopants, Zn, Ni are believed to substitute for Cu on the cooper-oxide plane and causes effective changes to the local electronic structure without much change of hole concentration. Simple valence counting suggests that if the Zn and Ni impurities maintain a nominal Cu²⁺ charge, the Zn²⁺ would have a $(3d)^{10}$, S=0 configuration and acts as a nonmagnetic impurity while the Ni²⁺ would have a $(3d)^8$, S=1configuration and acts a magnetic impurity. Although it is natural that the spin-1 impurities carry an onsite magnetic moment (Mendels et al., 1999) expected to give rise to the Kondo physics, the behavior associated with the nonmagnetic impurities is completely unexpected. Nuclear magnetic resonance (NMR) experiments performed with nonmagnetic spin-0 (Zn,Li,Al) in doped cuprates (Alloul et al., 1991; Ishida et al., 1993, 1996; Mahajan et al., 1994, 2000; Mendels et al., 1999) showed clearly that each impurity, itself carrying no magnetic moment, induces a local $S = \frac{1}{2}$ moment sitting on the nearest-neighbor Cu orbitals. It was also demonstrated that the magnetic properties associated with the substitution of these impurities strongly depends on the hole doping: In the underdoped regime, the moments retain their Curie law below the superconducting transition temperature T_c while near the optimal doping, the Kondo screening might persist even to $T \to 0$ though strongly reduced. From the NMR, it is known that the induced moment is distributed around the impurity. We would like to emphasize that this moment is merely a particular bound state of conduction electrons near the impurity and the precise form of the interaction between the induced moment with other conduction electrons is a priori unknown. At this stage, we are unable to make a definitive conclusion about its importance for our understanding of high-temperature cuprates. However, in a broader sense, the magnetic impurity embedded in superconductors is a very-well defined theoretical issue. Generally, the system Hamiltonian with a magnetic impurity consists of a d-wave BCS state \mathcal{H}_{BCS} , a potential scattering term \mathcal{H}_{pot} , and a magnetic term \mathcal{H}_{mag} . The magnetic term can described by the Anderson impurity model or Kondo spin exchange model, and the impurity spin can be either coupled to a single site or be spatially distributed. For the Anderson model with the single-site coupling, the magnetic term is given by:

$$\mathcal{H}_{mag} = \sum_{k\sigma} [V_{kd} c_{k\sigma}^{\dagger} d_{\sigma} + H.c.] + \epsilon_d \sum_{\sigma} d_{\sigma}^{\dagger} d_{\sigma} + U_d n_{d\uparrow} n_{d\downarrow} .$$
(10.7)

In the strong U_d limit, the Anderson model can be mapped onto a Kondo s-d exchange model through the Schrieffer-Wolff transformation:

$$\mathcal{H}_{mag} = J\mathbf{s}_0 \cdot \mathbf{S} , \qquad (10.8)$$

where $\mathbf{s}_0 = \frac{1}{2} \sum_{\sigma\sigma'} c_{0\sigma}^{\dagger} \boldsymbol{\sigma}_{\sigma\sigma'} c_{0\sigma'}$ is the spin operator for the conduction electron at the impurity site. The corresponding models for the multi-site coupling case are given by:

$$\mathcal{H}_{mag} = \sum_{I\sigma} [V_{Id}c_{I\sigma}^{\dagger}d_{\sigma} + H.c.] + \epsilon_d \sum_{\sigma} d_{\sigma}^{\dagger}d_{\sigma} + U_d n_{d\uparrow} n_{d\downarrow} ,$$
(10.9)

and

$$\mathcal{H}_{mag} = \sum_{I} J_{I} \mathbf{s}_{I} \cdot \mathbf{S} , \qquad (10.10)$$

respectively. We point out that in the large U_d limit, the Schrieffer-Wolff transformation will map the model as described by Eq. (10.9) onto to a Hamiltonian nonequivalent to the Kondo model described by Eq. (10.10). Therefore, Eq. (10.10) comes from different origin.

The Anderson impurity model for a single-site coupling in d-wave superconductors, Eq. (10.7), was studied by Zhang, Hu, and Yu (Zhang et al., 2001). A sharp localized resonance above the Fermi energy, showing a marginal Fermi liquid behavior, was predicted for the impurity states. The same logarithmic dependence of self-energy and a linear frequency dependence of the relaxation rate were also obtained, indicating a new universality class for the strong coupling fixed point. Almost at the same period of time, the multi-site coupling Anderson impurity model, Eq. (10.9) was considered by Zhu and Ting (Zhu and Ting, 2001b,c) while

the multi-site coupling Kondo impurity was studied by Polkovnikov, Sachdev, and Vojta (Polkovnikov, 2002; Polkovnikov et al., 2001). All these works show the existence of Kondo resonance. However, the low energy structure of spectral weight of the conduction electrons depends delicately on the local environment surrounding the dynamic impurity. The on-site potential scattering was taken to be either zero (Zhang et al., 2001) or very weak (Polkovnikov, 2002; Polkovnikov et al., 2001) so that the resonance peak is located very close to the Fermi energy. Zhu and Ting (Zhu and Ting, 2001b) took into account the quasiparticle scattering from a geometrical hole, where electrons are allowed to hop onto the four neighbors of the impurity site, and obtained a double-peak structure around the Fermi energy. They further (Zhu and Ting, 2001c) considered the potential scattering term to be in the unitary limit $(U \to \infty)$, and found that the Kondo resonance effect is weaved into that from the strong potential scattering to determine the low energy quasiparticle states. The delicate influence of the potential scattering on the Kondo physics as well as the local electronic structure in d-wave superconductors has been re-emphasized by Vojta and Bulla (Vojta and Bulla, 2001).

To be concrete, we present a discussion based on the multi-site coupling Kondo impurity model, as given by Eq. (10.10). As demonstrated in previous sections, the problem of a single-site potential scattering can be exactly solved. In the Nambu space, the Green's function is given by

$$\mathcal{G}(i,j;i\omega_n) = \mathcal{G}^0(i,j;i\omega_n) + \mathcal{G}^0(i,0;i\omega_n)T(i\omega_n)\mathcal{G}^0(0,j;i\omega_n)$$
(10.11)

where the T-matrix due to the potential scatterer is

$$T^{-1}(i\omega_n) = \tau_3/U - \mathcal{G}^0(0,0;i\omega_n) , \qquad (10.12)$$

and \mathcal{G}^0 is the Green's function for the system in the absence of impurities and has been given in early discussions. In the presence of both a potential scattering and a Kondo impurity, the system Green's function is found to be:

$$\tilde{\mathcal{G}}(i,j;i\omega_n) = \mathcal{G}(i,j;i\omega_n) + \sum_{l,l'} \varphi_l \varphi_{l'} \mathcal{G}(i,l;i\omega_n) \mathcal{T}_K(i\omega_n) \times \mathcal{G}(l',j;i\omega_n) .$$
(10.13)

Here l and l' label the sites neighboring to the impurity site at (0,0), and \mathcal{T}_K is the T-matrix for the Kondo impurity. The variables φ_l have different meaning depending on the approach to the \mathcal{T}_K . In the large-N approximation (equivalent to the slave-boson mean-field approximation), where

$$\mathcal{T}_K^{-1} = i\omega_n - \lambda \tau_3 - \sum_{l,l'} \varphi_l \varphi_{l'} \tau_3 \mathcal{G}(l,l';i\omega_n) \tau_3 , \quad (10.14)$$

where φ_l are the complex Hubbard-Straonovich fields, and are determined, together with the Lagrange multiplier λ , by the saddle point solution. However, in

the numerical renormalization group technique, when the strongest d-wave-like channel is considered, the variables are taken to be $\varphi_l = +(-)1$ depending on the bond orientation. Note that this d-wave-like pattern is merely a band structure effect and has nothing to do with the d-wave symmetry of the superconducting order parameter of the host. The LDOS in the presence of both types of impurities is obtained as:

$$\rho_i(\omega) = -\frac{1}{\pi} \text{Im} \{ \text{Tr} \left[\tilde{\mathcal{G}}(i, i; \omega + i0^+) \frac{1 + \tau_3}{2} \right] \}.$$
(10.15)

Figures 19 through 21 show the LDOS for a foursite Kondo impurity different various strength of the potential scattering, calculated using the NRG technique (Vojta and Bulla, 2001), which removes some artifacts of the slave-boson method. It is shown clearly that the Kondo effect is very sensitive to the strength of the potential scattering. In the absence of the potential scattering, sharp resonance peak show up directly on the impurity site, and on its next-nearest neighbors with reduced intensity, which is consistent with the experimental observation (Pan et al., 2000b). For a moderate value of the potential scattering, as shown in Fig. 20, the global particle-hole asymmetry changes its sign and the Kondo peak appears at the opposite side of the Fermi level compared to Fig. 19. For a strong potential scattering, the resonance peak directly from the impurity scattering becomes dominant, and the Kondo effect is weaved into the overall structure of the LDOS. In this case, the intensity of the peak is strongly suppressed by the on-site potential scattering and a double-peak structure with enhanced intensity is seen in the LDOS at the sites nearestneighboring to the impurity site. This result was also obtained by Zhu and Ting (Zhu and Ting, 2001b) based on the Anderson impurity model. It is expected that, in the unitary limit of the potential scattering, the LDOS has a zero intensity at the impurity site and a sharp single peak at its nearest neighbors. Consequently, the spatial shape of the resulting pattern is more compatible with the experiment after the filter effect (Martin et al., 2002; Zhu et al., 2000c), as seen in Sec. XIII, is taken into account. It is also shown in this simple model that the large LDOS from the resonance state induced by the strong potential scatterer reduces dramatically the critical Kondo coupling, indicating the determination of the Kondo effect by the local rather than global environment in which the magnetic impurity is embedded.

XI. DYNAMICAL IMPURITIES

A. Inelastic scattering from a single spin in d-wave superconductors

We will address the inelastic tunneling features due to the scattering off a local spin impurity. Assume that we have localized magnetic atom with spin S on a surface of a d-wave superconductor. We will treat the problem following (Balatsky *et al.*, 2003; Morr and Nyberg, 2003). Electrons in a superconductor interact with the localized spin via point-like exchange interaction at one site $J\mathbf{S} \cdot \boldsymbol{\sigma}$:

$$H = \sum_{\mathbf{k}} \xi(\mathbf{k}) c_{\mathbf{k}\sigma}^{\dagger} c_{\mathbf{k}\sigma} + \sum_{\mathbf{k}} [\Delta(\mathbf{k}) c_{\mathbf{k}\uparrow}^{\dagger} c_{-\mathbf{k}\downarrow}^{\dagger} + h.c.]$$

$$+ \sum_{\mathbf{k}, \mathbf{k}', \sigma, \sigma'} J \mathbf{S} \cdot c_{\mathbf{k}\sigma}^{\dagger} \boldsymbol{\sigma}_{\sigma\sigma'} c_{\mathbf{k}'\sigma'} + g\mu_{B} \mathbf{S} \cdot \mathbf{B} , (11.1)$$

where $c_{\mathbf{k}\sigma}$ is annihilation operator for the conduction electron of spin σ , $\xi(\mathbf{k})$ is the energy of the electrons, $\Delta(\mathbf{k}) = \frac{\Delta}{2}(\cos k_x - \cos k_y)$ is the d-wave superconducting gap of magnitude $\Delta \simeq 30 meV$ in typical high-T_c materials. The local spin S is a |S| = 1/2. We focus here on the effect of the Zeeman splitting of the otherwise degenerate local spin state in the external magnetic field B with splitting energy $\omega_0 \equiv \omega_L = g\mu_B B$. Below we use a mean field description of superconducting state at low temperatures $T \ll T_c$. Assuming field $B \ll H_{c2}$ we will ignore the orbital and Zeeman effect of the field on the conduction electrons ⁸.

We are interested in a local effect of inelastic scattering of electrons. Thus only local properties will determine the conduction electron self-energy. Results we obtain will also hold for a normal state with linearly vanishing DOS, such as a pseudogap state of high-Tc superconductors. In the case of a normal state one would model normal pseudogap state with a single particle Hamiltonian $H_0 = \sum_{\mathbf{k}} \epsilon(\mathbf{k}) c_{\mathbf{k}\sigma}^{\dagger} c_{\mathbf{k}\sigma}$ with $N(\omega) \sim \omega$.

Because of the vanishing DOS in a d-wave superconducting state Kondo singlet formation for occurs only a coupling constant exceed-(Cassanello and Fradkin, ing some critical value Gonzalez-Buxton and Ingersent, 1996; 1998; Withoff and Fradkin, 1990). For a particle-hole symmetric spectrum Kondo singlet is not formed for arbitrarily large values of J. Another situation where Kondo effect is irrelevant is the case of ferromagnetic coupling J. This allows us, quite generally, to consider a single spin in a d-wave superconductor that is not screened and we ignore the Kondo effect.

In the presence of magnetic field $\mathbf{B}||\hat{\mathbf{z}}$ spin degeneracy is lifted and components of the spin $\mathbf{S}||\hat{\mathbf{z}}$ and $\mathbf{S} \perp \mathbf{B}$ will have different propagators. It is obvious that only transverse components of the spin will contain information about level splitting at $\omega_0 = \omega_L$. We have therefore focused on S^+, S^- components only. The propagator in imaginary time τ is $\chi(\tau) = \langle T_{\tau}S^+(\tau)S^-(0)\rangle$ with Fourier transform and continuing to real frequency $\chi_0(\omega) = \frac{\langle S^z \rangle}{\omega_0^2 - (\omega + i\delta)^2}$. For free spin we have $\langle S_z \rangle = \tanh(\omega_0/2T)/2$. For more general case of magnetic anisotropy this does not have to be the case. To be general we will keep $\langle S_z \rangle$.

We begin with evaluation of the DOS correction due to coupling to localized spin. Self-energy correction is:

$$\Sigma(\omega_l) = J^2 T \sum_{\mathbf{k} \Omega_n} G(\mathbf{k}, \omega_l - \Omega_n) \chi^{+-}(\Omega_n) , \qquad (11.2)$$

where $G^0(\mathbf{k},\omega_l)=[i\omega_l-\xi(\mathbf{k})][(i\omega_l)^2-\xi^2(\mathbf{k})-\Delta^2(\mathbf{k})]^{-1}$ is the particle Green's function in d-wave superconductor, $G^{-1}=G^{(0)-1}-\Sigma$, $F^0(\mathbf{k},\omega_l)=[\Delta(\mathbf{k})][(i\omega_l)^2-\xi^2(\mathbf{k})-\Delta^2(\mathbf{k})]^{-1}$; $\Omega_l=2\pi l T$ is the bosonic Matsubara frequency and $\omega_l=(2l+1)\pi T; l=0,1,2...$ is the fermionic frequency. Using spectral representation and analytical continuation onto real axis $i\omega_n\to\omega+i\delta$ we find for imaginary part of self energy $\Sigma(\omega)$:

$$\operatorname{Im}\Sigma(\omega) = -J^{2}\langle S_{z}\rangle \operatorname{Im}G(\omega - \omega_{0})[n_{F}(\omega - \omega_{0}) - n_{B}(\omega_{0}) - 1],$$
(11.3)

where $n_F(\omega) = 1/[1 + \exp(\beta \omega)], n_B(\omega) = 1/[\exp(\beta \omega) - 1]$ are Fermi and Bose distribution functions. This local self-energy leads to the modifications of the DOS. In this solution we treat the self-energy effects in G to all orders, i.e. G in Eq. (11.3) is full Green's function $G^{-1}=G_0^{-1}-\Sigma(\omega)$ and solution for Σ is found selfconsistently for a local vibrational mode. The modifications of the superconducting order parameter and bosonic propagator were ignored in this calculation. Results are presented in Fig. 22. To proceed with analytic treatment, unless stated otherwise, we limit ourselves below to second order scattering in Σ . Difference between self-consistent solution and second order calculation are only quantitative and small for small coupling. Corrections to the Green's function $G(\mathbf{r}, \mathbf{r}', \omega) = G^0(\mathbf{r}, \mathbf{r}', \omega) +$ $G^{0}(\mathbf{r},0,\omega)\Sigma(\omega)G^{0}(0,\mathbf{r}',\omega) + F^{0}(\mathbf{r},0,\omega)\Sigma(\omega)F^{*0}(0,\mathbf{r},\omega).$ For simplicity we define $K(T, \omega, \omega_0) = -[n_F(\omega - \omega_0)$ $n_B(\omega_0) - 1 \simeq \Theta(\omega - \omega_0)$ which becomes a step function at low $T \ll \omega_0$, the limit we will focus on hereafter. Correction to the local density of states as a function of position comes from the correction to the bare Green's function $G^0: \delta N(\mathbf{r}, \omega) = 1/\pi \text{Im}[G^0(\mathbf{r}, 0, \omega)\Sigma(\omega)G^0(0, \mathbf{r}, \omega) \pm$ $F^{0}(\mathbf{r},0,\omega)\Sigma(\omega)F^{*0}(0,\mathbf{r},\omega)$, where keeping it general, the plus sign corresponds to the coupling to the local vibrational mode and minus – to the spin scattering respectively. The strongest effect will be at the impurity site. For on-site density of states we have:

$$\frac{\delta N(\mathbf{r} = 0, \omega)}{N_0} = \frac{\pi^2}{2} (JSN_0)^2 \frac{\omega - \omega_0}{\Delta} K(T, \omega, \omega_0)
\times \left(\frac{2\omega}{\Delta} \ln\left(\frac{\Delta}{\omega}\right)\right)^2, \quad \omega \ll \Delta,$$
(11.4)

$$\frac{\delta N(\mathbf{r} = 0, \omega)}{N_0} = 2\pi^2 (JSN_0)^2 K(T, \omega, \omega_0) \ln^2 \left(\frac{|\omega - \Delta|}{4\Delta}\right) \times \ln \left(\frac{4\Delta}{|\omega + \omega_0 - \Delta|}\right) + (\omega_0 \to -\omega_0), \ \omega \simeq |\Delta|, \quad (11.5)$$

where we used for on-site Green's function $G^0(0,0,\omega) = N_0\left[\frac{2\omega}{\Delta}\ln(\frac{4\Delta}{\omega}) + i\pi\frac{|\omega|}{\Delta}\right]$, for $\omega \ll \Delta$ and we retained

⁸ To minimize the orbital effect of magnetic field one can apply it parallel to the surface of superconductor. The magnetic field is penetrating the surface sheath on the scale of penetration depth so that its effect on the conduction electrons for d-wave SC is small.

only dominant real part of G^0 . In opposite limit $\omega \simeq \Delta$ we retained only dominant imaginary part of $G^0(0,0,\omega)=i\pi N(\omega)=-2iN_0\ln(\frac{|\omega-\Delta|}{4\Delta})$. At $\mathbf{r}=0$ we have $F^0(0,0,\omega)=0$. Complete DOS $N(\omega)$ and derivative $\frac{dN(\omega)}{d\omega}$ are shown on Fig. 22. For arbitrary position $N(\mathbf{r},\omega)$ we would have to add a Friedel oscillation factor $\Lambda(\mathbf{r})=[|G^0(\mathbf{r},\omega)|^2\pm|F^0(\mathbf{r},\omega)|^2]\sim\frac{\sin(k_Fr)}{(k_Fr_{||})^2+(r_{\perp}/\xi)^2}$ that describes the real space dependence of the Green's function on distance for small $\omega\ll\Delta$. Here $\mathbf{r}_{\perp}||\mathbf{k}_{F\perp}$ is the component of $\mathbf{r}=(\mathbf{r}_{\perp},\mathbf{r}_{||})$ that is along the Fermi surface near the nodal point of the gap and $\mathbf{r}_{||}||\mathbf{k}_{F||}$ is the component perpendicular to the Fermi surface at nodal point. Existence of the nodes in d-wave case results in the power law decay of $\Lambda(\mathbf{r})$ in all directions and it has a four fold modulation due to gap anisotropy (See detailed discussions in (Salkola et al., 1997)), also Sec. VII). The final result is our Eqs. (11.4-11.5).

It follows immediately that

$$\delta \frac{dI}{dV} / \frac{dI}{dV} \sim \delta N(\mathbf{r} = 0, V) / N_0 \sim (JSN_0)^2 \frac{V - \omega_0}{\Delta} \Theta(V - \omega_0) ,$$

$$\delta \frac{d^2I}{dV^2} \sim (JSN_0)^2 \Theta(V - \omega_0) . \tag{11.6}$$

Here we have used the fact that the derivative of $(\omega - \omega_0)\Theta(\omega - \omega_0)$ with respect to ω yields $\Theta(\omega - \omega_0)$. Thus in a d-wave superconductor and in a metal with vanishing DOS $N(\omega) = N_0 \frac{\omega}{\Delta}$ one should expect a step discontinuity in d^2I/dV^2 at the energy of a local mode with the strength $J^2N_0^2$ (see Fig. 22). This result is qualitatively different from the case of conventional metal. For metal with energy independent DOS we have from Eq. (11.4) for $T \ll \omega_0$

$$\frac{dI}{dV} \sim \delta N(\mathbf{r} = 0, V) \sim J^2 N_0^3 \Theta(V - \omega_0) , \qquad (11.7)$$

and the second derivative will reveal a delta function $d^2I/dV^2 \sim J^2N_0^3\delta(\omega-\omega_0)$ The effect in d-wave superconductor is clearly smaller than correction to DOS in a normal metal with the same coupling strength.

For completeness we also give the result for inelastic scattering in a metal with the more general DOS $N(\omega) = 1/\pi \text{Im} G^0(0,0,\omega) = (\omega/\Delta)^{\gamma} N_0$ with power $\gamma > 0$ that is determined by the microscopic properties of the material. Then, from Eqs. (11.3-11.4) we have for $\omega \ll \Delta$:

$$\delta \frac{dI}{dV} / \frac{dI}{dV} \sim \delta N(\mathbf{r} = 0, V) / N_0 \sim (V - \omega_0)^{\gamma} \Theta(V - \omega_0) ,$$

$$\delta \frac{d^2 I}{dV^2} \sim (V - \omega_0)^{\gamma - 1} \Theta(V - \omega_0) . \tag{11.8}$$

Depending on the value, we get divergent singularity at ω_0 for $\gamma < 1$, or a power law rise for $\gamma \geq 1$. In case of $\gamma = 1$ we recover the result for d-wave superconductor and for a pseudogap normal state.

Quite generally one can express the results in terms of the spectrum of superconductor. We can write $\text{Im}\Sigma(\omega)$ using spectral representation for $G(\mathbf{r}, \omega)$. In superconducting case, using Bogoliubov $u_{\alpha}(\mathbf{r}), v_{\alpha}(\mathbf{r})$ for eigenstate α , we have

$$G(\mathbf{r},\omega) = \sum_{\alpha} \left[\frac{|u_{\alpha}(\mathbf{r})|^2}{\omega - E_{\alpha} + i\delta} + \frac{|v_{\alpha}(\mathbf{r})|^2}{\omega + E_{\alpha} + i\delta} \right]. \quad (11.9)$$

Taking imaginary part of $G(\mathbf{r}, \omega)$ we arrive for $T \ll \omega_0$ at:

$$\operatorname{Im}\Sigma(\omega) = \frac{\pi J^2}{2\omega_0} \langle S_z \rangle [|u_\alpha(\mathbf{r} = 0)|^2 \delta(\omega - \omega_0 - E_\alpha) + |v_\alpha(\mathbf{r} = 0)|^2 \delta(\omega - \omega_0 + E_\alpha)] , \omega > 0.11.10)$$

At negative $\omega < 0$ one has to replace $\omega_0 \to -\omega_0$ in Eq.(11.10). For example, consider a magnetic impurity resonance in d-wave superconductor at energy ω_{imp} , such as a Ni induced resonance (Hudson *et al.*, 2001; Salkola *et al.*, 1997). Then only the term with resonance level $E_{\alpha} = E_{imp}$ will dominate the sum over eigenstates α in the vicinity of impurity site. Inelastic scattering off this impurity induced resonance will produce additional satellite *split away from the impurity level by* ω_0 , see Fig. 23. Sharp coherence peaks will also produce split satellites. Again, for a local phonon mode one gets a similar splitting of impurity level with ω_0 now being the phonon energy.

 (ω_0) , These results suggest the possibility of single spin de-(11.6) tection as one monitors the feature in d^2I/dV^2 as a function of position and external magnetic field. If we take experimentally seen DOS $N_0 \simeq 1/eV$ with $JN_0 \simeq$ in 0.14, $\Delta = 30meV$ (Hudson et al., 2001) and assuming the field of $\sim 10T$ we have $\omega_0 = 1meV$ (corresponding to the Zeeman splitting of $\sim 1meV$ in a magnetic field, we have from Eqs. (11.4-11.6)

$$\delta N(\mathbf{r} = 0, \omega)/N_0 \simeq 10^{-2} \frac{\omega - \omega_0}{\Lambda} \Theta(\omega - \omega_0)$$
. (11.11)

Result is expressed in terms of the relative change of DOS of a metal N_0 . For observation of this effect one would have to sample DOS in the vicinity of $eV = \omega_0 \propto B$. Assuming $\omega - \omega_0 = \omega_0$ we have from Eq. (11.11) $\delta \frac{dI}{dV} / \frac{dI}{dV} \sim 10^{-2}$. Expressed as a relative change of DOS of a superconductor $N(\omega) = N_0 \omega / \Delta$ effect is:

$$\delta \frac{dI}{dV} / \frac{dI}{dV} \sim \delta N(\mathbf{r} = 0, \omega) / N(\omega_0) \sim 10^{-2} \frac{\omega - \omega_0}{\omega_0} \Theta(\omega - \omega_0)$$
 (11.12)

It is of the same order of magnitude as the observed vibrational modes of localized molecules in inelastic electron tunneling spectroscopy STM, IETS-STM (Hahn and Ho, 2001; Stipe et al., 1998). The satellites at $\Delta + \omega_0$ produce the effect on the scale of unity and clearly seen even for small coupling. The important difference is that for localized spin the kink in DOS is tunable with magnetic field and this should make its detection easier.

B. Localized vibrational modes in d-wave superconductors

When a localized vibrational mode is coupled to electrons in a superconductor, the Hamiltonian is given by:

$$H = \sum_{k\sigma} \xi_k c_{k\sigma}^{\dagger} c_{k\sigma} + \sum_{k} [\Delta_k c_{k\uparrow}^{\dagger} c_{-k\downarrow}^{\dagger} + h.c.] + g \sum_{\sigma} (b^{\dagger} + b) c_{0\sigma}^{\dagger} c_{0\sigma} , \qquad (11.13)$$

Up to a second order in coupling constant g calculations are very similar if not identical to the ones in the previous section. For more detailed analysis see (Morr and Nyberg, 2003).

The proposed extension of the inelastic tunneling spectroscopy on the strongly correlated electrons states, such as a d-wave superconductor and pseudogap normal state would open up possibilities to study the dynamics of local spin and vibrational excitations. The DOS in these systems has a nontrivial energy dependence of general form $N(\omega) \sim \omega^{\gamma}, \gamma > 0$. This technique could allow for a Zeeman level spectroscopy of a single magnetic center, thus, in principle, allowing a single spin detection. There is a feature in $dI/dV \sim (\omega - \omega_0)^{\gamma - 1} \Theta(\omega - \omega_0)$ near the threshold energy ω_0 that indicates the inelastic scattering. One also finds strong satellite features near the gap edge due to coherence peak for a superconducting case. The singularity is a power law and qualitatively different from the results for a simple metallic DOS (Hahn and Ho, 2001; Stipe et al., 1998). For the relevant values of parameters for high- T_c the feature is on the order of several percents and makes the feature observable in these materials. Similar predictions are also applicable to the local vibrational modes, where ω_0 becomes a vibrational mode frequency.

XII. INTERPLAY BETWEEN COLLECTIVE MODES AND IMPURITIES IN *d*-WAVE SUPERCONDUCTORS

Conventional wisdom dictates that local probes have poor momentum resolution, and therefore cannot identify collective modes that exist at specific wave vectors. However, recent progress in relating the STM observations with ARPES (McElroy et al., 2003) by using a Fourier transform of the image taken over a large area opens up the possibility to study connections of STM measurements with other spectroscopies. Since the ability of the STS to identify the Fermi wave vector is most naturally explained by the sensitivity of the technique to Friedel oscillations in the electron density due to impurities, we now look into the DOS features arising from the interplay between dynamic scattering of of the collective mode and static disorder.

Neutron scattering is one of the spectroscopic measurements which revealed a resonance excitation, the so called 42 meV peak that is commonly present in a number of materials. It has been proposed that STM may be used to detect neutron mode (Zhu et al., 2004a). The main tool for such a measurement is the Inelastic Electronic Tunneling Spectroscopy (IETS), see Sec. XI. Specifically the proposal is to use Fourier transform (FT) tunneling maps and search for features that represent an IETS signature.

We limit our consideration to the example of a well defined mode at wave vector (π, π) with energy ω_0 . The ultimate goal is to detect the bosonic spectral function, be it magnetic spin mode or some lattice modes. Recent efforts indicate possible connective

tion between the kink in ARPES data on quasiparticle dispersion and phonon modes and, possibly, superconductivity (Damascelli et al., 2003; Gweon et al., 2004; Lanzara et al., 2004). It was suggested that the full Eliashberg function in frequency and momentum space may be extracted from ARPES data (Vekhter and Varma, 2003), and the challenge is to design a similar procedure for its determination from the FT IETS STM. Efforts to relate the data from ARPES, STM, and transport measurements in cuprates have recently intensified (Scalapino et al., 2004; Zhu et al., 2004c).

We need the impurity scattering to produce features that can be analyzed using Fourier transform. We consider weak Born scattering from distributed scalar potential $U(\mathbf{r}_i) = U_i$, i is the lattice site index. We find indeed that disorder potential can strongly modify the features as seen in local DOS. One of the interesting findings is that characteristic wave vectors of the impurity potential $U_{\mathbf{q}} = \sum_i U_i \exp(i\mathbf{q} \cdot \mathbf{r}_i)$ do play a crucial role in defining characteristic wave vectors of the DOS modulation.

To explain the method we point out that FT STM data do contain momentum information. However all the analysis up to date on FT STM data was done within the framework of elastic scattering that considers the natural quasiparticle excitations at the Fermi surface (Hoffman et al., 2002b). No inelastic scattering processes off the collective mode were included in the analysis. To consider the scattering of quasiarticles off the collective mode one has to explicitly keep track of the self-energy effects that result from scattering. In this case simple noninteracting quasiparticle picture is not adequate. Inelastic scattering of quasiparticles requires us to consider excitations off shell, for example to consider excitations at energies that are typically $\Delta + \Omega_0 \sim 70 meV$. At these energies the combination of the Fermi surface effects, typical wavevectors of the collective mode and typical wavevectors of the random potential all enter in determining the momentum of the inelastic tunneling features as seen in FT STM.

We limit ourselves to the second order scattering between carriers and bosonic excitations and at this level there is no conceptual difference in the method as applied to spin or phonon bosonic mode.

We start with a model Hamiltonian describing twodimensional electrons coupled to a collective spin mode and in the presence of inhomogeneity:

$$\mathcal{H} = \mathcal{H}_{BCS} + \mathcal{H}_{sp} + \mathcal{H}_{imp} . \tag{12.1}$$

Here the BCS-type Hamiltonian is given by $\mathcal{H}_{BCS} = \sum_{\mathbf{k},\sigma} (\varepsilon_{\mathbf{k}} - \mu) c_{\mathbf{k}\sigma}^{\dagger} c_{\mathbf{k}\sigma} + \sum_{\mathbf{k}} (\Delta_{\mathbf{k}} c_{\mathbf{k}\uparrow}^{\dagger} c_{-\mathbf{k}\downarrow}^{\dagger} + \Delta_{\mathbf{k}}^{*} c_{-\mathbf{k}\downarrow} c_{\mathbf{k}\uparrow}),$ where $c_{\mathbf{k}\sigma}^{\dagger}$ ($c_{\mathbf{k}\sigma}$) creates (annihilates) a conduction electron of spin σ and wavevector \mathbf{k} , $\varepsilon_{\mathbf{k}}$ is the normal state energy dispersion for the conduction electrons, μ the chemical potential, and $\Delta_{\mathbf{k}} = \frac{\Delta_{0}}{2}(\cos k_{x} - \cos k_{y})$ the d-wave superconducting energy gap. The coupling between the electrons and the resonance mode is modeled

by an interaction term $\mathcal{H}_{sp} = g \sum_i \mathbf{S}_i \cdot \mathbf{s}_i$, where the quantities g, \mathbf{s}_i , and \mathbf{S}_i are the coupling strength, the electron spin operator at site i, and the operator for the collective spin degrees of freedom, respectively. The dynamics of the collective mode will be specified below. The quasiparticle scattering from impurities in the Hamiltonian is given by, $H_{imp} = \sum_{i\sigma} U_i c_{i\sigma}^{\dagger} c_{i\sigma}$, where U_i is the strength of the impurity scattering potential. For simplicity, only the case of nonmagnetic scattering is considered here. By introducing a two-component Nambu spinor operator, $\Psi_i = (c_{i\uparrow}, c_{i\downarrow}^{\dagger})^T$, one can define the matrix Green's function for the full Hamiltonian system, $\hat{G}(i,j;\tau,\tau') = -\langle T_{\tau}[\Psi_i(\tau) \otimes \Psi_j^{\dagger}(\tau')] \rangle$. An algebra leads to the full electron Green's function with impurity scattering:

$$\mathcal{G}_{11}(i,j;i\omega_n) = \tilde{\mathcal{G}}_{11}^{(0)}(i,j;i\omega_n)
+ \sum_{j'} U_{j'} [\tilde{\mathcal{G}}_{11}^{(0)}(i,j';i\omega_n) \tilde{\mathcal{G}}_{11}(j',j;i\omega_n)
- \tilde{\mathcal{G}}_{12}^{(0)}(i,j';i\omega_n) \tilde{\mathcal{G}}_{21}(j',j;i\omega_n)] . (12.2)$$

Here $\tilde{\mathcal{G}}^{(0)}$ is the dressed Green's function, with its Fourier component given by:

$$[\tilde{\mathcal{G}}^{(0)}]^{-1}(\mathbf{k}; i\omega_n) = \begin{pmatrix} i\omega_n - \xi_{\mathbf{k}} - \Sigma_{11} & -\Delta_{\mathbf{k}} - \Sigma_{12} \\ -\Delta_{\mathbf{k}} - \Sigma_{21} & i\omega_n + \xi_{\mathbf{k}} - \Sigma_{22} \end{pmatrix},$$
(12.3)

where $\xi_{\mathbf{k}} = \varepsilon_{\mathbf{k}} - \mu$, $\omega_n = (2n+1)\pi T$ is the fermionic Matsubara frequency for fermions. When the inelastic scattering of quasiparticles from the collective mode occurs, the self-energy is obtained to the second order in the coupling constant as:

$$\hat{\Sigma}(\mathbf{k}; i\omega_n) = \frac{3g^2T}{4} \sum_{\mathbf{q}} \sum_{\Omega_l} \chi(\mathbf{q}; i\Omega_l) G_0(\mathbf{k} - \mathbf{q}; i\omega_n - i\Omega_l) ,$$
(12.4)

where $\chi(\mathbf{q};i\Omega_l)$ is the dynamical spin susceptibility $\chi_{ij}(\tau) = \langle T_{\tau}(S_i^x(\tau)S_j^x(0)) \rangle$ and $\Omega_l = 2l\pi T$ the bosonic Matsubara frequency, and G_0 is the bare superconducting Green's function. We have also assumed that the d-wave pair potential is real. For a single-site impurity, the equation of motion for the full Green's function can be exactly solved. For the case of multiple impurities and especially the inhomogeneous situation, some approximation needs to be taken. We consider here the case of the weak impurity scattering limit so that the Born approximation can be used. With this ansatz, we arrive at:

$$\mathcal{G}_{11}(i,j;i\omega_n) = \tilde{\mathcal{G}}_{11}^{(0)}(i,j;i\omega_n) + \delta \mathcal{G}_{11}(i,j;i\omega_n) \quad (12.5)$$

with

$$\delta \mathcal{G}_{11}(i,j;i\omega_n) = \sum_{j'} U_{j'} [\tilde{\mathcal{G}}_{11}^{(0)}(i,j';i\omega_n) \tilde{\mathcal{G}}_{11}^{(0)}(j',j;i\omega_n) - \tilde{\mathcal{G}}_{12}^{(0)}(i,j';i\omega) \tilde{\mathcal{G}}_{21}^{(0)}(j',j;i\omega_n)] . \tag{12.6}$$

The LDOS at the i-th site, summed over two spin components, is

$$\rho(\mathbf{r}_i, E) = -\frac{2}{\pi} \text{Im} \mathcal{G}_{11}(i, i; E + i\gamma) , \qquad (12.7)$$

where $\gamma = 0^+$. We are especially interested in the correction to the LDOS from the impurity scattering:

$$\delta\rho(\mathbf{r}_i, E) = -\frac{2}{\pi} \text{Im}\delta\mathcal{G}_{11}(i, i; E + i\gamma) . \qquad (12.8)$$

Its Fourier transform is:

$$\begin{split} \delta\rho(\mathbf{q},E) &= \sum_{i} \delta\rho(i,E) e^{-i\mathbf{q}\cdot\mathbf{r}_{i}} \\ &= -\frac{U_{\mathbf{q}}}{N\pi i} \sum_{\mathbf{k}} [\tilde{\mathcal{G}}_{11}^{(0)}(\mathbf{k}+\mathbf{q};E+i\gamma)\tilde{\mathcal{G}}_{11}^{(0)}(\mathbf{k};E+i\gamma) \\ &- \tilde{\mathcal{G}}_{11}^{(0)*}(\mathbf{k}-\mathbf{q};E+i\gamma)\tilde{\mathcal{G}}_{11}^{(0)*}(\mathbf{k};E+i\gamma) \\ &- \tilde{\mathcal{G}}_{12}^{(0)}(\mathbf{k}+\mathbf{q};E+i\gamma)\tilde{\mathcal{G}}_{21}^{(0)}(\mathbf{k};E+i\gamma) \\ &+ \tilde{\mathcal{G}}_{12}^{(0)*}(\mathbf{k}-\mathbf{q};E+i\gamma)\tilde{\mathcal{G}}_{21}^{(0)*}(\mathbf{k};E+i\gamma)] \ (12.9) \end{split}$$

where the Fourier transform of the scattering potential is

$$U_{\mathbf{q}} = \sum_{i} U_{i} e^{-i\mathbf{q} \cdot \mathbf{r}_{i}} . {12.10}$$

The corresponding Fourier (wave-vector) spectrum is defined as

$$P(\mathbf{q}, E) = |\delta \rho(\mathbf{q}, E)|. \tag{12.11}$$

Up to now discussion and formulation are quite general and can be used to study the effects of any dynamic mode once the susceptibility χ is known. Consider now specific case of magnetic mode with susceptibility taking a phenomenological form (based on the inelastic neutron scattering observations), see also (Eschrig and Norman, 2000):

$$\chi(\mathbf{q}; i\Omega_l) = -\frac{\delta_{\mathbf{q}, \mathbf{Q}}}{2} \left[\frac{1}{i\Omega_l - \Omega_0} - \frac{1}{i\Omega_l + \Omega_0} \right] , \quad (12.12)$$

where we denote the wavevector $\mathbf{Q} = (\pi, \pi)$ and the mode energy by Ω_0 . This form captures the essential feature of resonant peak observed by neutron scattering experiments in the superconducting state of cuprates (Zhu et al., 2004a). For the normal-state energy dispersion, we use $\varepsilon_{\mathbf{k}} = -2t(\cos k_x + \cos k_y)$ – $4t'\cos k_x\cos k_y$, where t and t' are the nearest and nextnearest neighbor hopping integral. Unless specified explicitly, the energy is measured in units of t. We choose t' = -0.2 to model the band structure of the hole-doped cuprates. Since the maximum energy gap for most of the cuprates at the optimal doping is about 30 meV while the resonance mode energy is in the range between 35 and 47 meV, we take $\Delta_0 = 0.1$ and $\Omega_0 = 0.15$ (i.e., $1.5\Delta_0$). The chemical potential ($\mu \approx -1.15$) is tuned to give an optimal doping value 0.16. To mimic the intrinsic life time broadening, in our numerical calculation we take γ of Eq. (12.7) to be $0.08\Delta_0$. A system size of $N = N_x \times N_y = 256 \times 256$ is taken in the numerical calculation.

Figure 24 plots the density of states in a clean system for various values of coupling constant g. Without the electron-mode coupling (g = 0), the density of states is peaked only at the maximum gap edges $\pm \Delta_0$. When there exists the electron-mode coupling, for example g = 0.2 as shown in the figure, several new effects emerge. As a result of the additional anomalous self-energy introduced through the coupling, the maximum gap edge is renormalized to Δ_{ren} , which is larger than Δ_0 . More importantly, the singularity in the quasiparticle self-energy causes additional poles in the Green's function, and new peaks show up at the energy $\pm E_r = \pm (\Delta_r + \Omega_0)$. A strong implication of this result is that regardless of the renormalization of the energy gap, the position of the new peaks relative to the superconducting coherent peak is shifted by Ω_0 . In addition, with the appearance of the peaks away from the gap edge, the intensity of the superconducting coherent peaks is reduced such that the sum rule is obeyed. The intensity of the peaks at negative energies is stronger than that at positive energies since the van Hove singularity is below the Fermi energy. These results, for the clean case, are consistent with earlier studies of the ARPES (Abanov et al., 1999: 2002: Campuzano et al., Dessau et al., 1991: Eschrig and Norman, 2000; Kee et al., 2002; Norman and Ding, 1998; Shen and Schrieffer, 1997) and DOS (Abanov and Chubukov, 2000). The shift of states due to inelastic scattering is also expected for scattering off of local mode (Balatsky et al., 2003).

We now turn to the Fourier spectrum in the presence of disorder. An accurate description of this problem requires an extremely high energy and spatial resolution. Therefore, a very large system size should be considered. For the quasiparticle scattering off a single impurity, as considered in the work by Zhu et al. (Zhu et al., 2004a), one can first calculate the LDOS within a small window around the impurity site in a very big system size (e.g., $N=1000\times1000$), then perform a Fourier transform over the window size and even with masking of sites. This procedure and flexibility does not exist in the case of disorder and inhomogeneity with multiple scattering centers. Summation over the wave-vector in the Brillouin zone constrains us to consider a moderate system size.

In Fig. 25, we show the Fourier spectrum at the energy $-E_r$ for the coupling constant g=0.2 with a structurless scattering potential $U_{\bf q}=U_0$. This structureless $u_{\bf q}$ corresponds to a single-site impurity in real space. In the absence of the electron-mode coupling (g=0), the Fourier spectrum has a strongest intensity at ${\bf q}=(0,0)$ and its equivalent points, and a moderately strong weight along the edges of the square around ${\bf q}=(\pi,\pi)$. When there exists the electron-mode coupling, as shown in Fig. 25, the spectrum has the strongest intensity point at four corners of the square, and a moderately strong intensity at the four ridges of the square. This implies that as one takes line cuts along the diagonal the first feature at $\pm E_r$ always will be at the wavevector $(\pi - \delta, \pi - \delta)$ before the (π, π) point. Regardless of whether the electrons

are coupled to the collective mode, the spectrum has a minimum in intensity at $\mathbf{q}=(\pi,\pi)$, which is different from the results when the pre-dominant Friedel oscillation is filtered out of the Fourier transform. When the scattering potential has a clear stucture, which might be relevant to the inhomogeneity in high- T_c cuprates, the pattern of the Fourier spectrum changes dramatically. As an ansatz, we propose the following stucture for the scattering potential:

$$U_{\mathbf{q}} = \frac{U_0 q_0^2}{q_0^2 + 4[\cos^2(q_x/2) + \cos^2(q_y/2)]}, \qquad (12.13)$$

where the parameter q_0 describes the extent of the peak at $\mathbf{q}=(\pi,\pi)$. This structure factor has a highly nontrivial consequence on the Fourier spectrum of the local density of states. This is because overall modulation $\delta\rho(\mathbf{q},\omega)\propto U_{\mathbf{q}}$ and for $U_{\mathbf{q}}$ peaked at (π,π) FT DOS $\delta\rho(\mathbf{q})$ will also be peaked at this wavevector. As shown in Fig. 26, the Fourier spectrum now has a strongest intensity at the four ridges, which are located along the diagonals of the first Brillouin zone, and a secondly strongest intensity at $\mathbf{q}=(\pi,\pi)$. Except in the four small lobes around the corners, the spectrum has moderate intensity inside the square.

Here we have considered the situation where all impurities have identical potential scattering strength. If one dopes a strong scattering impurity, for example Zn substituted for Cu, into a high- T_c cuprate which has inhomogeneity coming from weak potential scatterers, the pattern of the Fourier spectrum of the local density of states is mostly determined by the scattering off the strong impurity.

To summarize, the main results of this section are: 1. the energy of the inelastic feature is at $E_r = \Delta_0 + \Omega_0 \sim 70 meV$ for optimal doping. Given that the gap is position dependent in observed spectra, this energy will be position dependent. 2. the typical wave vectors along diagonals where the inelastic features are seen are determined by a number of factors: the momentum of the disorder potential $U(\mathbf{q})$, the doping and positions of the "diamonds" seen in Figs. 25 and 26. 3. the first feature that is seen in FT IETS STM in our calculation is occurring at wavevectors that are inside (π, π) vectors.

XIII. SCANNING TUNNELING MICROSCOPY RESULTS

A. STM results around a single impurity

The STM has established itself as a remarkably powerful and versatile tool for studying the electronic properties of solids. Its remarkable energy and spatial resolution makes it particularly well suited for materials characterized by small energy and short length scales. It measures the tunneling current varying with the voltage bias and the tip positions. In the tunneling Hamiltonian formalism, the differential tunneling conductance—the derivative of the current with respect to the voltage bias, is

given by

$$\frac{dI}{dV} \propto -\int d\omega \sum_{\mathbf{k},\sigma} |T_{\mathbf{k}}|^2 A_{\sigma}(\mathbf{k},\omega) f'_{FD}(\omega - eV) , \quad (13.1)$$

where f_{FD} is the Fermi distribution function, and $A_{\sigma}(\mathbf{k},\omega)$ is the electron spectral function of the The tunneling matrix element, $|T_{\mathbf{k}}|^2$ $\sum_{\mathbf{q}} |M_{\mathbf{k}\mathbf{q}}|^2 A_{tip}(\mathbf{q},\omega)$, where $M_{\mathbf{k}\mathbf{q}}$ is the matrix element representing the overlap of the electronic states on the tip and sample. Using a tip with featureless DOS around the Fermi energy, we can assume $|T_{\mathbf{k}}|^2$ is energy independent. If we further assume a k-independent tunneling matrix element, one can find that the tunneling conductance is proportional to the local density of state at the tip position, which we have chosen to be the origin, $\rho(eV) = -\int d\omega \sum_{\mathbf{k},\sigma} A(\mathbf{k},\omega) f'(\omega - eV)$. At zero temperature, it is simply given by the imaginary part of the electronic Green's function we have used heavily for the discussion throughout the work, that is $\rho(\mathbf{r}, eV) = -\frac{1}{\pi} \sum_{\sigma} \text{Im} G_{\sigma}(\mathbf{r}, \mathbf{r}; \omega = eV)$. Here we have labeled the tip position by \mathbf{r} .

The experimental attempts to detect and accurately resolve the sub-gap features in the density of states in superconductors with impurities have a long history. This feature was observed in the planar junctions doped with magnetic impurities in earlier years. However, a direct observation of the sub-gap states induced by a magnetic impurity did not occur until late 1990's. In 1997, Yazdani and co-workers (Yazdani et al., 1997) deposited adatoms, Mn, Gd and Ag, on the (110)-oriented surface of a superconducting Nb sample, and examined the local electronic structure around them. Figure 27 shows their STM tunneling spectrum measurement. The main fundings are: (1) The local density of states has no much difference for the tunneling through Ag impurity atoms and far away from them, since Ag impurity atoms are believed to be non-magnetic in nature; (2) The LDOS at energies less than the Nb's gap is enhanced when the tunneling is through Mn and Gd magnetic atoms. The enhancement happens at the length scale of 10Å, indicating the bound nature of the impurity states; (3) The LDOS spectra are asymmetric about the Fermi energy. Within the framework of the BdG theory, the authors used a twoparameter magnetic impurity model, where the electrons are coupled with the impurity through an magnetic exchange interaction J and experience a nonmagnetic potential scattering U. The obtained results, consistent with the Yu-Shiba-Rusinov prediction and more recent theoretical works, fit the experimental data. However, the model calculation required the value of J of the order of 4 eV, in the strong coupling limit, and failed to capture the detailed spatial dependence of the spectra around Gd site.

The pioneering STM experimental research on the local electronic structure around single defects and impurities in high- T_c cuprates was carried out by two groups led by Eigler at IBM Almaden Research Center (Yazdani *et al.*, 1999) and Davis at UC Berke-

ley (Hudson et al., 1999). Since the high- T_c cuprates have a d-wave pairing symmetry, even nonmagnetic impurity scattering would affect the superconductivity. Byers, Flatte, and Scalapino (Byers et al., 1993) were the first to suggest the use of STM to study the spatial variations of the tunneling conductance near impurities. In particular, it was theoretically predicted (Balatsky et al., 1995; Salkola et al., 1996) that quasiparticle resonance states are induced around a nonmagnetic impurity in a d-wave superconductor, in striking contrast to swave systems. The sample used by Yazdani and coworkers is overdoped Bi₂Sr₂CaCu₂O₈ with a superconducting transition temperature of 74K and a transition width of 3K. The sample used by the Berkeley group is $Bi_2Sr_2CaCu_2O_{8+\delta}$ with a transition temperature of 87K and a transition width of 5K. The STM experiments were operated at 5K and 4.2K, respectively. The STM spectroscopy on these samples, which were nominally undoped with known impurities, shows clearly the enhancement of the local density of states near the zero voltage bias in regions where the chemically induced defects in the sample are located. The experiments provided a strong evidence for the existence of low-energy quasiparticle resonance states around single nonmagnetic impurities, as predicted theoretically. The asymmetric or splitting of the measured resonance near the zero bias may come from the fact that the particlehole symmetry may be broken by impurities and defects locally or the underlying realistic band structure of BSCCO (Flatte and Byers, 1998; Zhu et al., 2000a). However, in these two experiments, the location in the crystal and the identity of these scattering centers are unknown. Moreover, since the enhancement of the local density of states at these scattering centers is not dramatically large and the coherence of high-Tc superconductors is so short, it is very difficult to investigate in detail the local electronic structure around them at an atomic scale.

New STM study on the impurity effects in BSCCO was reported by the Berkeley group (Pan et al., 2000b). The samples were $Bi_2Sr_2Ca(Cu_{1-x}Zn_x)_2O_{8+\delta}$ single crystals with intentionally doped with x = 0.6% Zn. The crystals have the transition temperature of 84K and a width of 4K. To search for low-energy quasiparticle states associated with the Zn atoms, the authors first mapped the differential tunneling conductance at zero sample bias in a larger window of the surface and found a number of randomly distributed bright sites corresponding to the areas of high LDOS. Then they measured the tunneling spectroscopy exactly at the center of a bright scattering site. As shown in Fig. 28, the spectrum showed a very strong DOS peak at the energy $\Omega = -1.5 \pm 0.5$ meV. The peak intensity can be up to six times greater than the normal-state conductance. At the same time, the intensity at the superconducting coherence peak is strongly suppressed, indicating the almost complete local destruction of superconductivity. These phenomena is consistent with the theoretically predicted characteristics of quasiparticle scattering off a nonmagnetic unitary impurity in a d-wave superconductor. The strong intensity of the near-zero-bias peak allows the authors to give a close inspection of the electronic structure around the Zn impurity. As shown in Fig. 30, the STM differential conductance imaging at $\Omega = -1.5 meV$ exhibits two novel features: Firstly, it has strongest intensity directly at the impurity site and local maxima at the sites belonging to the sublattice containing the impurity site, while local minima at the sites belonging to the other sublattice. Secondly, the intensity decays much faster along the gap nodal direction than along the bond direction. These new features are totally unexpected. The theory based on a potential scattering model would predict a vanishingly small intensity at the impurity in the unitary limit. The first feature motivated theorists to study the electronic structure around a Kondo impurity in a d-wave superconductor (Polkovnikov et al., 2001; Zhang et al., 2001; Zhu and Ting, 2001b), and consider the importance of the BiO layer which is the exposed surface (Martin et al., 2002; Zhu and Ting, 2001c; Zhu et al., 2000c).

The STM study on the local electronic structure around a magnetic Ni atom in BSCCO was also reported by the same Berkeley group (Hudson et al., 2001). It was found that there two spin-resolved resonance states induced by the Ni atom, in contrast to the case of Zn atom in previous experiment where only a spin-degenerate resonance state is induced. The energy of four resonance peaks in the tunneling spectrum are, $\pm \Omega_1$ and $\pm \Omega_2$, with $\Omega_1 = 9.2 \pm 1.1$ mev and $\Omega_2 = 18.6 \pm 0.7$ meV. The experimental result is reasonable agreement with a theoretical model with both nonmagnetic and magnetic scattering (Salkola et al., 1997; Tsuchiura et al., 2000). By substituting the values of $\Omega_{1,2}$ and the maximum superconducting energy gap $\Delta_0 = 28$ meV into the theoretical formula (Salkola et al., 1997):

$$\Omega_{1,2} = -\frac{\Delta_0}{2N_F(U_0 \pm J) \ln|8N_F(U \pm W)|}$$
(13.2)

with N_F the normal-state density of states at the Fermi energy, U and W the strength of nonmagnetic and magnetic scattering, one can find $N_F U = -0.67$ and $N_F W = 0.14$. This result indicates that, despite Ni atoms possess a magnetic moment, the scattering off them is dominated by potential interactions. In addition, the experiment also showed that the intensity at the gap edge in the tunneling conductance directly at the Ni impurity site is almost unaffected, in comparison with that far away from the impurity, supporting the scenario that the high-Tc superconductivity is magnetically mediated (Pines, 1997).

B. Spatial distribution of particle and hole components

Spatial distribution of tunneling intensity clearly exhibits alternation between positive and negative bias, see

for example, Fig. 29. It appears as a rotation of an impurity induced cross upon changing the sign of the bias. Since the effect is so explicit in the images we will address it here.

Apparent rotation of the impurity intensity can be understood as a result of interplay between particle and hole components of the Bogoliubov quasiparticle. This effect is a general property of superconductivity and is seen in both s-wave and d-wave superconductors (Hudson et al., 2001; Pan et al., 2000a; Yazdani et al., 1997), see also Sec. IX. The Bogoliubov quasiparticles, that are native excitations in superconductor, have both particle and hole component. The sites where there is a large particle components will have large intensity on positive bias site and hence will be show up as bright sites on positive bias. Sites with large hole component will be bright on negative bias, Fig. 32.

Let us define the respective amplitudes of particle and hole amplitudes of the Bogoliubov quasiparticle, $u_n(i)$ and $v_n(i)$ for site i and for particular eigenstate n. They obey the normalization condition $\sum_{n} |u_n(i)|^2 + |v_n(i)|^2 =$ 1 for any fixed site i. Consider now a site where, say, $u_n(i)$ is large and close to 1 for particular eigenvalue. It follows therefore that for the same site the $v_n(i)$ would have to be small, since the normalization condition is almost exausted by $|u_n(i)|^2$ term alone. Similarly, for the sites where $v_n(i)$ has large magnitude, $u_n(i)$ would have to be small. Large $u_n(i)$ component would mean that quasiparticle has a large electron component on this site. Hence the electron will have large probability to tunnel into superconductor on this site and the tunneling intensity for electrons positive sample bias will be large. Conversely, for those sites the hole amplitude is small $|v_n(i)||u_n(i)|$ and the hole intensity negative sample bias will be small. Similarly, for sites with large hole amplitudes $|v_n(i)||u_n(i)|$ the electron amplitude will be suppressed and this site will be bright on the hole bias. Therefore if there is a particular pattern for the large particle amplitude (sampled on positive bias) on certain sites i, the complimentary pattern of bright sites for hole tunneling (on negative bias) will develop as a consequence of the inherent particle-hole mixture in superconductor. This is the physics behind what appears as the cross rotation upon bias switch, seen in experiments (Hudson et al., 2001; Pan et al., 2000a), see Fig. 29.

C. Fourier-transformed STM Measurement

The ingredient of the Fourier-transform STM technique is to collect a large set of tunneling conductance data (at a fixed voltage bias) in the real space, and then to perform a Fourier transform. This technique was first applied by Hoffman et~al., 2002a to study the quasiparticle states generated by a quantized magnetic vortex in the mixed state of slightly overdoped high- T_c superconductor, ${\rm Bi_2Sr_2CaCu_2O_{8+\delta}}$. A Cu-O bond-oriented "checkboard" pattern with $4a_0$ period-

The $4a_0$ modulation periodicity is one half of that $(8a_0)$ of the field-induced SDW modulation observed in neutron scattering (Khaykovich et al., 2002; Lake et al., 2001, 2002) on other cuprate materials. This field-induced "checkerboard" pattern has been interpreted as the induction of two-dimensional spin density wave around the vortex core where the superconductivity is suppressed (Andersen and Hedegård, 2003; Takigawa et al., 2003; Zhu et al., 2002), the nucleation of the antiferromagnetic order brought about by local quantum fluctuations of a vortex (Franz et al., 2002), and the frozen of d-wave hole pairs into a crystal by the magnetic field (Chen et al., 2002). Most of the theories rely on the proximity of the system to a quantum critical point so that it is very sensitive to external perturbations. The same kind of checkerboard pattern has also been predicted around a single strong impurity with induced local moment in the optimally doped cuprates (Chen and Ting, 2003, 2004; Liang and Lee, 2002; Zhu et al., 2002).

The challenge comes from the experimental observation of a similar checkerboard pattern even at zero field in the same doping regime (Hoffman et al., 2002b; Howald et al., 2003; McElroy et al., 2003). experiments by Hoffman et al., 2002b; McElroy et al., 2003, the Fourier analysis of the images of the energydependent modulations yields the dispersion of wavevectors. Instead, Howard and co-workers observed the existence of static striped density of electronic states, i.e., the four-period peaks in the Fourier transform of the data are present at all energies, including very low energies. One can understand these two effects separably. Those peaks showing energy dispersion comes from the a quasiparticle scattering from impurities (Byers et al., 1993; Wang and Lee, 2003; Zhang and Ting, 2003, 2004). A heuristic model based upon the electronic band structure is as follows (McElroy et al., 2003): In BSCCO, four nodes exist in the superconducting gap Δ_k . Below the gap maximum Δ_0 , the contours in k-space along which quasiparticle exist at a given energy are bananashaped, as shown in Fig. 33. The quasiparticle density of states at energy $E = \omega$, $\rho(E = \omega)$ is proportional to $\int_{E_k=\omega} |\nabla_k E_k|^{-1} dk$, where the integral is performed over the contour $E_k = \omega$. Each 'banana' exhibits its largest rate of increase with energy, $|\nabla_k E_k|^{-1}$, near its two ends. Therefore, the primary contributions to $\rho(E)$ are from the octet of momentum-space regions centered around $\mathbf{k}_{i}(E)$, $j=1,2,\ldots,8$, at the end of the 'banana's. (Red circles in Fig. 33.) In the presence of impurities, quasiparticles will be elastically scattered. A quasiparticle located in momentum-space near one element of the octet is highly likely to be scattered to the vicinity of another element of the octet, because of the large density of final states there. For each \mathbf{k}_i in a representative octet, there are seven characteristic scattering wavevectors. This octet-model then predicts a total of 56 scattering wavevectors. Of these, 32 constitute a complete set of inequivalent wavevectors and therefore 16 distinct $\pm \mathbf{q}$ pairs can be detected by Fourier-transformed scanning tunneling spectroscopy. The experimental data (McElroy et al., 2003) are in good agreement with this model. From the material point of view, although no external impurities were introduced in a controlled manner into the sample of these experiments, the source of quasiparticle scattering may be closely related to the experimentally observed nanoscale inhomogeneity (Howald et al., 2001; Lang et al., 2002; Pan et al., 2001).

In contrast, the observed non-dispersive LDOS modulations (Howald et al., 2003) should be interpreted by invoking a static (or fluctuating) charge- or spinordered state (Kivelson et al., 2003; Podolsky et al., 2003; Polkovnikov et al., 2003). The emergence of a competing ordering is due to the quantum criticality with or without the aid of the inhomogeneity in the sample. An even stronger evidence of the competing ordering is provided by recent observation that the electronic states at low energies within the pseudogap state in $Bi_2Sr_2CaCu_2O_{8+\delta}$ exhibit spatial modulations with an energy-independent incommensurate periodicity (Vershinin et al., 2004). Theoretically, a complete microscopic model with all these elements has not yet been developed.

D. Filter

We point out that for unitary scattering impurity in any model it is difficult if not impossible to produce large intensity on the impurity site. Unitary scattering produces a node in the wave function. Yet, experimentally, the impurity site is bright (Pan et al., 2000b). One explanation is that the image seen by STM is not the real intensity of the impurity state that is buried below the exposed layer in STM experiments. One needs to have a model on how intensity is transmitted to the top layer. The idea of a filter then comes in naturally. Martin et al. (Martin et al., 2002) proposed an idea of filter that intensity as seen at the top layer by STM is a convolution of initial intensity due to impurity scattering and filter function that comes from the effective hopping matrix element between CuO planes, $t_k \propto |\cos k_x - \cos k_y|^2$.

The reasoning goes as follows. In order to tunnel between layers it is advantageous to involve tunneling between s-wave orbitals that extend out of the Cu-O plane. These orbitals are off the chemical potential and virtual hopping on these orbitals would bring large energy denominators in any perturbation scheme. Still it pays to engage s-wave orbitals of Cu because one gains on the exponential overlap factors between s-orbitals in adjacent planes. The electronic orbitals near chemical potential are essentially $d_{x^2-y^2}$ orbitals of Cu (hybridized with porbitals but we ignore this hybridization). The $d_{x^2-y^2}$ orbitals on the impurity site are orthogonal to the s-orbital of the impurity site. The next available s orbitals are on the nearest Cu sites. Therefore electron hops virtually on

to p_x or p_y orbitals of nearest O and then onto s-orbital. The amplitude for the hops Cu $d_{x^2-y^2} \to O$ $p_{x,y} \to Cu$ s would be different for hops along horizontal and vertical directions, as one can verify from Fig. (34).

For example the hopping to the Cu site on the right one would get for and amplitude $A_{i,i+x(y)}$:

$$A_{i,i+x} \propto \frac{\langle d_i | p_x \rangle \langle p_x | s_{i+x} \rangle}{[E_p - E_d][E_s - E_p]} \sim \frac{(-1) \exp(ik_x a)}{[E_p - E_d][E_s - E_p]}$$

$$A_{i,i+y} \propto \frac{\langle d_i | p_y \rangle \langle p_y | s_{i+y} \rangle}{[E_p - E_d][E_s - E_p]} \sim \frac{(+1) \exp(ik_x a)}{[E_p - E_d][E_s - E_p]},$$
(13.3)

in the second equation we considered a plane waves that describe the states without impurity scattering. One immediately can see that the signature for the horizontal and vertical amplitudes is opposite in sign regardless of the phase assignment of p-orbitals for pure case and for general amplitudes of the states produced by impurity scattering. For a quantum mechanical process to hop from one site to nearest neighbor s-orbitals one would have to add the amplitudes:

$$A_{tot} = A_{i,i+x} + A_{i,i-x} + A_{i,i+y} + A_{i,i-y}$$

$$\sim \cos(k_x a) - \cos(k_y a) .$$
(13.4)

Again, second equation refers to the pure plane wave analysis to make contact with the bands structure calculations for the tunneling matrix element (Andersen et al., 1995). Upon hopping on the s-orbitals electron hops to the next layer and retraces its path exactly in reversed sequence as described above. Therefore the amplitude for the hopping will be proportional to the square of the A_{tot} . The net hopping matrix element has the from consistent with $|d_{x^2-y^2}|$ modulations:

$$|A_{tot}|^2 \propto |A_{i,i+x} + A_{i,i-x} + A_{i,i+y} + A_{i,i-y}|^2$$
 (13.5)

This particular filter is directly connected to the interplane hopping matrix element obtained within the band structure calculation (Andersen *et al.*, 1995). However the idea that one has to involve the *s*-orbitals of the Cu-O plane is relevant also for an exposed Cu-O layer as one would need to tunnel from the *s*-orbitals of the tip onto relevant *s*-orbitals of the Cu-O plane (Misra *et al.*, 2002).

Alternative filter due to blocking of certain hopping matrix elements has been considered by Zhu et al. (Zhu et al., 2000c). For an analysis of the local effects of impurity one need to consider a local tunneling matrix elements that has to connect impurity orbitals to s-orbitals on neighboring Cu atoms that have a greatest overlap between Cu-O layers. The net effect of the filter is to produce large spectral intensity on an impurity site and nearest neighbor sites to be dark. More recently, the measured quasi-continuous data has been converted to a set of LDOS defined on a two-dimensional lattice (Wang and Hu, 2004), which is suitable for a rigorous comparison between the tight-binding model studies and the STM experimental data.

Another important observation one can make by comparing STM and local NMR results available in Li doped YBCO superconductor (Bobroff et al., 2001). In case of Li impurity NMR revealed that maximum intensity in NMR signal comes from four nearest neighbor Cu sites and is quite localized near impurity. This observation would be consistent with the notion that strongly scattering impurity produces large density of states on nearest sites. The crucial difference between NMR and STM is that NMR observation does not require electronic tunneling. Magnetic field is measured instead. Hence there is no filter to apply to native electronic states in Cu-O plane to obtain NMR real space distribution. Therefore, depending on the type of measurement one might need or need not to use the filters. Details depend on the nature of the measurement.

XIV. AVERAGE DENSITY OF STATES IN SUPERCONDUCTORS WITH IMPURITIES

The Green's function formalism is well suited to the analysis of the combined effect of many uncorrelated impurities in the bulk of a superconductor. The first treatment of the superconducting properties using this technique was given by Abrikosov and Gor'kov (Abrikosov and Gorkov, 1960) in a pioneering paper. The basic assumptions underlying such calculations were given in Sec. III.B. After averaging over different impurity distributions following Eq. (3.14), the translational symmetry in the system is restored, and therefore the Green's function takes the general form

$$\widehat{G}^{-1}(\mathbf{k},\omega) = i\omega_n - \xi(\mathbf{k})\tau_3 - \Delta_0\sigma_2\tau_2 - \widehat{\Sigma} \quad (14.1)$$

$$\equiv i\widetilde{\omega} - \widetilde{\varepsilon}(\mathbf{k})\tau_3 - \widetilde{\Delta}\sigma_2\tau_2. \quad (14.2)$$

Here the second line explicitly takes into account the matrix structure of the self-energy, $\hat{\Sigma}$. The superconducting gap in the presence of impurities is determined by the self-consistency condition, Eq. (2.21), which reads here

$$\Delta(\widehat{\Omega}) = \pi T N_0 \sum_{\omega_n} \int d\widehat{\Omega}' V(\widehat{\Omega}, \widehat{\Omega}') \frac{\widetilde{\Delta}(\widehat{\Omega}')}{\sqrt{\widetilde{\omega}_n^2 + \Delta^2(\widehat{\Omega}')}}.$$
(14.3)

The transition temperature is the temperature at which a non-trivial solution of the self-consistency equation first appears. Together with the recipe for computing the self-energy these equations form a general basis for treating ensembles of impurities in superconductors. We note here that we always ignore the contribution of Σ_3 , which is equivalent to the renormalization of the chemical potential. This is always allowed in computing the density of states, although the corrections may need to be taken into account in evaluating the response functions (Hirschfeld *et al.*, 1988). The basic assumption for computing the self-energy is that, in addition to neglecting the interaction between spins on different impurity sites, see Sec. III.B, we can neglecting the interference

effects of scattering on different impurities (which the order $(p_F l)^{-1}$, where l is the mean free path).

A. s-wave

1. Born approximation and the AG Theory

In a seminal paper Abrikosov and Gorkov analysed the effect of the impurity scattering on superconductivity in the Born approximation. We briefly review this analysis to compare its outcome with the results of theories going beyond Born approximation. We follow the treatment of Maki, 1969.

Consider a general impurity potential combining the potential and the magnetic scattering,

$$\widehat{U}_{imp}(\mathbf{k} - \mathbf{k}') = U_{pot}(\mathbf{k} - \mathbf{k}')\tau_3 + J(\mathbf{k} - \mathbf{k}')\mathbf{S} \cdot \boldsymbol{\alpha}, (14.4)$$

where α is defined in Eq. (3.5). AG considered the self energy in the Born approximation,

$$\widehat{\Sigma}(\omega, \mathbf{k}) = n_{imp} \int \frac{d\mathbf{k}'}{(2\pi)^3} \widehat{U}_{imp}(\mathbf{k} - \mathbf{k}') \widehat{G}(\mathbf{k}', \omega) \widehat{U}_{imp}(\mathbf{k}' - \mathbf{k}).$$
(14.5)

Integrating over \mathbf{k}' we find

$$\widetilde{\omega} = \omega_n + \frac{1}{2} \left(\frac{1}{\tau_p} + \frac{1}{\tau_s} \right) \frac{\widetilde{\omega}}{\sqrt{\widetilde{\omega}_n^2 + \Delta^2}}, \quad (14.6)$$

$$\widetilde{\Delta} = \Delta + \left(\frac{1}{\tau_p} - \frac{1}{\tau_s}\right) \frac{\widetilde{\Delta}}{\sqrt{\widetilde{\omega}_n^2 + \Delta^2}},$$
 (14.7)

where the potential (τ_p) and spin-flip (τ_s) scattering times are given by

$$\frac{1}{\tau_p} = n_{imp} N_0 \int d\widehat{\Omega} |U_{pot}(\mathbf{k} - \mathbf{k}')|^2, \qquad (14.8)$$

$$\frac{1}{\tau_s} = n_{imp} N_0 S(S+1) \int d\widehat{\Omega} |J(\mathbf{k} - \mathbf{k}')|^2. \quad (14.9)$$

Here we averaged over all possible directions of the impurity spin.

In the absence of spin-flip scattering both Δ and ω are renormalized identically, and it follows from Eq. (14.3) that the gap remains unchanged compared to the pure case. This is in accordance with Anderson's theorem. The spin flip scattering time (which violates the time-reversal symmetry) enters the equations for $\widetilde{\omega}$ and $\widetilde{\Delta}$ with the opposite sign. Therefore, introducing $u = \widetilde{\omega}/\widetilde{\Delta}$, we find

$$\frac{\omega}{\Delta} = u \left(1 - \frac{(\Delta \tau_2)^{-1}}{\sqrt{1 + u^2}} \right). \tag{14.10}$$

It follows that the gap in the single particle spectrum is $E_{gap} = \Delta (1-(\Delta \tau_s)^{-2/3})^{3/2}$ for $\Delta \tau_s > 1$, and vanishes for $\Delta \tau_s < 1$. This gapless region starts at the value of pairbreaking parameter α

$$\alpha' = \tau_s^{-1} = \Delta_{00} \exp(-\pi/4),$$
 (14.11)

where Δ_{00} is the gap in the pure material at T = 0. The transition temperature is determined from

$$\psi\left(\frac{1}{2} + \frac{1}{2\pi\tau_s T_c}\right) - \psi\left(\frac{1}{2}\right) = \ln\frac{T_{c0}}{T_c},$$
 (14.12)

where $\psi(x)$ is the digamma function and T_{c0} is the transition temperature of the pure material. Consequently, superconductivity is destroyed $(T_c = 0)$ when

$$\alpha_c = \tau_s^{-1} = \pi T_{c0}/2\gamma = \Delta_{00}/2 > \alpha',$$
(14.13)

where $\gamma \approx 1.78$. As $\alpha' \approx 0.912\alpha_c$ AG predicted that a regime of gapless superconductivity exists for a range of impurity scattering (Abrikosov and Gorkov, 1960). This was first confirmed in experiments by Woolf and Reif (Woolf and Reif, 1965).

The evolution of the density of states with increasing disorder was investigated in detail (Ambegaokar and Griffin, 1965; Skalski et al., 1964), and is shown in Fig. 35. For $\alpha < \alpha'$ a hard gap in the single particle spectrum persists up to the critical impurity concentration, as shown in Fig. 36. This result is clearly at odds with our discussion in Sec. VI, which shows that even a single magnetic impurity creates a localized state in the superconducting gap.

2. Shiba impurity bands

In the AG theory the impurity concentration and the strength of the exchange coupling contribute to the suppression of superconductivity as a single pairbreaking parameter, $\alpha = \tau_s^{-1} = (2n_{\rm imp}/\pi N_0) \sin^2 \delta_0 \propto n_{imp} J^2 S(S +$ 1) for isotropic exchange, see Eq. (14.9). This is a result of the Born approximation; in general, the phase shift δ_0 and the concentration of impurities $n_{\rm imp}$ are separate variables that control different aspects of impurity scattering. For example, in the limit of dilute concentration of strong magnetic impurities, the AG approach yields a small scattering rate, and a single-particle spectral gap virtually identical to that in a pure limit. On the other hand, we have learned that in this regime each impurity is accompanied by a bound state with the energy below the gap, and therefore we expect a finite number of these sub-states to exist in a superconductor. This section addresses this dichotomy.

Analysis of the strong scattering regime requires going beyond the Born approximation, and here we use the self-consistent T-matrix approach (Hirschfeld et~al., 1986; Schmitt-Rink et~al., 1986), where the self-energy $\widehat{\Sigma}(\mathbf{p},\omega)=n_{imp}\widehat{T}_{\mathbf{p},\mathbf{p}}$, and

$$\widehat{T}_{\mathbf{p},\mathbf{p}'} = \widehat{U}_{\mathbf{p},\mathbf{p}'} + \int d\mathbf{p}_1 \widehat{U}_{\mathbf{p},\mathbf{p}_1} \widehat{G}(\mathbf{p}_1,\omega) \widehat{T}_{\mathbf{p}_1,\mathbf{p}'}. \quad (14.14)$$

Following the treatment described in Sec. VI, we analyse the pairbreaking in different angular momentum channels. The effective pairbreaking parameter in the

l-th channel is $\alpha_l = n_{imp}(1 - \epsilon_l^2)/(2\pi N_0)$, where ϵ_l is the position of the corresponding bound state, see Eq. (6.10). In analogy with the AG treatment, we find that the ratio $u_n = \widetilde{\omega}_n/\widetilde{\Delta}(\omega_n)$ satisfies the equation (Chaba and Nagi, 1972; Rusinov, 1969)

$$\frac{\omega_n}{\Delta} = u_n \left[1 - \sum_{l=0}^{\infty} (2l+1) \frac{\alpha_l}{\Delta} \frac{\sqrt{1 + u_n^2}}{\epsilon_l^2 + u_n^2} \right], \quad (14.15)$$

where the gap is determined self-consistently from

$$\Delta = 2\pi T N_0 g \sum_n (1 + u_n^2)^{-1/2}.$$
 (14.16)

This equation should be contrasted with Eq. (14.10). The pairbreaking parameter, α_l now depends separately on the position of the single-impurity resonance state, ϵ_l and the impurity concentration, in contrast to the AG theory.

The growth of the impurity band has been investigated for the spherically symmetric case of purely magnetic scattering (Chaba and Nagi, 1972; Rusinov, 1969; Shiba, 1968). The critical concentration of impurities at which the transition temperature vanishes is obtained by setting $T_c = 0$ in the gap equation,

$$\ln \frac{T_{c0}}{T_c} = \psi(1/2 + \alpha/2\pi T_c) - \psi(1/2), \qquad (14.17)$$

where now (Ginzberg, 1979)

$$\alpha = \sum_{l} (2l+1)\alpha_{l}. \tag{14.18}$$

Since the gap equation is identical to that considered by AG, the critical pairbreaking, $\alpha_{cr} = \Delta_0/2$. However, now the critical concentration of impurities depends on the phase shift of scattering by individual impurities, and on the position of the single impurity resonance, see Fig. 37,

3. Quantum spins and density of states

In the fully quantum treatment of the impurity spin, Sec. X, we discussed the competition between gapping the density of states due to superconductivity, and the onset of the Kondo screening of the impurity moment. The main conclusion was that, in contrast to classical impurity spin, the position of the bound state is not simply given by the value of the bare exchange coupling but depends sensitively on the ratio T_K/T_c . Once the position of the bound state is established, in the limit of independent impurities one can consider the growth of the impurity band in analogy with the previous section. As discussed previously, for ferromagnetic coupling of the impurity to the conduction electrons, the bound state is always close to the gap edge, the scattering is weak, and we can expect that the Abrikosov-Gor'kov theory gives

$$n_{cr} = \pi N_0 \Delta_0 \left[\sum_l (2l+1)(1-\epsilon_l^2) \right]^{-1}$$
. (14.19)

The width of the gapless regime now also depends on the details of scattering. For l=0 channel only the gap vanishes when the pairbreaking exceeds the value (Rusinov, 1969; Shiba, 1968)

$$\frac{\alpha'}{\alpha_{cr}} = 2\epsilon_0^2 \exp[-\pi \epsilon_0^2 / 2(1 + \epsilon_0)]. \tag{14.20}$$

In the Born approximation (weak scattering) the bound state moves to the gap edge, $\epsilon_0 = 1$, and we regain the result of Abrikosov and Gorkov. For stronger scattering, $\epsilon_0 < 1$, the realm of gapless superconductivity is enhanced compared to the AG theory. As higher order harmonics are included, the threshold at which the density of states at the Fermi energy becomes non-zero shifts even lower (Ginzberg, 1979).

For l=0 in the limit $\alpha_0 \ll \Delta$ the width of the impurity band around E_0 is estimated to be $W=(8\alpha_0\Delta)^{1/2}(1-\epsilon_0)^{1/4}$, and therefore varies as $n_{imp}^{1/2}$ (Shiba, 1968). Therefore if the resonance state at E_0 is sufficiently close to the gap edge, the concentration, c_0 , at which the top of the impurity band merges with the continuum above Δ is smaller than the critical concentration, c', at which the bottom of the impurity band reaches the Fermi surface and the superconductor becomes gapless (Shiba, 1968), see Fig. 38. In fact, the AG result is an extreme example of this behavior when the states due to individual impurities are infinitely close to the gap edge, and therefore the effect of increasing impurity concentration is an apparent decrease of the gap until the onset of the gapless behavior.

correct results.

When Kondo screening is effective, for antiferromagnetic coupling, the behavior of the density of state and the transition temperature was studied a series of papers by Müller-Hartmann and co-workers (Müller-Hartmann, 1973; Müller-Hartmann and Zittartz, Schuh and Müller-Hartmann, 1978; Zittartz et al., 1972). The main new result was the prediction of the re-entrant behavior for small $T_K/T_c \lesssim 1$. In that case the phase shift of the scattering increases upon lowering temperature, but remains moderate at T_c enabling the transition to the superconducting state. Upon further decrease in temperature, scattering becomes stronger and suppresses superconductivity in a range of phase diagram of Fig. 39. Finally, at lowest temperatures below T_K , the system re-enters local Fermi liquid regime with weak scattering and superconductivity may re-appear.

While further work (Jarrell, 1990; Matsuura et al., 1977) cast doubt on the existence of the third transition, region of two solutions for $T_c(n_{imp})$ was confirmed by theoretical studies. In particular, a combination of quantum Monte Carlo technique with Eliashberg equations gave the dependence of the re-entrance transition on the electron-phonon coupling constant, while accounting non-perturbatively for the Kondo effect (Jarrell, 1990), see Fig. 39. Moreover, the initial decrease of T_c with increasing impurity concentration is fast (Jarrell, 1990; Müller-Hartmann and Zittartz, 1971), and depends on the coupling strangth (Jarrell, 1990). The behavior of the density of states in this limit was investigated in detail (Bickers and Zwicknagl, 1987; Jarrell et al., 1990). The overall shape of the transition temperature as a function of impurity concentration with re-entrant transition was observed in (LaCe)Al₂ alloy series (Maple, 1973).

B. d-wave

For completeness we briefly consider the growth of the impurity band with finite concentration of impurities. As was mentioned above, scalar (non-magnetic) impurities are pair-breakers for any nonconventional superconductor, and substantially change the low-energy spectrum of superconducting quasiparticles. This problem has been addressed in great detail in the framework of the self-consistent T-matrix approximation (for example, see (Balatsky et al., 1994; Gorkov and Kalugin, 1985; Hirschfeld and Goldenfeld, 1993; Hirschfeld et al., 1986, 1988; Lee, 1993; Pethick and Pines, 1986b; Schmitt-Rink et al., 1986)), which leads to the finite density of states at the Fermi level. Here we briefly review the main steps and give results for the quasiparticle scattering rate and low-energy density of states for completeness.

For finite impurity concentration, the self-consistent Green's function, averaged over impurity positions, was given in Eq. (3.21) as

$$\widehat{G}^{-1}(\mathbf{k},\omega) = \widehat{G}_0^{-1}(\mathbf{k},\omega) - \widehat{\Sigma}(\omega). \tag{14.21}$$

with $\widehat{\Sigma}(\omega) = n_{\rm imp} \widehat{T}(\omega)$. In the case of particle-hole symmetry (Hirschfeld *et al.*, 1988), and unconventional gap (defined by us as having a zero average over the Fermi surface, see Sec. I) the only non-vanishing component of the T-matrix is proportional to τ_0 ,

$$T_0(\omega) = \frac{g_0(\omega)}{c^2 - g_0(\omega)}. (14.22)$$

The T-matrix has to be determined self-consistently with $g_0(\omega)\rangle = \frac{1}{2\pi N_0} \sum_{\mathbf{k}} \mathrm{Tr} \widehat{G}(\mathbf{k}, \omega) \widehat{\tau}_0$. Solution of this equation leads to a finite density of

Solution of this equation leads to a finite density of states at the Fermi level. This result was first obtained for Born scattering (Gorkov and Kalugin, 1985; Udea and Rice, 1985), leading to an exponentially small $N(0)/N_0 \approx 4\tau^2\Delta_0^2\exp(-2\Delta_0\tau)$, where τ is the normal state scattering rate. The results are much more dramatic for unitarity scattering (c=0) (Hirschfeld *et al.*, 1986; Schmitt-Rink *et al.*, 1986), when straightforward algebra yields

$$\gamma \simeq \sqrt{n_{\rm imp}(\Delta_0/\pi N_0)},\tag{14.23}$$

where $\gamma = -\mathrm{Im}\,\Sigma(\omega \to 0)$ is the scattering rate for low-energy quasiparticles. For $\omega \lesssim \gamma$, the density of states is determined by impurities and is finite: $N_{\mathrm{imp}}(0)/N_0 = 2\gamma/\pi\Delta_0$. The characteristic width of the impurity-dominated region is $\omega^* \simeq \gamma \propto \sqrt{n_{\mathrm{imp}}}$.

The origin of the finite density of states is the impurity band, grown from the impurity-induced states (consider c=0). Scaling of the impurity bandwidth $\gamma \propto \sqrt{n_{\rm imp}}$ has been obtained earlier for the case of paramagnetic impurities in an s-wave superconductor (Shiba, 1968). The fact that $\gamma \propto \sqrt{n_{\rm imp}}$ is obeyed in the case of a d-wave superconductor with scalar impurities as well is consistent with the claim that the low-energy states in a disordered d-wave superconductor are indeed formed from the bound states at finite concentration. Many questions about the exact nature of the interference between impurity sites in unconventional superconductors remain as of now unanswered. We briefly reviewed some of the relevant work in the introduction, but do not discuss it in depth here.

Notice that the results above are for isotropic impurity scattering. Anisotropic impurities may preferentially scatter electrons between regions with the same, or close values of the gap, so that the scattering is inefficient in suppressing T_c . For general impurity phase shifts this has been considered by Choi, 1999, while for the model with dominant small angle scattering in cuprates (Abrahams and Varma, 2000) the effect was considered by Kee (Kee, 2001).

XV. OPTIMAL FLUCTUATION

A. Introduction

So far we concentrated on discussing the effect of a single impurity on its immediate surrounding and on the combined effect of an ensemble of scattering centers on the spatially averaged properties of a superconductor. In the case of a single pairbreaking impurity the characteristic length is simply the superconducting coherence length, ξ_0 . In the Abrikosov-Gorkov approach the gap is assumed to be uniformly suppressed. If the coherence length is short, this assumption breaks down as the energy cost of local suppression of the order parameter becomes smaller than the cost of uniform reduction of the gap. In this case again the length scale of this suppression is of the order of ξ_0 . These results are obtained by carrying out a standard impurity averaging procedure at the mean field level, i.e. averaging over all the possible configurations of impurity atoms (Abrikosov et al., 1963).

It is clear, however, that some physics is missing in such an approach. Among all the realizations of the impurity distribution in a sample of size L_0 there exist regions where the local impurity concentration, on some characteristic scale $L \ll L_0$, differs significantly from the average concentration, n. If the local impurity concentration is sufficiently high, for $L > \xi_0$ superconductivity may be locally destroyed of sufficiently suppressed to generate a bound quasiparticle state at an energy $E \ll \Delta_0$.

Of course, such regions are rare. There is a high entropy cost in creating an impurity droplet with the concentration significantly different from the average and hence the probability of encountering these regions is small. However, the states localized in these droplets make a non-perturbative contribution to the density of states averaged over the entire sample, N(E), and qualitatively modify its behavior compared to the mean field (Abrikosov-Gorkov and Shiba) treatment. Quite dramatically, they make any s-wave superconductor with a small concentration of magnetic impurities ($\Delta \tau_s \gg 1$) gapless (Balatsky and Trugman, 1997). It is due to such a dramatic modification that the interest in these "tail" states stretching below the mean field gap edge has peaked in recent years.

The problem of tail states did not originate in the study of superconductivity. The contribution of regions of anomalous impurity concentration to the net density of states below the gap edge was first considered in doped semiconductors by Lifshitz (Lifshitz, 1964a,b, 1967). He was the first to show that such rare impurity configurations create a local profile in the Coulomb potential that can have bound states, and therefore gives rise to the non-vanishing density of states below the bottom of the band, E_g . Henceforth the states localized in the droplets of impurities have become known as 'Lifshitz tails', and have been extensively studied (Halperin and Lax, 1966; Van Mieghem, 1992; Zittartz and Langer, 1966).

While, in retrospect, it is natural that inhomogeneities lead to a low-energy tail in the density of states in superconductors in much the same way, little attention has been paid to this problem until the paper by Balatsky and Trugman (Balatsky and Trugman, 1997). Their study was stimulated by the experimental observations that the tunneling density of states in s-wave superconductors with magnetic impurities is far greater at low energies than the Abrikosov-Gorkov theory suggests (Bader et al., 1975; Edelstein, 1967; Woolf and Reif, 1965). A number of theoretical studies of the tail states followed, and this topic is now a subject of active interest.

Below we first briefly review the physical picture of the tail states in semiconductors, and then describe how it is applied to the subgap states in superconductors with impurities.

B. Tail states in semiconductors and optimal fluctuation

In a semiconductor there are two distinct situations: a) heavily doped, and b) lightly doped with impurity atoms. In the former case a localized tail state with energy $E < E_q$ forms in the impurity-rich region, and the extent of its wave function greatly exceeds the average distance between individual shallow sites. Therefore the exact impurity potential can be replaced by a smooth function, averaged over regions containing many impurities. The probability of realization of the potential with the "right" energy of the bound state among all the possible impurity distributions determines its contribution to the DOS. In the latter case the number of impurity sites needed to form a bound state depends on how deep below the band edge the energy of such a state is. For example, if each impurity binds an electron at energy E_1 , while E_2 is the energy of the state bound by two impurities on neighboring lattice sites, to obtain a localized state below E_1 but above E_2 , one simply needs to find a region where the two impurities are at a particular finite distance from each other. The probability of finding such an impurity pair determines the density of states (Lifshitz, 1964b, 1967). As we go to energies below E_2 we need to position three impurities etc.

For energy, E, the most probable (albeit still very rare) configuration of impurities that creates a potential U, with a bound state from the solution of Schrödinger's equation $[H_{band} + U]\psi = \mathcal{E}[U]\psi$, such that $\mathcal{E}[U] = E$, and therefore contributes the most to N(E) is called the optimal fluctuation. Given the probability density for the impurity potential, P[U], and the density of states in this potential,

$$N(E) = \int \mathcal{D}UP[U]\delta(E - \mathcal{E}[U]), \qquad (15.1)$$

the optimal fluctuation is obtained by using the saddle point approximation and minimizing the resulting functional with respect to U. This approach finds the cheapest (from the entropy consideration) impurity potential that creates a bound state at E. Therefore it optimizes the non-uniform impurity distribution (fluctuation from the uniform average) to the given energy, hence the name "optimal fluctuation". The general technical difficulty of minimization lies in its essential nonlinearity: the optimal potential depends on the wave function of the particle in this potential.

Let us consider the example of many uncorrelated shallow impurity centers forming an extended potential. It is described by the Gaussian probability density,

$$P[U] \propto \exp\left[-\frac{1}{2U_0} \int d^d \mathbf{r} U^2(\mathbf{r})\right].$$
 (15.2)

Saddle point approximation for Eq.(15.1) gives

$$\ln \frac{N(E)}{N_0} \approx -\mathcal{S}[U_{opt}],\tag{15.3}$$

where the optimal fluctuation is obtained by minimizing the functional

$$S[U] = \frac{1}{2U_0^2} \int d^d \mathbf{r} U^2(\mathbf{r}) + \lambda \left(\mathcal{E}[U] - E \right)$$
 (15.4)

with respect to the potential U and the Lagrange multiplier λ . At the simplest level it is sufficient to consider only the potentials where $\mathcal{E}[U] = E$ is the lowest energy state in the potential U; fluctuations where E coincides with the higher eigenstates are exponentially less probable. In a semiconductor the kinetic energy of the quasiparticles is $p^2/2m^*$, where m^* is the effective mass. Consequently, in a potential well of depth U (all energies are measured from the band edge) and size L the energy of the localized state is of the order of $U + 1/(mL^2) = E$ $(\hbar = 1)$. In the optimal fluctuation $E \sim U \sim L^{-2}$, so that the action for such fluctuation is $S[U] \approx L^d U^2/U_0^2$, or $\ln[N(E)/N_0] \approx -|E|^{2-d/2}/U_0^2$ (Halperin and Lax, 1966; Lifshitz, 1964b). Importantly, the characteristic size of the optimal fluctuation, $L \propto |E|^{-1/2}$ increases as the energy approaches the band edge, while its depth, $|U| \sim |E|$ decreases: the potential becomes more shallow and ex-

More formally, note that the energy of the bound state is the expectation value of the hamiltonian over the wave function of the bound state, $\psi(\mathbf{r})$, is equal to E,

$$\mathcal{E}[U] = \langle \widehat{H} \rangle = \langle \psi | \frac{\mathbf{p}^2}{2m^*} + U | \psi \rangle = E \tag{15.5}$$

Minimization of the action in Eq.(15.4) with respect to U dictates that

$$U(x) = -\lambda U_0^2 \langle \psi | \frac{\delta \widehat{H}}{\delta U} | \psi \rangle = -\lambda U_0^2 \psi^2(x), \qquad (15.6)$$

while minimization with respect to λ dictates that, in this potential, the bound state is at energy E, i.e. (setting $m^* = 1$ for simplicity)

$$\left[-\frac{1}{2}\nabla^2 - \lambda U_0^2 \psi^2(\mathbf{r}) \right] \psi(\mathbf{r}) = E\psi(\mathbf{r}). \tag{15.7}$$

In one dimension this equation is exactly solved to give (Halperin and Lax, 1966)

$$\psi(x) = \sqrt{\frac{\kappa}{2}} \operatorname{sech} \kappa x, \qquad (15.8)$$

$$\lambda U_0^2 = 8\kappa, \tag{15.9}$$

with $E = -\kappa^2/2$. Therefore the "optimal action" $S(U_{opt}) \simeq \kappa^2/U_0^2 \sim |E|^{3/2}$ as expected.

In higher dimensions the corresponding equation is not solvable, however, one can extract the energy dependence of the action by assuming a spherically symmetric optimal fluctuation and an exponentially decaying at large distances bound state to find the Lifshitz tail $N(E) \propto \exp(-|E|^{2-d/2})$ (Lifshitz, 1964b; Lifshitz et al., 1988). To obtain the pre-exponential factor one needs to consider all the wave functions in the potential, and the corresponding analysis has only been carried out in low dimensions (Halperin and Lax, 1966).

C. S-wave superconductors

1. Magnetic and non-magnetic disorder

Since the effect of the tails is most dramatic for fully gapped superconductors, most studies focused on conventional, s-wave superconductors with pairbreaking magnetic impurities. The general route followed in all the investigations is similar to the approach described above: given the probability density of different impurity configurations, and the hamiltonian of the system with the potential of each impurity distribution, we find the most probable configuration of impurities that gives rise to a state at a given energy within the gap. Technical implementations of this algorithm vary depending on the specifics of the problem at hand, see below.

There are important differences between the physics of the optimal fluctuation in such a superconductor and an optimal potential well for quasiparticles below the band gap discussed in the previous section. First, since the superconducting quasiparticles consist of electron pairs close to the Fermi surface, their kinetic energy is not simply that of a band particle, but is given instead by the Hamiltonian

$$\widehat{H} = \widehat{\xi}\tau_3 + \Delta(\mathbf{r})\tau_1\sigma_2, \tag{15.10}$$

where τ_i and σ_i are the Pauli matrices in the particlehole and the spin space respectively, so that $\tau_i\sigma_j$ is a 4×4 direct product. Therefore, while the envelope of the tail state wave function still varies smoothly over the length scale of inhomogeneities in the impurity distribution, the rapid oscillations on the atomic scale associated with the Fermi surface have to be taken into account. As will be seen below, these considerations substantially modify the behavior of the tail states.

Second, the scattering potential is a matrix in particlehole and spin space. In general, an impurity site acts both as a potential and a magnetic scatterer, so that the total scattering potential is

$$\widehat{\mathbf{U}}(\mathbf{r}) = \sum_{i} \left[U_0 \tau_3 \delta(\mathbf{r} - \mathbf{r}_i) + J(\mathbf{r} - \mathbf{r}_i) \mathbf{S}_i \cdot \boldsymbol{\alpha} \right], (15.11)$$

using the Nambu notations. The potential part of the scattering, U_0 , is not pairbreaking in accordance with Anderson's theorem. However, since the size of the optimal fluctuation is large compared to the correlation length, it is necessary to distinguish between the cases where the motion of quasiparticles within the optimal fluctuation is diffusive (strong potential scattering, $\Delta \tau \ll 1$, $\tau \ll \tau_s$, where τ is the transport lifetime) and ballistic (weak potential scattering, $\tau \gg \tau_s$). Moreover, we should also distinguish between strong and weak magnetic scattering: if the magnetic scattering is strong there are resonance (Shiba-Rusinov) states in the gap, and the tails stretch not from the mean-field gap edge, but from the localized impurity band. If the magnetic scattering can be treated in the self-consistent Born approximation, the tail states

emerge below the Abrikosov-Gorkov renormalized single particle spectral gap, $\Delta_0 = \Delta (1-(\Delta \tau_s)^{-2/3})^{3/2}$, where Δ is the self-consistent value of the superconducting order parameter. In the AG limit the probability density for the magnetic impurity potential is gaussian, as it is averaged over a large number of impurity sites. In contrast, in the unitarity scattering limit there are subgap states localized on one or a few impurities; consequently, we deal with the Poisson density distribution. These various possibilities provide for a rich variety of behavior that is still a subject of active interest.

All models of tail states due to magnetic impurities studied so far ignore interactions between the impurity spins: it was shown in Ref. (Larkin and Ovchinnikov, 1972) that the RKKY interaction and glassy behavior of impurity spins modify the AG results very weakly. The models also treat impurity spins as classical Heisenberg spins, and therefore cannot account for the Kondo effect. This is justified either when the Kondo temperature of individual impurity sites is much smaller than the superconducting transition temperature, $T_K \ll T_c$ (and depletion of states at the Fermi level prevents screening of the local moment), or in the opposite limit, $T_K \gg T_c$, when the moments are quenched already in the normal state (Müller-Hartmann and Zittartz, 1971).

To our knowledge, the first paper discussing the influence of non-uniform impurity distribution on the transition temperature in analogy with Lifshitz's work appeared in 1968 (Kulik and Itskovich, 1968). These authors found that, in the limit of average impuritity concentration $n \ll n_{cr}$ of the Abrikosov-Gorkov theory, there are localized regions that become superconducting at a temperature $T_c' > T_c(n)$, where $T_c(n)$ is the corresponding AG transition temperature. The difference between the two was evaluated for parabolic one-dimensional variation of the effective impurity potential. Kulik and Itskovich, 1968 also noted that their results will be modified if there is non-magnetic as well as magnetic scattering, but did not address this question further.

2. Diffusive limit, weak magnetic scattering

If the scattering on individual magnetic impurities is weak, the optimal fluctuation is created by large droplets of these scattering centers. Since the impurities are uncorrelated, the probability density for the impurity potential is Gaussian, which greatly simplifies the analysis.

Historically, most of the studies have been carried out in the diffusive limit. One of the first papers investigated the smearing of the gap edge due to local fluctuations in the effective interaction between electrons (Larkin and Ovchinnikov, 1972). If the correlation length of the inhomogeneities, $r_c \gg \xi$, where ξ is the coherence length of the dirty superconductor, $\xi \sim (D/\Delta)^{1/2}$, and D is the diffusion constant, the order parameter simply locally adjusts to the value of the inter-

action and the density of state is determined by the local gap amplitude,

$$N(E) = \int_{0}^{\infty} N(E, \Delta)W(\Delta)d\Delta, \qquad (15.12)$$

where $W(\Delta)$ is the probability density of the gap.

In the opposite limit of short-range correlations in the pairing interaction, the finite density of states below the mean field gap edge is due to the states spatially localized in correlated droplets of size $r_0 \sim \xi[(\Delta_0 - E)/\Delta]^{-1/4}$ (increasing rapidly as $E \to \Delta_0$ as in a semiconductor), which leads to $N(E) \propto \exp(-[(\Delta_0 - E)/\Delta]^{5/4}$ in d=3. As in semiconductors, the high entropy cost of a large droplet is offset by the lowering of the kinetic energy of the bound state. Indeed, in a clean system with $\Delta \tau_s \gg 1$, and therefore $\delta_0 \approx \Delta$, we find the characteristic kinetic energy, $D/r_0^2 \simeq \sqrt{\Delta_0^2 - E^2}$.

Recently it was argued that the above result is flawed since it does not account properly for the rapid oscillations of the wave function of the bound state on the scale of the Fermi wavelength (Meyer and Simons, 2001). These authors used a field-theoretical approach that maps the disordered superconducting system onto a non-linear σ -model (for a review, see Altland et~al., 2000) to show that, while the droplet size for the optimal fluctuation is identical to that obtained by Larkin and Ovchinnikov, the subgap density of states is $N(E) \propto \exp\{-[(\Delta_0 - E)/\Delta]^{(6-d)/4}\}$, which gives the exponent 3/4, rather than 5/4, for d=3.

The paper that brought the investigation of the subgap states in superconductors into the limelight after a quarter-century-long hiatus was the study of the density of states due to regions where the impurity concentration is sufficient to locally destroy superconductivity (Balatsky and Trugman, 1997). In that case the spectrum of the fluctuation region is similar to that of a disordered metallic grain of the same size, L, and depends on the mean level spacing of the grain, δ_L . The average density of states was obtained in two steps. First, an average over all realizations of disorder for grains of size L yielded $N_L(E) \sim \delta_L^{-1}$. Second, the probability of finding a fluctuation region of size L with the critical concentration of impurities, n_c , for a given average impurity concentration, n, $P_L(n_c; n)$ was used to define the average density of states over the entire sample, $N(E) \sim \int dV P_L(n_c; n) N_L(E)$. This integral was estimated to find

$$N(E) \sim \delta_{L_0}^{-1} \exp[-L_0^d(n_c \ln(n_c/n) - n_c + n)],$$
 (15.13)

as $E \to 0$. Here $L_0 = (\xi_0 l)^{1/2}$ is of the order of the coherence length in a dirty superconductor with $l \ll \xi_0$.

At energies closer to the gap edge, in the spirit of optimal fluctuation, it is not necessary to destroy superconductivity completely to generate the tail states. Using the instanton approach for the nonlinear σ -model, Lamacraft and Simons demonstrated how these states arise out of inhomogeneous instanton configurations for

the action (Lamacraft and Simons, 2000, 2001). The resulting optimal action reads

$$S_0 = a_d (\Delta_0 \tau_s)^{2/3} (1 - \Delta_0 \tau_s)^{-2/3})^{-(2+d)/8} \left(\frac{\Delta_0 - E}{\Delta}\right)^{(6-d)/4}.$$
(15.14)

density of states, varies as $N(E) \sim \exp[-4\pi g(\xi/L)^{d-2}S_0] \sim \exp\{-[(\Delta_0 - E)/\Delta]^{(6-d)/4}\}$. Here g is the bare conductance and $a_d \sim 1$

That approach appears sufficiently general to analvse nucleation of domains in a variety of sys-It was used to re-derive within this frametems. work (Lamacraft and Simons, 2001) the universal gap fluctuations in small metallic grains, first obtained using random-matrix theory (Vavilov et al., 2001), namely $N(E) \sim \exp[-(\Delta_0 - E)^{3/2}]$, valid for $\Delta_0 - E \ll \Delta_0$. In this regime the spatial extent of the optimal fluctuation is greater than the size of the grain, so that effectively we are in zero dimensions, d=0, and the exponent 3/2agrees with the general result of Lamacraft and Simons, (6-d)/4. In the same zero-dimensional limit, but at lower energies, $E \ll \Delta_0$, the random matrix theory gives $N(E) \sim (|E|/\delta^{3/2}\Delta^{1/2}) \exp[-\pi \tau_s (\Delta_0 - E)^2/\delta],$ where δ is the mean level spacing in the grain (Beloborodov et al., 2000).

3. Diffusive limit, strong scattering

Recently the field theoretical treatment been extended to the case of strong scatterers (Marchetti and Simons, 2002). In that case the probability distribution of scattering strength is Poissonian rather than Gaussian. In the field theoretical language this implies that the action cannot be expanded to second order in the magnetic potential, as it was for the weak potential. Marchetti and Simons circumvented this difficulty by considering the dominant contribution of droplets densely populated by magnetic impurities, so that $\xi \ll l_s \ll l$. As we saw above, an impurity band emerges within superconducting gap in the limit of nearunitary scattering already at the level of the mean field theory. Consequently, the tail states extend from the edge of the continuum above Δ_0 as well as from the top and bottom of the impurity band, see Fig. 41. According to Marchetti and Simons in all these cases the density of states varies as $N(E) \propto \exp[-(|E - E_i|/\Delta)^{(6-d)/4}]$, where E_i is the appropriate band edge. Therefore the exponent of the action is identical to that found in other systems in the diffusive limit.

4. Ballistic limit, weak scattering

It was noticed early on that in some systems the magnetic scattering is dominant: upon increasing the concentration of impurities the increase in residual resistivity ratio correlates with the suppression of the superconducting transition temperature (Edelstein, 1967). Since both

magnetic and nonmagnetic scattering contribute to the resistivity, but only the magnetic part suppresses T_c , this is an indication of almost purely spin-dependent scattering. Shytov and co-workers (Shytov et al., 2003) considered the subgap states in this limit in clean $(l \gg \xi_0)$ or $\Delta \tau_s \gg 1$ limit, when the spectral gap obtained in the self-consistent Born approximation nearly coincides with the order parameter, $\Delta_0 \approx \Delta$.

Once again, since the impurities are assumed to be weak, the optimal fluctuation for states not too far from the gap edge is large and shallow, and the spin-dependent potential has the Gaussian probability density. When the size of the optimal fluctuation is much greater than the superconducting coherence length, $l\gg L\gg \xi_0$, the motion of the quasiparticles in this potential is ballistic. As a result, direct mapping on the non-linear σ -model is not feasible, and the problem requires quantum mechanical treatment akin to that in a semiconductor discussed above.

As in that case, we first consider the one-dimensional problem. An important assumption (discussed below) is that a ferromagnetic fluctuation maximizes the effect of the impurity potential. Choosing the direction of the impurity spins along the y axis, performing rotation $\sigma_2 \rightarrow \sigma_3$, we remove the vector character of the slowly varying potential \mathbf{U} , and consider the hamiltonian

$$\widehat{H}_{\pm} = \widehat{\xi}\tau_3 \pm \Delta_0 \tau_1 \pm U(\mathbf{r}). \tag{15.15}$$

The hamiltonian, however, still remains a matrix in the particle-hole space, and the wave functions of the optimal fluctuation are the Nambu spinors Ψ .

Let us again discuss the physical behavior of the optimal fluctuation qualitatively. We linearize the kinetic energy near the Fermi surface, so that typical kinetic energy in an OF of size L is $\xi \simeq v_F/L$. Then the energy of a quasiparticle in the optimal fluctuation (measured from the Fermi energy) is $E \simeq U + \sqrt{\Delta_0^2 + v_F^2/L^2}$. For the energies close to the superconducting gap, $(\Delta_0 - E)/\Delta_0 \ll 1$, the OF is large $(L \gg \xi_0 = v_F/\Delta_0)$ and shallow $(|U|/\Delta_0 \ll 1)$, so that $E - \Delta_0 \approx U + v_F^2/(\Delta_0 L^2)$. Introducing the dimensionless energy $\epsilon = E/\Delta_0$, we obtain, in analogy with the arguments above, $|U|/\Delta_0 \simeq \xi_0^2/L^2 \simeq 1 - \epsilon$. Notice that the size of the fluctuation is $L \simeq \xi_0/\sqrt{1-\epsilon} \gg \xi_0$. As a result, we find $S[U] \approx LU^2/U_0^2 = \Delta_0^2 \xi_0 (1-\epsilon)^{3/2}/U_0^2$. From the definition of U_0 it follows that

$$-\ln \frac{N(E)}{N_0} \approx \mathcal{S}[U_{opt}] \simeq (\Delta_0 \tau_s) (1 - \epsilon)^{3/2}.$$
 (15.16)

The energy dependence in Eq. (15.16) is identical to the result of Lifshits in d=1, despite the linear, rather than quadratic, dependence of the kinetic energy on the size of the droplet. This follows from the smallness of this energy compared to the gap: even though $\xi \propto 1/L$, the expansion is in ξ^2 .

The minimization of the saddle-point action proceeds exactly following the steps in section XV.B. For spin "up" particles $\mathcal{E}_{+}[U] = \langle \Psi | \widehat{H}_{+} | \Psi \rangle$. Minimization with respect to U gives

$$U(x) = -\lambda U_0^2 \langle \Psi | \frac{\delta \hat{H}_+}{\delta U} | \Psi \rangle. \tag{15.17}$$

In principle this variational derivative includes the effect of the self-consistent suppression of the gap. However, it can be explicitly demonstrated (Shytov et al., 2003) that the effect of self-consistency is small. Then, in exact analogy to the semiconductor problem, $U(x) = -\lambda U_0^2(\Psi^*(x)\Psi(x))$, where $(\Psi^*\Psi)$ denotes the scalar product in particle-hole space. In turn, Schrödinger equation takes the form

$$\left[-iv_F \frac{\partial}{\partial x} \tau_3 + \Delta_0 \tau_1 - \lambda U_0^2 (\Psi^* \Psi)\right] \Psi = E \Psi. \quad (15.18)$$

This equation is solved by introducing the bilinear forms $\Psi^{\star}(x)\tau_{i}\Psi(x)$. These bilinears play the role of the Halperin-Lax wave function in the Nambu space, and yield

$$R_0 = \frac{1 - \epsilon^2}{\xi_0 \arccos \epsilon} \frac{1}{\epsilon + \cosh(2x\sqrt{1 - \epsilon^2}/\xi_0)}, (15.19)$$

$$R_1 = R_0(\epsilon + \xi_0 R_0 \arccos \epsilon), \tag{15.20}$$

$$R_2 = \sqrt{R_0^2 - R_1^2}, (15.21)$$

and $R_3 = 0$ (Shytov *et al.*, 2004). The physical potential of the optimal fluctuation is (Shytov *et al.*, 2003)

$$\frac{U(x)}{2\Delta_0} = -\frac{1 - \epsilon^2}{\epsilon + \cosh(2x\sqrt{1 - \epsilon^2}/\xi_0)}.$$
 (15.22)

which corresponds to the value of the action

$$S[U] = 8\pi(\Delta_0 \tau_s) \left[\sqrt{1 - \epsilon^2} - \epsilon \arccos \epsilon \right].$$
 (15.23)

For $\epsilon \approx 1$ the length scale of the optimal fluctuation is $\xi_0/\sqrt{1-\epsilon^2}$, its depth is $U \sim \Delta_0(1-\epsilon^2)$, and the density of states $N(E) \sim \exp[-(1-\epsilon^2)^{3/2}]$, in complete agreement with qualitative estimates.

The most important observation of Shytov $et\ al.$, 2003 is that in higher dimensions the optimal fluctuation is strongly anisotropic, in contrast to both the conventional semiconductors and superconductors in the diffusive limit. This is a direct consequence of the composite nature of superconducting quasiparticles: they are made out of objects that move with the Fermi velocity. The wave function of the subgap state is concentrated along the quasiclassical trajectory, which is a chord in a potential of any shape. Consequently, there is little energy cost in reducing the size of the OF in the "transverse" direction, while the smaller volume makes such fluctuations more probable, see Fig. 40. As a result, the optimal fluctuation is strongly elongated in one (x) direction. The wave function of the bound state can be written as

 $\Psi(x, \mathbf{y}) = \exp(ik_F x)\Phi(x, \mathbf{y})$, where \mathbf{y} denotes the transverse d-1 coordinates, and Φ is a slowly varying function. The kinetic energy of the quasiparticle is

$$\hat{\xi}\Psi \approx -e^{ik_Fx} \left(iv_F \frac{\partial}{\partial x} + \frac{\nabla_y^2}{2m} \right) \Phi \sim \left(\frac{v_F}{L_x} + \frac{1}{mL_y^2} \right) \Psi.$$
(15.24)

The transverse size of the fluctuation can therefore be reduced until the second term becomes comparable to the first, i.e. $L_y \simeq (\lambda_F L_x)^{1/2}$, where $\lambda_F \simeq k_F^{-1}$ is the Fermi wavelength. Consequently, $|U|/\Delta_0 \sim 1 - \epsilon$ and $L_x \sim \xi_0/\sqrt{1-\epsilon}$, and

$$S[U_{opt}] \simeq L_x L_y^{d-1} \frac{U^2}{U_0^2} \simeq (\Delta_0 \tau_s) \left(\frac{E_F}{\Delta_0}\right)^{\frac{d-1}{2}} (1 - \epsilon)^{\frac{7-d}{4}},$$
(15.25)

where E_F is the Fermi energy. Consequently, the density of states, $N(E) \sim \exp[-(1 - \epsilon)^{(7-d)/4}]$.

The action for this anisotropic fluctuation is smaller than that for an isotropic droplet with the same energy of the bound state, by a factor of $(E_F/\Delta_0)^{(d-1)/2}(1-\epsilon)^{-(d-1)/4}$, so that the corresponding DOS is exponentially higher.

Since the optimal fluctuation is a result of a saddle point approximation for the functional integral, Eq. (15.1), it is only valid when $S[U_{opt}] \gg 1$, or

$$1 - \epsilon \gg (\Delta_0 \tau_s)^{\frac{4}{d-7}} \left(\frac{\Delta_0}{E_F}\right)^{\frac{2(d-1)}{7-d}}.$$
 (15.26)

For d=1 this condition becomes $1-\epsilon\gg (\Delta_0\tau_s)^{-2/3}$, while for d=3 it does not depend on the gap amplitude, $1-\epsilon\gg (k_Fl)^{-1}$.

It is possible to compare the densities of states given by different approaches at the crossover scale between the diffusive and the ballistic regimes (Vekhter et al., 2003). A transition to the diffusive regime occurs when the size of OF $L \geq v_F \tau_s$, or $1 - \epsilon \leq (\Delta_0 \tau_s)^{-2}$. The result of Ref.(Lamacraft and Simons, 2000) for $\Delta_0 \tau_s \gg 1$ is $S_D = (\Delta_0 \tau_s)^{5/3} (E_F/\Delta_0)^{d-1} (1-\epsilon)^{(6-d)/4}$. Consequently, at the crossover point the action from Eq. (15.25) is smaller, $S_D/S_0 \simeq (E_F/\Delta_0)^{(d-1)/2} (\Delta_0 \tau_s)^{7/6} \gg 1$, and the OF found by Shytov et al. corresponds to a greater DOS. Therefore the structure of the OF near the crossover between the ballistic and diffusive regimes still resembles closely that given above. As the size of the OF increases even further, the anisotropic fluctuation becomes insupportable due to diffusive motion.

Balatsky and Trugman (Balatsky and Trugman, 1997) considered only the DOS at E=0 due to the suppression of superconductivity by paramagnetic impurity potential. They needed a large volume fluctuation, $V \geq \xi^d$, which is less probable and yields lower DOS than that of Eq. (15.25). Vekhter *et al.*, 2003 checked whether local suppression of the gap from Δ_0 to E due to a large number of impurities with *uncorrelated* spins (as opposed to a ferromagnetic OF above) is advantageous. For $1 - \epsilon \ll 1$

the local pairbreaking rate, γ , needed to reduce the gap to E is $\gamma \tau_s \approx 1 + (1 - \epsilon)(\Delta_0 \tau_s)^{2/3}$, and the volume of the region has to be at least equal to that of the anisotropic OF to avoid high kinetic energy cost (this is an underestimate since it ignores proximity coupling to bulk). In that case the optimal action $S_{BT}/S_0 \approx (\Delta_0 \tau_s)^{1/3} (E_F/\Delta_0) \bar{c}$, where $\bar{c} = n_{imp} \lambda_F^d$ is the atomic concentration of impurity atoms. As a result, for realistic values of \bar{c} and clean samples $S_{BT} \gg S_0$, and the DOS given by the action in Eq. (15.25) is higher.

Therefore the ballistic limit of the action obtained by Shytov *et al.*, 2003 is expected to be valid near the crossover between the ballistic and the diffusive regimes.

5. Ballistic regime, strong scattering

As of today, we are not aware of any investigations of the structure of the optimal fluctuation in the ballistic regime, when there exist bound states on individual magnetic impurities. It is reasonable to assume that the result differs from the standard Lifshitz formula for the same reason as in the section above: the wave functions of the states localized on magnetic impurities in superconductors oscillate with the Fermi wavelength, see Sec. VI. As a result, in the dilute impurity limit, the shift of the energy level localized on, for example, two impurities located at distance $R \gg p_F^{-1}$, will be suppressed by the typical factor $\exp(-R/\xi_0)$ (Rusinov, 1968). Consequently, the states significantly below the impurity band must be created by a large number of impurities or impurities located on neighboring lattice sites. This problem still awaits further investigation.

6. Summary

In s-wave superconductors with magnetic impurities the density of states does not vanish irrespective of the concentration and nature of the impurity scattering. The tails of the density of states extend into the mean field gap. Therefore all superconductors with magnetic impurities are gapless. This behavior is qualitatively illustrated in Fig. 41.

XVI. SUMMARY AND OUTLOOK

While considering the role of impurities in conventional and unconventional superconductors, this review focused on theoretical and experimental results that highlight the new physics beyond standard Abrikosov-Gor'kov theory, Anderson theorem and average lifetime effects. The studies of disorder in s-wave superconductors were carried out in detail in the 1960's. We discussed more recent results in this field. Our main emphasis has been on how individual impurities influence local electronic states in their immediate vicinity, and on deviations from the standard

Abrikosov-Gorkov theory on mesoscopic scales. This focus is dictated both by the advances in experimental techniques, which can now use NMR methods and STS measurements to probe electronic states with atomic spatial resolution, at the scales where impurities perturb their surrounding, (Fischer and et al, 2004), and the concomitant development of new theoretical approaches.

The stimulus for such extensive studies is that impurities are markers that allow to reveal the nature of correlations and pairing of the state where impurities are placed. Indeed particular pattern of impurity-induced electronic states is closely connected to the symmetry of the superconducting gap and helps us to understand the nature of superconducting pairing. If strong electronic correlations in the ground state are present, they also are reflected in details of impurity induced states. Therefore watching the waves created by throwing a pebble in the pond of correlated electrons helps us understand the properties of the underlying electronic liquid.

We kept the discussion general to allow applications to other systems and materials. For instance, this was our rationale for employing the BCS state to describe superconductivity. We believe that it is a good approximation in heavy fermion, organic superconductors and SrRuO₄, at very low energy. At the same time, deviations from this mean field picture may provide additional details on the underlying physics of the particular material. Majority of the data at a moment are obtained in high- T_c materials. It is clear that similar local effects are present around impurities in other unconventional superconductors, e.g. in $Na_xCoO_2 \cdot yH_2O$ superconductors (Wang and Wang, 2004), although we are not aware of any data on single impurity states in these materials. Given the importance of the impurity states, this field will undoubtedly be extended to other systems by future experiments.

Outlook for the future. New ideas and directions continue to emerge in the studies of electronic properties induced by impurities. The suite of new experimental tools that address local electronic effects, such as STM, will help to clarify the role of interference between several impurities, and pave the way towards connecting the microscopic local states with average properties. Recent theoretical work addressed some aspects of this subject (Andersen, 2003; Atkinson et al., 2003; Morr and Balatsky, 2003; Morr and Stavropoulos, 2003; Zhu et al., 2003, 2004b), and is awaiting direct comparison with experiment.

Another promising avenue is combining the spatial resolution of STM-STS with the time resolution. The subject is still in its infancy, both theoretically and experimentally, but hold immense promise for the future. Sec. XI reviewed some of very recent work in this direction. Temporal and spatial characterization of the states generated by dynamical impurities allow exploration of the correlations inside the electronic state in which impurity is placed. One obvious example where such characterization is crucial is the Kondo effect in a supercon-

ducting state. It is desirable to have a time resolved measurements that allow to visualize the Kondo effect in a superconductor. Another interesting problem that needs further elaboration is a role of collective modes in impurity-induced states. We are only starting to investigate these questions, as discussed in Sec. XII.

Real progress on these problems will be made when we have real data. As usual, one should expect that the data will have surprises that were not anticipated in simple theoretical models. This will motivate further theoretical studies, stimulate more measurements, and therefore will lead to a rapid further development of the field. They can provide space (and time) resolved window into the intimate workings of the correlated electron matter. We have every reason to be enthusiastic and optimistic about the future the field of impurity states in superconductors, and in other correlated electron systems.

Acknowledgments

We would like to thank many of our colleagues for useful discussions. We are especially grateful to our collaborators over many years who were instrumental in our work on the subjects that are reviewed here. Without their insights and knowledge this work would be impossible. We thank Ar. Abanov, E. Abrahams, B. Altshuler, A. R. Bishop, A. H. Castro Neto, J. C. Davis, D. Eigler, L. P. Gor'kov, M. J. Graf, I. A. Gruzberg, P. J. Hirschfeld, W. Ho, C. R. Hu, T. K. Lee, D. K. Morr, I. Martin, D. Pines, A. Rosengren, M. I. Salkola, J. A. Sauls, D. J. Scalapino, J. R. Schrieffer, A. V. Shytov, Q. Si, C. S. Ting, M. Vojta, Z. D. Wang, and J. Zaanen for fruitful discussions. This work was supported by the U.S. Department of Energy (A.V.B. and J.X.Z.) and by the Board of Regents of Louisiana (I. V.).

List of Symbols

Quantity	Explanation
a	Lattice parameter
$b(b^\dagger)$	Bosonic annihilation (creation) operators
$c(c^\dagger)$	Fermionic ahhihilation (creation) operators
d	Spatial dimension
D	Half energy bandwidth
Δ_0	Superconducting energy gap
Δ_k	Momentum-dependent superconducting energy gap
$\phi_n(\mathbf{r})$	Electron eigenfunction
E_F	Electron Fermi energy
$G(\tau, \tau'), G(\tau, \mathbf{r})$	Electron Green's function in coordinate space
$G(\omega_n, \mathbf{k}), G(\mathbf{k}, \omega_n)$	Electron Green's function in Matsubara frequency and momentum space
H, \mathcal{H}, H_{int}	Hamiltonian
J, J_0, J_c	Exchange coupling
L	Linear dimension of a system
μ	Chemical potential
$N(\epsilon)$	Electron density of states
$N(\epsilon, \mathbf{r}), N(E, i)$	Electron local density of states
$\psi(\mathbf{r}(\psi^{\dagger}(\mathbf{r}))$	Fermionic field operators in continuum space
$ \Psi angle,\;\; \Psi_0 angle$	BCS variational wavefunction
$ \Psi_{-1}\rangle, \Phi_{-1}\rangle$	Excited variational wavefunction with single particle excitation present
r	Spatial coordinates
au	Pauli matrices in spin space
au	Pauli matrices in Nambu space
$V_{lphaeta\gamma\delta}, ilde{V}_{lphaeta}$	Superconducting pairing interaction
\mathbf{S}	Local spin operator
t,t'	Electron hopping integral
ι	Electron-like Bogoliubov quasiparticle wavefunction amplititude
$T(\omega)$	T-matrix
T	Temperature
v	Hole-like Bogoliubov quasiparticle wavefunction amplititude
U	Hubbard on-site electron-electron interaction
U_0	Impurity scattering potential
W	Half energy bandwidth
$W_{\mathbf{k}}$	D-density-wave order parameter
ξ_0	BCS superconducting coherence length at low temperatures
$\xi(T)$	BCS temperature dependent coherence length

References

Abanov, A., and A. V. Chubukov, 2000, Phys. Rev. B **61**, R9241.

Abanov, A., A. V. Chubukov, M. Eschrig, M. R. Norman, and J. Schmalian, 2002, Phys. Rev. Lett. 89, 177002.

Abrahams, E., and C. M. Varma, 2000, Proc. Natl. Acad. Sci. **97**, 5714.

Abrikosov, A. A., and L. P. Gorkov, 1960, Zh. Eksp. Teor. Fiz. 39, 1781, [Sov. Phys. JETP 12, 1243 (1961)].

Abrikosov, A. A., L. P. Gorkov, and I. E. Dzyaloshinski, 1963,

Methods of Quantum Field Theory in Statistical Physics (Dover Publications, Inc., New York).

Adagideli, I., P. M. Goldbart, A. Shnirman, and A. Yazdani, 1999, Phys. Rev. Lett. 83, 5571.

Affleck, I., and J. B. Marston, 1988, Phys. Rev. B **37**, 3774. Alloul, H., P. Mendels, H. Casalta, J.-F. Marucco, and J. Arabski, 1991, Phys. Rev. Lett. **67**, 3140.

Altland, A., B. D. Simons, and D. Taras-Semchuk, 2000, Adv. Phys. 49, 321.

Altland, A., and M. Zirnbauer, 1997, Phys. Rev. B 55, 1142.
 Ambegaokar, V., and A. Griffin, 1965, Phys. Rev. 137, A1151.

- Andersen, B. M., 2003, Phys. Rev. B 68, 094518.
- Andersen, B. M., and P. Hedegård, 2003, Phys. Rev. B 67, 172505.
- Andersen, O. K., A. I. Lichtenstein, O. Jepsen, and F. Paulsen, 1995, J. Phys. Chem. Solids **56**, 1573.
- Anderson, P. W., 1959, Phys. Rev. Lett. 3, 325.
- Anderson, P. W., 1970, J. Phys. C 3, 2436.
- Anderson, P. W., G. Yuval, and D. R. Hamann, 1970, Phys. Rev. B 1, 4464.
- Andrei, N., 1980, Phys. Rev. Lett. 45, 379.
- Annett, J., 1990, Adv. Phys. 39, 83.
- Aprili, M., M. Covington, E. Paraoanu, B. Niedermeier, and L. H. Greene, 1998, Phys. Rev. B 57, R8139.
- Arfi, B., H. Bahlouli, C. Pethick, and D. Pines, 1988, Phys. Rev. Lett. 60, 2206.
- Atkinson, W. A., and P. J. Hirschfeld, 2002, Phys. Rev. Lett. 88, 187003.
- Atkinson, W. A., P. J. Hirschfeld, A. H. MacDonald, and K. Ziegler, 2000, Phys. Rev. Lett. 85, 3926.
- Atkinson, W. A., P. J. Hirschfeld, and L. Zhu, 2003, Phys. Rev. B **68**, 054501.
- Bader, S. D., N. E. Phillips, M. B. Maple, and C. A. Luengo, 1975, Solid State Commun. 16, 1263.
- Balatsky, A., 1998, Phys. Rev. Lett. 80, 1972.
- Balatsky, A., 2000, Phys. Rev. B 61, 6940.
- Balatsky, A., and E. Abrahams, 1992, Phys. Rev. B 45, 13125.
 Balatsky, A. V., A. Abanov, and J.-X. Zhu, 2003, Phys. Rev. B 68, 214506.
- Balatsky, A. V., A. Rosengren, and B. L. Altshuler, 1994, Phys. Rev. Lett. 73, 720.
- Balatsky, A. V., M. I. Salkola, and A. Rosengren, 1995, Phys. Rev. B 51, 15547.
- Balatsky, A. V., and S. A. Trugman, 1997, Phys. Rev. Lett. **79**, 3767.
- Barash, Y. S., A. Grishin, and M. Sigrist, 1997, Zh. Eksp. Teor. Fiz 112, 304, [JETP 85, 168 (1997)].
- Beloborodov, I. S., B. N. Narozhny, and I. L. Aleiner, 2000, Phys. Rev. Lett 85, 816.
- Berezinskii, V., 1974, Pisma Zhurn. Eksp. Teor.Fiz. **20**, 628, [JETP Lett. **20**, 287 (1974)].
- Berlinsky, A. J., D. A. Bonn, R. Harris, and C. Kallin, 2000, Phys. Rev. B 61, 9088.
- Bhaseen, M. J., J. S. Caux, I. I. Kogan, and A. M. Tsvelik, 2001, Nucl. Phys. B 618, 465.
- Bickers, N. E., and G. E. Zwicknagl, 1987, Phys. Rev. B ${\bf 36},$ 6746.
- Blonder, G. E., M. Tinkham, and T. M. Klapwijk, 1982, Phys. Rev. B **25**, 4515.
- Blount, E. I., 1985, Phys. Rev. B 32, 2935.
- Bobroff, J., H. Alloul, W. MacFarlane, P. Mendels, N. Blanchard, G. Collin, and J. Marucco, 2001, Phys. Rev. Lett. 86, 4116.
- Borkowski, L. S., and P. J. Hirschfeld, 1992, Phys. Rev. B **46**, 9274.
- Borkowski, L. S., and P. J. Hirschfeld, 1994, J. Low Temp. Phys. 96, 185.
- Buchholtz, L. J., and G. Zwicknagl, 1981, Phys. Rev. B 23, 5788.
- Bulaevskii, L., V. Kuzii, and A. Sobyanin, 1977, Pisma Zh. Eksp. Teor. Phys 25, 314, [JETP Lett. 25, 290 (1977)].
- Bulla, R., M. T. Glossop, D. E. Logan, and T. Pruschke, 2000, J. Phys.: Condens. Matter 12, 4899.
- Bulla, R., T. Pruschke, and A. C. Hewson, 1997, J. Phys.: Condens. Matter 9, 10463.

- Buzdin, A., L. Bulaevskii, and S. Panyukov, 1982, Pisma Zh. Eksp. Teor. Phys 35, 147, [JETP Lett. 35, 178 (1982)].
- Buzdin, A. I., 2004, Rev. Mod. Phys. ***, ****.
- Byers, J. M., M. E. Flatté, and D. J. Scalapino, 1993, Phys. Rev. Lett. 71, 3363.
- Campuzano, J. C., H. Ding, M. R. Norman, H. M. Fretwell, M. Randeria, A. Kaminski, J. Mesot, T. Takeuchi, T. Sato, T. Yokoya, T. Takahashi, T. Mochiku, et al., 1999, Phys. Rev. Lett. 83, 3709.
- Campuzano, J. C., M. R. Norman, and M. Randeria, 2004, in Physics of Superconductors (Springer, Berlin), volume II, p. 167.
- Carbotte, J. P., 1990, Rev. Mod. Phys. 62, 1027.
- Carr, G. L., R. P. S. M. Lobo, J. LaVeigne, D. H. Reitze, and D. B. Tanner, 2000, Phys. Rev. Lett. 88, 3001.
- Cassanello, C. R., and E. Fradkin, 1996, Phys. Rev. B 53, 15079.
- Cassanello, C. R., and E. Fradkin, 1997, Phys. Rev. B 56, 11246.
- Chaba, A. N., and A. D. S. Nagi, 1972, Can. J. Phys. 50, 1736.
- Chakravarty, S., R. B. Laughlin, D. K. Morr, and C. Nayak, 2001, Phys. Rev. B 63, 094503.
- Chen, D. C., D. Rainer, and J. Sauls, 1999, in Proceedings of the International Conference on Quasiclassical Methods in Superconductivity and Superfluidity, VERDITZ 96, edited by D. Rainer and J. A. Sauls.
- Chen, H.-D., J.-P. Hu, S. Capponi, E. Arrigoni, and S.-C. Zhang, 2002, Phys. Rev. Lett. 89, 137004.
- Chen, H. Y., and C. S. Ting, 2003, Phys. Rev. B 68, 212502.Chen, K., and C. Jayaprakash, 1995, J. Phys.:Condens. Matter 7, L491.
- Chen, Q., I. Kosztin, B. Janko, and K. Levin, 1998, Phys. Rev. Lett. 81, 4708.
- Chen, Y., and C. S. Ting, 2004, Phys. Rev. Lett. **92**, 077203. Chiao, M., R. W. Hill, C. Lupien, L. Taillefer, P. Lambert, R. Gagnon, and P. Fournier, 2000, Phys. Rev. B **62**, 3554.
- Choi, C., and P. Muzikar, 1990, Phys. Rev. B 41, 1812.
- Choi, C. H., 1999, Phys. Rev. B 60, 6884.
- Chubukov, A. V., A. Abanov, and D. N. Basov, 2003, Phys. Rev. B 68, 024504.
- Coleman, P., 1984, Phys. Rev. B 29, 3035.
- Coleman, P., 1985, J. Magn. Mater. 47, 323.
- Corson, J., J. Orenstein, S. Oh, J. O'Donnell, and J. N. Eckstein, 2000, Phys. Rev. Lett. 85, 2569.
- Covington, M., M. Aprili, E. Paraoanu, L. H. Greene, F. Xu,
 J. Zhu, and C. A. Mirkin, 1997, Phys. Rev. Lett. 79, 277,
 [Erratum: Phys. Rev. Lett. 79, 2598 (1997)].
- Cox, D. L., and A. Zawadowski, 1998, Adv. Phys. 47, 599.
- Damascelli, A., Z. Hussain, and Z.-X. Shen, 2003, Rev. Mod. Phys. **75**, 473.
- Dessau, D. S., B. O. Wells, Z. Shen, W. E. Spicer, A. J. Arko, R. S. List, D. B. Mitzi, and A. Kapitulnik, 1991, Phys. Rev. Lett. 66, 2160.
- Duffy, D., P. J. Hirschfeld, and D. J. Scalapino, 2001, Phys. Rev. B 64, 224522.
- Edelstein, A. S., 1967, Phys. Rev. Lett. 19, 1184.
- Emery, V. J., and S. A. Kivelson, 1995, Nature (London) **374**, 434.
- Eschrig, M., and M. R. Norman, 2000, Phys. Rev. Lett. 85, 3261.
- Fetter, A. L., 1965, Phys. Rev 140, A1921.
- Fetter, A. L., and J. D. Walecka, 1971, Quantum Theory of Many-Particle Systems (McGraw Hill, Inc., New York).

- Fischer, O., and et al, 2004, Rev. Mod. Phys. **, ****.
- Flatté, M. E., and J. M. Byers, 1997a, Phys. Rev. Lett. **78**, 3761.
- Flatté, M. E., and J. M. Byers, 1997b, Phys. Rev. B **56**, 11213.
- Flatte, M. E., and J. M. Byers, 1998, Phys. Rev. Lett. **80**, 4546.
- Flatté, M. E., and J. M. Byers, 1999, Solid State Physics 52, 137.
- Fogelström, M., D. Rainer, and J. A. Sauls, 1997, Phys. Rev. Lett. 79, 281.
- Franz, M., C. Kallin, and A. J. Berlinsky, 1996, Phys. Rev. B 54, R6897.
- Franz, M., D. E. Sheehy, and Z. Tešanović, 2002, Phys. Rev. Lett. 88, 257005.
- Franz, M., and Z. Tešanović, 1998, Phys. Rev. Lett. 80, 4763.
 Galitskii, V. M., and A. I. Larkin, 2002, Phys. Rev. B 66, 064526.
- de Gennes, P. G., 1989, Superconductivity of Metals and Alloys (Addison-Wesley, New York).
- Ghosal, A., and H. Y. Kee, 2004, Phys. Rev. B 69, 224513.
- Ghosal, A., M. Randeria, and N. Trivedi, 1998, Phys. Rev. Lett. 81, 3940.
- Ginzberg, D. M., 1979, Phys. Rev. B 20, 960.
- Glazman, L., and K. Matveev, 1989, Pisma Zh. Eksp. Teor. Phys. 49, 570, [JETP Lett.49, 660 (1989)].
- Gonzalez-Buxton, C., and K. Ingersent, 1998, Phys. Rev. B 57, 15254.
- Gorkov, L. P., and P. A. Kalugin, 1985, Pis'ma ZhETF 41, 208, [JETP Lett. 41, 253 (1985)].
- Graf, M., A. Balatsky, and J. Sauls, 2000, Phys. Rev. B 61, 3255.
- Graf, M. J., J. Sauls, and D. Rainer, 1995, Phys. Rev. B 52, 10588.
- Graf, M. J., S.-K. Yip, J. A. Sauls, and D. Rainer, 1996, Phys. Rev. B 53, 15147.
- Grimaldi, C., 1999, Europhys. Lett. 48, 681.
- Gweon, G.-H., T. Sasagawa, S. Y. Zhou, J. Graf, H. Takagi, D.-H. Lee, and A. Lanzara, 2004, Nature (London) 430, 187.
- Hahn, J. R., and W. Ho, 2001, Phys. Rev. Lett. 87, 166102.
- Halperin, B. I., and M. Lax, 1966, Phys. Rev. 148, 722.
- Hamann, D. R., 1967, Phys. Rev. 158, 570.
- Han, Q., Z. D. Wang, X.-G. Li, and L. y. Zhang, 2002, Phys. Rev. B 66, 104502.
- Han, Q., T. Xia, Z. D. Wang, and X.-G. Li, 2004, Phys. Rev. B 69, 224512.
- Harlingen, D. J. V., 1995, Rev. Mod. Phys. 67, 515.
- Heinrichs, J., 1968, Phys. Rev. 168, 451.
- Hettler, M. H., and P. J. Hirschfeld, 1999, Phys. Rev. B 59, 9606.
- Hewson, A. C., 1993, The Kondo Problem to heavy Fermions (Cambridge University Press).
- Hill, R. W., C. Lupien, M. Sutherland, E. Boaknin, D. G. Hawthorn, C. Proust, F. Ronning, L. Taillefer, R. Liang, D. A. Bonn, and W. N. Hardy, 2004, Phys. Rev. Lett. 92, 027001.
- Hirschfeld, P. J., and N. Goldenfeld, 1993, Phys. Rev. B , 4219.
- Hirschfeld, P. J., W. O. Putikka, and D. J. Scalapino, 1994, Phys. Rev. B 50, 10250.
- Hirschfeld, P. J., S. M. Quinlan, and D. J. Scalapino, 1997, Phys. Rev. B 55, 12742.
- Hirschfeld, P. J., P. Wölfle, D. Einzel, J. A. Sauls, and W. O.

- Putikka, 1989, Phys. Rev. B 40, 6695.
- Hirschfeld, P. J., P. Wölfle, and D. Vollhard, 1986, Sol. State Comm 59, 111.
- Hirschfeld, P. J., P. W. Wölfle, and D. Einzel, 1988, Phys. Rev. B 37, 83.
- Hoffman, J. E., E. W. Hudson, K. M. Lang, V. Madhavan, H. Eisaki, S. Uchida, and J. C. Davis, 2002a, Science 295, 466.
- Hoffman, J. E., K. McElroy, D.-H. Lee, K. M. Lang, H. Eisaki, S. Uchida, and J. C. Davis, 2002b, Science 297, 1148.
- Hosseini, A., R. Harris, S. Kamal, P. Dosanjh, J. Preston, R. Liang, W. N. Hardy, and D. A. Bonn, 1999, Phys. Rev. B 60, 1349.
- Hotta, T., 1993, J. Phys. Soc. Jpn 62, 274.
- Howald, C., H. Eisaki, N. Kaneko, M. Greven, and A. Kapitulnik, 2003, Phys. Rev. B 67, 014533.
- Howald, C., P. Fournier, and A. Kapitulnik, 2001, Phys. Rev. B 64, 100504.
- Howell, P. C., A. Rosch, and P. J. Hirschfeld, 2004, Phys. Rev. Lett. 92, 037003.
- Hsu, T. C., J. B. Marston, and I. Affleck, 1991, Phys. Rev. B 43, 2866.
- Hu, C.-R., 1994, Phys. Rev. Lett. 72, 1526.
- Hudson, E. W., K. M. Lang, V. Madhavan, S. H. Pan, H. Eisaki, S. Uchida, and J. C. Davis, 2001, Nature 411, 920.
- Hudson, E. W., S. H. Pan, A. K. Gupta, K.-W. Ng, and J. C. Davis, 1999, Science 285, 88.
- Hussey, N. E., 2002, Adv. Phys. 51, 1685.
- Ingersent, K., 1996, Phys. Rev. B 54, 11936.
- Ingersent, K., and Q. Si, 1998, eprint cond-mat/9810226.
- Ishida, K., Y. Kitaoka, N. Ogata, T. Kamino, K. Asayama, J. R. Cooper, and N. Athanassopoulou, 1993, J. Phys. Soc. Jpn. 63, 2803.
- Ishida, K., Y. Kitaoka, K. Yamazoe, K. Asayama, and Y. Yamada, 1996, Phys. Rev. Lett. 76, 531.
- Ishida, K., Y. Kitaoka, T. Yoshitomi, N. Ogata, T. Kamino, and K. Asayama, 1991, Physica C 179, 29.
- Itoh, Y., 1993, J. Phys. Soc. Jpn. 62, 2184.
- Janko, B., I. Kosztin, K. Levin, M. Norman, and D. Scalapino, 1999, Phys. Rev. Lett. 82, 4304.
- Jarrell, M., 1990, Phys. Rev. B 41, 4815.
- Jarrell, M., D. S. Silva, and B. Patton, 1990, Phys. Rev. B 42, 4804.
- Joynt, R., 1997, J. Low Temp. Phys. 109, 811.
- Kampf, A. P., and T. P. Devereaux, 1997, Phys. Rev. B 56, 2360.
- Kashiwaya, S., and Y. Tanaka, 2000, Rep. Prog. Phys. **63**, 1641.
- Kee, H. Y., 2001, Phys. Rev. B 64, 012506.
- Kee, H.-Y., S. A. Kivelson, and G. Aeppli, 2002, Phys. Rev. Lett. 88, 257002.
- Ketterson, J. B., and S. N. Song, 1999, Superconductivity (Cambridge University Press).
- Khaluillin, G., R. Kilian, S. Krivenko, and P. Fulde, 1997, Phys. Rev. B **56**, 11882.
- Khaykovich, B., Y. S. Lee, R. W. Erwin, S. H. Lee, S. Wakimoto, K. J. Thomas, M. A. Kastner, and R. J. Birgeneau, 2002, Phys. Rev. B **66**, 014528.
- Kilian, R., S. Krivenko, G. Khaliullin, and P. Fulde, 1999, Phys. Rev. B 59, 14432.
- Kivelson, S. A., I. P. Bindloss, E. Fradkin, V. Oganesyan, J. M. Tranquada, A. Kapitulnik, and C. Howald, 2003, Rev. Mod. Phys. 75, 1201.

- Koga, M., and M. Matsumoto, 2002a, Phys. Rev. B 65, 094434.
- Koga, M., and M. Matsumoto, 2002b, J. Phys. Soc. Jpn. 71, 943.
- Kondo, J., 1964, Prog. Theor. Phys. 32, 37.
- Kosterlitz, J. M., and D. J. Thouless, 1973, J. Phys. C 6, 1181.
- Kosterlitz, J. M., and D. J. Thouless, 1974, J. Phys. C 7, 1046.
- Krasnov, V. M., A. Yurgens, D. Winkler, P. Delsing, and T. Claeson, 2000, Phys. Rev. Lett. 84, 5860.
- Kruis, H. V., I. Martin, and A. V. Balatsky, 2001, Phys. Rev. B 64, 054501.
- Kuboki, K., and M. Sigrist, 1998, J. Phys. Soc. Jpn. 67, 2873.
 Kulik, I. O., and O. Y. Itskovich, 1968, Zh. Eksp. i Teor. Fiz.
 55, 193, [Sov. Phys. JETP. 28, 102 (1969)].
- Lake, B., G. Aeppli, K. N. Clause, D. F. McMorrow, K. Lefmann, N. E. Hussey, N. Mangkorntong, M. Nohara, H. Takagi, T. E. Mason, and A. Schröder, 2001, Science 291, 1759.
- Lake, B., H. M. RØnnow, N. B. Christensen, G. Aeppli, , K. Lefmann, D. F. McMorrow, P. Vorderwisch, P. Smeibidl, N. Mangkorntong, T. Sasagawa, M. Nohara, et al., 2002, Nature 415, 299.
- Lamacraft, A., and B. D. Simons, 2000, Phys. Rev. Lett. 85, 4783.
- Lamacraft, A., and B. D. Simons, 2001, Phys. Rev. B 64, 014514.
- Landau, L., and E. Lifshitz, 2000, Quantum Mechanics, vol. 3 (Butterworth-Heinemann, Oxford).
- Lang, K. M., V. Madhavan, J. E. Hoffman, E. W. Hudson, H. Eisaki, S. Uchida, and J. C. Davis, 2002, Nature 415, 412.
- Lanzara, A., P. V. Bogdanov, X. J. Zhou, S. A. Kellar, D. L. Feng, E. D. Lu, T. Yoshida, H. Eisaki, A. Fujimori, K. Kishio, J.-I. Shimoyama, T. Noda, et al., 2004, Nature (London) 430, 187.
- Larkin, A., 1965, JETP Lett. 2, 130.
- Larkin, A. I., V. I. Mel'nikov, and D. E. Khmelnitskii, 1971, Sov. Phys. JETP 33, 458.
- Larkin, A. I., and Y. N. Ovchinnikov, 1972, Sov. Phys. JETP 34, 1144.
- Laughlin, R. B., 1998, Phys. Rev. Lett. 80, 5188.
- Lee, P. A., 1993, Phys. Rev. Lett. 71, 1887.
- Lee, Y.-S., K. Segawa, Y. Ando, and D. N. Basov, 2004, Phys. Rev. B 70, 014518.
- Liang, S. D., and T. K. Lee, 2002, Phys. Rev. B 65, 214529.Lifshitz, I. M., 1964a, Adv. Phys. 13, 483.
- Lifshitz, I. M., 1964b, Usp. Fiz. Nauk 83, 617, [Sov. Phys. Usp. 7, 549 (1965)].
- Lifshitz, I. M., 1967, Zh. Eksp. i Teor. Fiz. 53, 743, [Sov. Phys. JETP 26, 462 (1968)].
- Lifshitz, I. M., S. A. Gredeskul, and L. A. Pastur, 1988, Introduction to the theory of disordered systems (John Wiley & Sons, New York).
- Logan, D. E., and M. T. Glossop, 2000, J. Phys.: Condens. Matter 12, 985.
- Loram, J. W., J. L. Luo, J. R. Cooper, W. Y. Liang, and J. L. Tallon, 2000, Physica (Amsterdam) C 341-348, 831.
- Ma, M., and P. A. Lee, 1985, Phys. Rev. B 32, 5658.
- Machida, K., and F. Shibata, 1972, Prog. Theor. Phys. **47**, 1817.
- Mackenzie, A. P., K. Haselwimmer, A. Tyler, G. Lonzarich, Y. Mori, S. Nishizaki, and Y. Maeno, 1998, Phys. Rev. Lett. 80, 161.

- Mackenzie, A. P., and Y. Maeno, 2003, Rev. Mod. Phys. **75**, 657.
- Mahajan, A. V., H. Alloul, G. Collin, and J.-F. Marucco, 1994, Phys. Rev. Lett. **72**, 3100.
- Mahajan, A. V., H. Alloul, G. Collin, and J.-F. Marucco, 2000, Eur. Phys. J. B 13, 457.
- Mahan, G. D., 2000, Many-Particle Physics (Kluwer Academic/Plenum Publishers, New York), 3rd edition.
- Maki, K., 1969, in *Superconductivity*, edited by R. D. Parks (Marcel Dekker, New York), p. 1035.
- Maple, M. B., 1973, in *Magnetism*, edited by H. Suhl (Academic Press, New York), volume V, p. 289.
- Marchetti, F. M., and B. D. Simons, 2002, J. Phys. A: Math. Gen. 35, 4201.
- Markowitz, D., and L. P. Kadanoff, 1963, Phys. Rev. **131**, 563
- Marston, J. B., and I. Affleck, 1989, Phys. Rev. B **39**, 11538. Martin, I., and A. V. Balatsky, 2000, Phys. Rev. B **62**.
- Martin, I., A. V. Balatsky, and J. Zaanen, 2002, Phys. Rev. Lett. 88, 097003.
- Matsumoto, M., and M. Koga, 2001, J. Phys. Soc. Jpn. **70**, 2860.
- Matsumoto, M., and M. Koga, 2002, Phys. Rev. B **65**, 024508. Matsuura, T., 1977, Progr. Theor. Phys. **57**, 1823.
- Matsuura, T., S. Ichinose, and Y. Nagaoka, 1977, Prog. Theor. Phys. **57**, 713.
- McElroy, K., R. W. Simmonds, J. E. Hoffman, D. H. Lee, J. Orenstein, H. Eisaki, S. Uchida, and J. C. Davis, 2003, Nature **422**, 592.
- Mendels, P., J. Bobroff, G. Collin, H. Alloul, M. Gabay, J.-F. Marucco, N. Blanchard, and B. Grenier, 1999, Europhys. Lett. 46, 678.
- Meyer, J. S., and B. D. Simons, 2001, Phys. Rev. B **64**, 134516.
- Millis, A. J., 2003, Solid State Commun. 126, 3.
- Misra, S., S. Oh, D. J. Hornbaker, T. DiLuccio, J. N. Eckstein, and A. Yazdani, 2002, Phys. Rev. Lett. 89, 087002.
- Moradian, R., J. F. Annett, B. L. Gyorffy, and G. Litak, 2001, Phys. Rev. B **63**, 024501.
- Morr, D. K., 2002, Phys. Rev. Lett. 89, 106401.
- Morr, D. K., and A. V. Balatsky, 2003, Phys. Rev. Lett. 90, 067005.
- Morr, D. K., and R. H. Nyberg, 2003, Phys. Rev. B 68, 060505.
- Morr, D. K., and N. A. Stavropoulos, 2003, Phys. Rev. B **67**, 020502.
- Movshovich, R., M. A. Hubbard, M. B. Salamon, A. V. Balatsky, R. Yoshizaki, J. L. Sarrao, and M. Jaime, 1998, Phys. Rev. Lett. 80, 1968.
- Müller-Hartmann, E., 1973, in *Magnetism*, edited by H. Suhl (Academic Press, New York), volume V, p. 353.
- Müller-Hartmann, E., and J. Zittartz, 1971, Phys. Rev. Lett. **26**, 428.
- Nagaoka, Y., 1965, Phys. Rev Ser. A 138, 1112.
- Nagaoka, Y., 1967, Progr. Theor. Phys. 37, 13.
- Nagaosa, N., and P. A. Lee, 1997, Phys. Rev. Lett. 79, 3755.Neils, W. K., and D. J. V. Harlingen, 2002, Phys. Rev. Lett. 88, 047001.
- Nersesyan, A., and A. Tsvelik, 1997, Phys. Rev. Lett. **78**, 3981.
- Nersesyan, A., A. Tsvelik, and F. Wenger, 1995, Nucl. Phys. B **438**, 561.
- Nicol, E. J., and J. P. Carbotte, 2003, Phys. Rev. B 67, 214506.

- Norman, M. R., and H. Ding, 1998, Phys. Rev. B 57, 11089.
 Norman, M. R., H. Ding, M. Randeria, J. C. Campuzano,
 T. Yokoya, T. Takeuchi, T. Takahashi, T. Mochiku,
 K. Kadowaki, P. Guptasarma, and D. G. Hinks, 1998, Nature (London) 392, 157.
- Ogura, J., and T. Saso, 1993, J. Phys. Soc. Jpn. **62**, 4364. Okabe, Y., and A. D. S. Nagi, 1983, Phys. Rev. B **28**, 1320.

Ong, P., and et al, 2004, Rev. Mod. Phys. **, ****.

- Pan, S. H., E. W. Hudson, A. K. Gupta, K.-W. Ng, H. Eisaki, S. Uchida, and J. C. Davis, 2000a, Phys. Rev. Lett. 85, 1536.
- Pan, S. H., E. W. Hudson, K. M. Lang, H. Eisaki, S. Uchida, and J. C. Davis, 2000b, Nature 403, 746.
- Pan, S. H., J. P. O'Neal, R. L. Badzey, C. Chamon, H. Ding, J. R. Engelbrechet, Z. Wang, H. Eisaki, S. Uchida, A. K. Gupta, K.-W. Ng, E. W. Hudson, et al., 2001, Nature 413, 282.
- Pepin, C., and P. A. Lee, 1998, Phys. Rev. Lett. **81**, 2779. Pepin, C., and P. A. Lee, 2001, Phys. Rev. B **63**, 054502.
- Pethick, C., and D. Pines, 1986a, Phys. Rev. Lett. **109**, 811. Pethick, C. J., and D. Pines, 1986b, Phys. Rev. Lett. **57**, 118. Pines, D., 1997, Physica C **282-287**, 273.
- Podolsky, D., E. Demler, K. Damle, and B. I. Halperin, 2003, Phys. Rev. B 67, 094514.
- Polkovnikov, A., 2002, Phys. Rev. B 65, 064503.
- Polkovnikov, A., S. Sachdev, and M. Vojta, 2001, Phys. Rev. Lett. 86, 296.
- Polkovnikov, A., S. Sachdev, and M. Vojta, 2003, Physica C 388-389, 19.
- Quinlan, S. M., P. J. Hirschfeld, and D. J. Scalapino, 1996, Phys. Rev. B 53, 8575.
- Quinlan, S. M., D. J. Scalapino, and N. Bulut, 1994, Phys. Rev. B 49, 1470.
- Read, N., 1985, J. Phys. C 18, 2651.
- Read, N., and D. M. Newns, 1983a, J. Phys. C 16, 3273.
- Read, N., and D. M. Newns, 1983b, J. Phys. C 16, L1055.
- Renner, C., B. Revaz, J.-Y. Genoud, K. Kadowaki, and Ø. Fischer, 1998, Phys. Rev. Lett. **80**, 149.
- Rusinov, A. I., 1968, Pis'ma ZhETF $\bf 9$, 146, [JETP Lett. $\bf 9$, 85 (1969)].
- Rusinov, A. I., 1969, Zh. Eksp. i Teor. Fiz. **56**, 2047, [Sov. Phys. JETP **29**, 1101 (1969)].
- Sakai, O., Y. Shimizu, H. Shiba, and K. Satori, 1993, J. Phys. Soc. Jpn. 62, 3181.
- Sakurai, A., 1970, Prog. Theor. Phys. 44, 1472.
- Salkola, M. I., A. V. Balatsky, and D. J. Scalapino, 1996, Phys. Rev. Lett. 77, 1841.
- Salkola, M. I., A. V. Balatsky, and J. R. Schrieffer, 1997, Phys. Rev. B 55, 12648.
- Samokhin, K., and M. Walker, 2001, Phys. Rev. B 64, 024507.
 Satori, K., H. Shiba, O. Sakai, and Y. Shimizu, 1992, J. Phys. Soc. Jpn. 61, 3239.
- Saxena, S. S., P. Agarwal, K. Ahilan, F. M. Grosche, R. K. W. Haselwimmer, M. J. Steiner, E. Pugh, I. R. Walker, S. R. Julian, P. Monthoux, G. G. Lonzarich, A. Huxley, et al., 2000, Nature. 406, 587.
- Scalapino, D. J., P. J. Hirschfeld, and T. Nunner, 2004, proceedings of SNS-2004 (Sitges), eprint unpublished.
- Schachinger, E., 1982, Z. Phys B 47, 217.
- Schachinger, E., and J. P. Carbotte, 1984, Phys. Rev. B 29, 165.
- Schachinger, E., J. M. Daams, and J. P. Carbotte, 1980, Phys. Rev. B 22, 3194.
- Schlottmann, P., 1976, Phys. Rev. B 13, 1.

- Schmitt-Rink, S., K. Miyaka, and C. M. Varma, 1986, Phys. Rev. Lett. 57, 2575.
- Schrieffer, J. R., 1964, *The Theory of Superconductivity* (Benjamin, New York).
- Schuh, B., and E. Müller-Hartmann, 1978, Z. Phys. B 29, 39.Segre, G. P., N. Gedik, J. Orenstein, D. A. Bonn, R. Liang, and W. N. Hardy, 2002, Phys. Rev. Lett. 88, 137001.
- Senthil, T., and M. P. A. Fisher, 1999, Phys. Rev. B **60**, 6893. Senthil, T., and M. P. A. Fisher, 2000, Phys. Rev. B **61**, 9690.
- Senthil, T., M. P. A. Fisher, L. Balents, and C. Nayak, 1998, Phys. Rev. Lett. 81, 4704.
- Sheehy, D. E., I. Adagideli, P. M. Goldbart, and A. Yazdani, 2001, Phys. Rev. B 64, 224518.
- Shen, Z. X., and J. R. Schrieffer, 1997, Phys. Rev. Lett. 78, 1991.
- Shiba, H., 1968, Prog. Theor. Phys. 40, 435.
- Shiba, H., 1973, Prog. Theor. Phys. 50, 50.
- Shnirman, A., I. Adagideli, P. M. Goldbart, and A. Yazdani, 1999, Phys. Rev. B **63**, 7517.
- Shytov, A. V., I. Vekhter, I. A. Gruzberg, and A. V. Balatsky, 2003, Phys. Rev. Lett. **90**, 147002.
- Shytov, A. V., I. Vekhter, I. A. Gruzberg, and A. V. Balatsky, 2004, eprint unpublished.
- Sidorov, V. A., M. Nicklas, P. G. Pagliuso, J. L. Sarrao, Y. Bang, A. V. Balatsky, and J. D. Thompson, 2002, Phys. Rev. Lett. 89, 157004.
- Sigrist, M., and K. Ueda, 1991, Rev. Mod. Phys. 63, 239.
- Simon, M. E., and C. M. Varma, 1999, Phys. Rev. B 60, 9744.
 Skalski, S., O. Betbeder-Matibet, and P. R. Weiss, 1964, Phys. Rev. 136, A1500.
- Soda, T., T. Matsuura, and Y. Nagaoka, 1967, Progr. Theor. Phys. 38, 551.
- Spivak, B., and S. Kivelson, 1991, Phys. Rev. B 43, 3740.
- Stamp, P. C. E., 1987, Journ. Magn. Magn. Materials. 63-64, 429.
- Stipe, B., M. Rezaei, and W. Ho, 1998, Science 280, 1732.
- Takegahara, K., Y. Shimizu, and O. Sakai, 1992, J. Phys. Soc. Jpn. **61**, 3443.
- Takigawa, M., M. Ichioka, and K. Machida, 2003, Phys. Rev. Lett. 90, 047001.
- Tanaka, K., and F. Marsiglio, 2000, Phys. Rev. B 62, 5345. Tanuma, Y., Y. Tanaka, M. Ogata, and S. Kashiwaya, 1998,
- J. Phys. Soc. Jpn. 67, 1118.Timusk, T., 2003, eprint cond-mat/0303383.
- Timusk, T., and B. Statt, 1999, Rep. Prog. Phys. 62, 61.
- Tinkham, M., 1996, Introduction to Superconductivity (McGraw-Hill, Inc., New York), 2nd edition.
- Tsuchiura, H., Y. Tanaka, M. Ogata, and S. Kashiwaya, 2000, Phys. Rev. Lett. 84, 3165.
- Tsuei, C. C., and J. R. Kirtley, 2000, Rev. Mod. Phys. **72**, 969.
- Tsuneto, T., 1962, Prog. Theor. Phys. 28, 857.
- Tu, J. J., C. C. Homes, G. D. Gu, D. N. Basov, and M. Strongin, 2002, Phys. Rev. B 66, 144514.
- Turner, P. J., R. Harris, S. Kamal, M. E. Hayden, D. M. Broun, D. C. Morgan, A. Hosseini, P. Dosanjh, G. K. Mullins, J. S. Preston, R. Liang, D. A. Bonn, et al., 2003, Phys. Rev. Lett. 90, 237005.
- Udea, K., and T. M. Rice, 1985, in *The Physics of Elementary Excitations*, edited by T. Kasuya and T. Sato (Springer-Verlag, Berlin).
- Van Mieghem, P., 1992, Rev. Mod. Phys. 64, 755.
- Varma, C. M., 1999, Phys. Rev. Lett. 83, 3538.
- Vavilov, M. G., P. W. Brouwer, V. Ambegaokar, and C. W. J.

- Beenakker, 2001, Phys. Rev. Lett. 86, 874.
- Vekhter, I., A. V. Shytov, I. A. Gruzberg, and A. V. Balatsky, 2003, Physica B 329-333, 1446.
- Vekhter, I., and C. M. Varma, 2003, Phys. Rev. Lett. 90, 237003.
- Vershinin, M., S. Misra, S. Ono, Y. Abe, Y. Ando, and A. Yazdani, 2004, Science 303, 1995.
- Vishveshwara, S., T. Senthil, and M. P. A. Fisher, 2000, Phys. Rev. B 61, 6966.
- Vojta, M., 2001, Phys. Rev. Lett. 85, 097202.
- Vojta, M., and R. Bulla, 2001, 65, 014511.
- Volovik, G. E., and L. P. Gor'kov, 1984, JETP Lett. **39**, 550. Wang, Q., and C.-R. Hu, 2004, Phys. Rev. B **70**, 092505.
- Wang, Q.-H., 2002, Phys. Rev. Lett. 88, 057002.
- Wang, Q.-H., and D.-H. Lee, 2003, Phys. Rev. B **67**, 020511. Wang, Q.-H., and Z. D. Wang, 2004, Phys. Rev. B **69**, 092502.
- Wiegmann, P. B., 1980, JETP Lett. 31, 367.
- Wilson, K. G., 1975, Rev. Mod. Phys. 47, 773.
- Withoff, D., and E. Fradkin, 1990, Phys. Rev. Lett. **64**, 1835. Woolf, M. A., and F. Reif, 1965, Phys. Rev. **137**, A557.
- Xiang, T., and J. M. Wheatley, 1995, Phye. Rev. B 51, 11721.
 Yashenkin, A. G., W. A. Atkinson, I. V. Gornyi, P. J. Hirschfeld, and D. V. Khveshchenko, 2001, Phys. Rev. Lett. 86, 5982.
- Yazdani, A., C. M. Howald, C. P. Lutz, A. Kapitulnik, and D. M. Eigler, 1999, Phys. Rev. Lett 83, 176.
- Yazdani, A., B. A. Jones, C. P. Lutz, M. F. Crommie, and D. M. Eigler, 1997, Science 275, 1767.
- Yoshioka, T., and Y. Ohashi, 1998, J. Phys. Soc. Jpn 67, 1332.
- Yoshioka, T., and Y. Ohashi, 2000, J. Phys. Soc. Jpn **69**, 1812.
- Yu, L., 1965, Acta Phys. Sin. 21, 75.
- Zhang, D., and C. S. Ting, 2003, Phys. Rev. B 67, 100506.
- Zhang, D., and C. S. Ting, 2004, Phys. Rev. B 69, 012501.
- Zhang, G.-M., H. Hu, and L. Yu, 2001, Phys. Rev. Lett. 86, 704.
- Zhu, J.-X., and A. Balatsky, 2002, Phys. Rev. B 65, 132502.
 Zhu, J.-X., W. Kim, C. S. Ting, and J. P. Carbotte, 2001, Phys. Rev. Lett. 87, 197001.
- Zhu, J.-X., T. K. Lee, C. R. Hu, and C. S. Ting, 2000a, Phys. Rev. B 61, 8667.
- Zhu, J.-X., I. Martin, and A. R. Bishop, 2002, Phys. Rev. Lett. 89, 067003.
- Zhu, J.-X., D. N. Sheng, and C. S. Ting, 2000b, Phys. Rev. Lett. 85, 4944.
- Zhu, J.-X., J. Sun, Q. Si, and A. V. Balatsky, 2004a, Phys. Rev. Lett. 92, 5017002.
- Zhu, J.-X., and C. S. Ting, 2001a, Phys. Rev. Lett. 87, 147002.
- Zhu, J.-X., and C. S. Ting, 2001b, Phys. Rev. B **63**, 020506. Zhu, J.-X., and C. S. Ting, 2001c, Phys. Rev. B **64**, 060501.
- Zhu, J.-X., C. S. Ting, and C. R. Hu, 2000c, Phys. Rev. B **62**, 6027.
- Zhu, L., W. A. Atkinson, and P. J. Hirschfeld, 2003, Phys. Rev. B 67, 094508.
- Zhu, L., W. A. Atkinson, and P. J. Hirschfeld, 2004b, Phys. Rev. B 69, 060503.
- Zhu, L., P. J. Hirschfeld, and D. J. Scalapino, 2004c, eprint cond-mat/0406304.
- Ziegler, K., 1996, Phys. Rev. B 53, 9653.
- Ziegler, K., M. H. Hettler, and P. J. Hirschfeld, 1996, Phys. Rev. Lett. 77, 3013.
- Zittartz, J., A. Bringer, and E. Müller-Hartmann, 1972, Sol.

- St. Commun. 10, 513.
- Zittartz, J., and J. S. Langer, 1966, Phys. Rev. **148**, 741. Zittartz, J., and E. Müller-Hartmann, 1970, Z. Phys. **232**, 11.

Figures

- FIG. 1 Multiple scattering on a single impurity. Thick (thin) line denotes full (bare) Green's function, and the dashed line denotes scattering process. The second line defines the T-matrix according to Eq. (3.19).
- FIG. 2 Impurity bound state in a metal at energy ω_0 is formed as a result of a multiple scattering.
- FIG. 3 Graphic solution of the Eq. (7.5) for large U_0 is shown. Only physically relevant intersections with small imaginary part Ω_0 " $\ll \Omega'_0$ are shown. In the region where the imaginary part of the local Green's function exceeds the real part, the resonance is broadened and merges with continuum. Resonances below (or above, for a different sign of U_0) the fermionic band are the sharpest, with most of spectral weight, and the virtual bound state inside the gap is well resolved for large U_0 (small c).
- FIG. 4 Illustration of the cross shaped nature of the impurity state. Shown is the spectral density $A_{\sigma}(\mathbf{r}, \pm \Omega_0)$ as a function of position and spin in units of $N_0\Delta_0$ for a) $\mu=0$ and b) $\mu=-W$, 2W is the bandwidth, in a two-dimensional d-wave superconductor as a function of position around a classical magnetic moment ($N_0J_0=10$ and $U_0=0$) located at $\mathbf{r}=0$; a is the lattice spacing. These results are computed self-consistently with $\xi=10a$. At half filling, the spectral density obeys particle-hole symmetry: $A_{\uparrow}(\mathbf{r},\Omega_0)=A_{\downarrow}(\mathbf{r},-\Omega_0)$. The energies of the shown virtual-bound states are a) $\Omega_0=0.05\Delta_0$ and b) $\Omega_0=0.5\Delta_0$. From (Salkola et al., 1997)
- FIG. 5 Self-consistently determined gap function near scalar impurity in a 2D *d*-wave superconductor. Gap suppression is strongly localized near impurity site aside from weak oscillating tails. From (Franz *et al.*, 1996)
- FIG. 6 The LDOS as a function of energy at the impurity site (left panels) and at one of its nearest neighbors (right panels) in a 2D lattice. The upper panels are for various values of repulsive potential, $U_0=0$ (black line), 2 (blue line), 5 (green line), and 10 (red line) while the lower panels are for various values of attractive potential, $U_0=0$ (black line), -2 (blue line), -5 (green line), and -10 (red line). The band structure parameter values are $t=1,\,t'=0$, and the chemical potential $\mu=0$.
- FIG. 7 Same as Fig. 6 except that the band structure parameter values are $t=1,\ t'=-0.2,$ and the chemical potential $\mu=-0.784.$

FIG. 8 Same as Fig. 6 except that the band structure parameter values $t=1,\ t'=-0.3$ and the chemical potential $\mu=-1.0$.

FIG. 9 An impurity state in a high T_c superconductor: (a) The DOS in the pseudogap regime used in this article (see also [11]) and (b) the DOS in the superconducting state as was used in [1]. In both phases there is a resonant state.

FIG. 10 (a) The density of states $N(\omega) = -g_0''(\omega)/\pi$. Around the pseudogap states are only partly depleted e.g. $N_0(\omega) = N_0|\omega|/\Delta_{PG}$, where $N_0(\omega) = N_0$ for $\Delta_{PG} < |\omega| < W/2$ with W the bandwidth. (b) The real part $g_0'(\omega)$ of Green's function together with $1/U_0$ and U_0 positive. Ω' is the real part of the solution of the equation $g_0(\Omega) = 1/U_0$ close to zero and therefore with sharp bandwidth. (c) The impurity induced resonance at $\Omega' = -\Delta_{PG}/2U_0N_0\ln(2U_0N_0)$. Because the other three solutions of Eq. (8.1) have much broader bandwidth, they are not depicted here. All the figures are taken on the impurity site. From Kruis, Martin and Balatsky (Kruis et~al., 2001)

FIG. 11 DDW-DOS for the clean case (solid line) and in the presence of a non-magnetic impurity with $U_0=1$ eV: (1) DOS on the impurity site, (2) DOS on the nearest-neighbor site, and (3) DOS on the next-nearest-neighbor site. The other parameter values are: $t=300meV,\ W_0=25meV,\ t'=0,$ and $\mu=0$. From Morr (Morr, 2002).

FIG. 12 (a) Fermi surface in the DDW state with $t'=-0.3t, \ \mu=-0.91t$ (corresponding to a hole-doping of 10%) and $W_0=25$ meV. The hole pockets are centered around $(\pm\pi/2,\pm\pi/2)$. (b) DOS in the DDW state with the same band parameters as in (a), for the clean case (solid line) and in the presence of a non-magnetic impurity with $U_0=1$ eV: (1) DOS on the impurity site, (2) DOS on the nearestneighbor site, and (3) DOS on the next-nearest-neighbor site. Inset: SC DOS for the same band parameters as in (a). From Morr (Morr, 2002)

FIG. 13 Local density of states with $\Delta_0 = 0.68t$, $\mu = -0.3t$ and $U_0 = 100t$. (a) $N(\mathbf{r}_{nn}, \omega)$ versus ω . Solid lines: $n_v = 10^{-6}, 10^{-4}, 10^{-3}$, and 5×10^{-3} with decreasing peaks. The dotted line is the LDOS at $n_v = 0$ and $U_0 = 0$ for comparison. (b) $N(\mathbf{r}, 0.05t)$ at $n_v = 0$. The impurity is at the center. (c) The same as (b) for $n_v = 5 \times 10^{-3}$. The gray scale is the same in (b) and (c). The other parameter t' = 0. From Wang (Wang, 2002).

FIG. 14 The local effect of a magnetic moment on the lowenergy spectral density in an s-wave superconductor. FIG. 15 Two variational states are shown schematically. $|\Psi_0\rangle$ is a standard BCS wave function that contains only paired particles and has unscreened impurity spin S. $|\Psi_1\rangle$ is a variational wave function that describes the formation of the bound state between particle with the spin opposite to the local spin (for antiferromagnetic coupling); this state is inherently a non BCS state and electonic spin quantum number differs by one unpaired spin compared to $|\Psi_0\rangle$.

FIG. 16 Energies of two variational states are shown. $|\Psi_0\rangle$ is a standard BCS state with energy E_0 . $|\Psi_1\rangle$ is a variational state that describes the formation of the bound state between particle with the spin opposite to the local spin with energy E_1 . Level crossing between states with different symmetry occurs at some critical value of the coupling J_{crit} . This is an example of a first order quantum phase transition with no divergent length or time scale associated with it.

FIG. 17 a) The bound-state energy Ω_0 , b) the spectral weight of the pole Z^{\pm} for positive and negative energies in units of $N_0J_0,N_0=N_F$, c) the spin polarization $\langle \mathbf{s}(\mathbf{r}=0)\rangle$, and d) the gap function $\Delta(\mathbf{r}=0)/\Delta_0$ at the impurity site $\mathbf{r}=0$ as a function of J_0 in the s-wave superconductor. Lines denote the T matrix results for the uniform order parameter and symbols the self-consistent mean-field results on a square lattice at half filling. The quantities of the impurity-induced intragap quasiparticle state belonging to the branch $J_0 < J_{crit}$ are denoted by solid lines and solid symbols, whereas those ones belonging to the branch $J_0 > J_{crit}$ are marked by dashed lines and open symbols. Taken from (Salkola et al., 1997).

FIG. 18 Cartoon of the intrinsic π junction near magnetic impurity in s-wave superconductor.

FIG. 19 Calculated tunneling density of states for the four-site Kondo impurity model at 15% hole doping with a realistic band structure ($t=0.15~{\rm eV},\,t'=-t/4,\,t''=t/12$), $\Delta_0=0.04~{\rm eV}$, and $\mu=-0.14~{\rm eV}$. The Kondo coupling is $J=0.09~{\rm eV}$, the potential scattering U=0. Top: Local DOS vs. energy for the impurity site (red) and the nearest (blue) and second (green) neighbor sites. Bottom: Spatial dependence of the local DOS at $\omega=-2~{\rm meV}$. Left: Local DOS in the CuO₂ plane. Right: Local DOS after applying the filter effect proposed by Martin, Balatsky, and Zaanen (Martin et~al., 2002). From Vojta and Bulla (Vojta and Bulla, 2001)

FIG. 20 Same as Fig. 19, but with potential scattering U=t=0.15 eV. Here, J=0.065 eV. The lower panel shows the local DOS at $\omega=+2$ meV. From Vojta and Bulla (Vojta and Bulla, 2001).

FIG. 21 Same as Fig. 19, but with potential scattering U=4t=0.6 eV. Here, J=0.04 eV. The lower panel shows the local DOS at $\omega=+3$ meV. From Vojta and Bulla (Vojta and Bulla, 2001).

FIG. 22 The solution for the DOS (black line) and its energy derivative (red line) are presented for a local boson mode scattering in a d-wave superconductor. The normal self-energy was treated self-consistently as a full solution of the Eq. (11.3), ignoring vertex corrections and gap modifications. Apart from the feature at $\omega = \omega_0$ we get also strong satellite peaks at $\Delta + \omega_0$ that are a consequence of a coherence peak in DOS of a d-wave superconductor. These satellites are a specific property of a superconducting state and will not be present in a pseudogap state. These features are best seen in $\frac{dN}{d\omega}$. Energy scale is given in units of Δ , the dimensionless coupling constant is taken to be 1. For comparison we plot the results for local mode frequency $\omega_0/\Delta = 0.2, 0.4, 0.6$ in the first three panels. The lower panel gives the results for the asymptotic analytic solution, that assumes $\omega_0 \ll \Delta$ using Eq. (11.1), for $\omega_0 = 0.4$. The overall features are similar for both cases, however the analytic solution shows a somewhat larger feature. Taken from (Balatsky et al., 2003)

FIG. 23 Appearance of the satellite peaks for an impurity resonance ω_{imp} at $\omega_{imp} \pm \omega_0$ is shown schematically. The satellites will have different spectral weight. Imagine we inject into system an electron at energy $\omega_{imp} + \omega_0$. To create a peak at ω_{imp} one need to excite local mode and the energy of the electron will be equal to the difference between local state and local mode energies. Similarly, to obtain the peak at ω_{imp} from injected electron at energy $\omega_{imp} - \omega_0$ one needs to add local mode energy to an electron. For this process to occur the local mode has to be excited to begin with and hence this process will have very low weight at low T. These two processes will also have different matrix elements. Overall relative weight of the side peaks is proportional to $J^2N_0^2$ which we assumed to be small. In case of magnetic scattering, when $\omega_0 = g\mu_B B$ the splitting will be tunable by the field. Taken from (Balatsky et al., 2003)

FIG. 24 The density of states for a clean system with g=0 and 0.2.

FIG. 25 Fourier spectrum at $E = -E_r$ for the constant g = 0.2 and the structure factor $U_{\mathbf{q}} = U_0$. The parameter $U_0 = 0.3$

FIG. 26 Fourier spectrum at $E = -E_r$ for the constant g = 0.2 and the structure factor $u_{\bf q} = U_0 q_0^2/\{q_0^2 + 4[\cos^2(q_x/2) + \cos^2(q_y/2)]\}$. The parameter $U_0 = 0.3$ and $q_0 = 0.5$.

FIG. 27 Left panel: The dI/dV spectra measured near (A) Mn, (B) Gd, and (C) Ag atoms and far away from the impurity where local density of states can be fit by the BCS theory. Right panel: Constant-current topographs and simultaneously acquired dI/dV images show the spatial extent of the bound state near Mn and Gd adatoms. (A) Constantcurrent (32 Å by 32 Å) topograph of a Mn adatom. (B) Image of dI/dV near the Mn adatom, acquired simultaneously with the topograph in (A) by using an ac detection. The areas where dI/dV is reduced (dark) show the extent of the bound state. This reversed contrast comes about because a dc bias voltage was chosen well above the energy of the bound state, where the bound state affects dI/dV only indirectly by contributing to the total current I. (C) Constant-current (32 \mathring{A} by 32 Å) topograph of a Gd adatom. (D) Image of dI/dV near the Gd adatom, acquired simultaneously with the topograph in (C). From Yazdani (Yazdani et al., 1997).

FIG. 28 Differential tunneling spectra taken at the Zn-atom site (open circles) and a location far away from the impurity (filled circles). Note that even on the impurity site one has peaks at both positive and negative bias albeit of very different magnitude that are reflection of the particle hole character of the impurity resonance. To fit the data one can use a simple potential scattering model with essentially unitary scattering phase shift $\theta=0.48\pi$. Phase shift is related to a impurity potential U_0 via simple formula: $\cot\theta=\frac{1}{\pi N_F U_0}$. From Pan et al. (Pan et al., 2000b).

FIG. 29 Differential conductance spectra above the Ni atom and at several nearby locations. Differential conductance spectra obtained at four positions near the Ni atom showing the maxima at $eV=\pm\Omega_1$. Intensity as a function of position relative to impurity site reverses upon change of the bias sign. This effect is explained as a result of particle and hole components of the impurity state. From Hudson et al. (Hudson et al., 2001).

FIG. 30 High-spatial-resolution image of the differential tunneling conductance at a negative tip voltage bias eV = -1.2mV at a $60 \times 60 \mathring{A}^2$ square. Also shown d-wave gap nodes orientation and lattice sites to indicate that impurity state is registered to lattice. From Pan *et al.* (Pan *et al.*, 2000b).

FIG. 31 Tunneling DOS for tunneling on Ni impurity site. Note that there are always states at opposite bias as well. The peak intensity is largest on either positive or negative bias depending on the position. To fit the data one need to use both U_0 and J. From Hudson *et al.* (Hudson *et al.*, 2001).

FIG. 32 The particle and hole components of the impurity wave function for a magnetic impurity in a s-wave superconductor is shown. A) Impurity wave function $\Psi_B(r)$ and B) $r^2\Psi_B(r)$ are shown. The maxima of particle and hole components occur at different positions. This results in the different image of the impurity state, seen on positive and negative bias. This effect is a general property of a superconductor regardless of the symmetry of the pairing state. From (Yazdani et al., 1997).

FIG. 33 A representative set of seven scattering vectors $\mathbf{q}_i(E)$ of the 'octet' model. Reproduced with permission from (McElroy et al., 2003).

FIG. 34 The real space image of different orbitals on Cu, nearest O and nearest Cu sites are shown. Quantum mechanical interference produces the filter effect that changes the distribution of the impurity state intensity (Martin *et al.*, 2002).

FIG. 35 Density of states in the Abrikosov-Gorkov theory of magnetic impurities in superconductors. Here $\Gamma = \tau_s^{-1}$. Reproduced with permission from (Skalski *et al.*, 1964).

FIG. 36 Plot of the dependence of the order parameter, Δ , transition temperature, T_c , and the single particle spectral gap, Ω_G here, on the scattering rate $\Gamma = \tau_s^{-1}$. Reproduced with permission from (Skalski *et al.*, 1964).

FIG. 37 Evolution of the spectral gaps and density of states for strong magnetic impurities ($\epsilon_0 \ll \Delta_0$). Left panel shows the available states (shaded) as a function of the impurity concentration. Right panel shows the qualitative features of the density of states for different values of the impurity concentration, labeled by vertical lines A, B, C, D on the left. Critical concentration of impurities corresponds to line B, when the impurity band first touches $\omega=0$. At the same time, spectral gap between the top of the impurity band and the bottom of the continuum states persists to higher impurity concentration (line D).

FIG. 38 Evolution of the spectral gaps and density of states for weak magnetic impurities ($\epsilon_0 \lesssim \Delta_0$). Left panel shows the available states (shaded) as a function of the impurity concentration. Right panel shows the qualitative features of the density of states for different values of the impurity concentration, labeled by vertical lines A, B, C on the left. The impurity band and the continuum above the gap merge at a low impurity concentration,see line B, and further evolution of the density of states is very close to the predictions of the AG theory. Critical concentration (line C) marks the onset of gapless superconductivity.

FIG. 39 Reduced transition temperature normalized to pure system as a function of the impurity concentration for different eleteron-phonon coupling, λ_0 . The impurity concentration $\bar{c} = n_{imp}/(2\pi)^2 N_0 T_{c0}$. From (Jarrell, 1990).

FIG. 40 The spatial structure of the optimal fluctuation in the ballistic and the diffusive limits.

FIG. 41 Qualitative picture of the density of states in an s-wave superconductor with magnetic impurities. Blue shade denotes regions where the mean field density of states is finite. Red shading signifies the finite DOS induced by the deviations of the local impurity distribution from the average. The density of states in these tails is exponentially small but finite. If the impurities are weak, the well-defined impurity band is absent and the tail extend from the mean field gap edge.

Tables

	S-WAVE	$P ext{-WAVE}$	$D ext{-WAVE}$
POTENTIAL SCATTERING	_	+	+
MAGNETIC SCATTERING	+	+	+

TABLE I Effects of potential and magnetic impurity scattering on the s-, p- and d-wave superconductors is shown qualitatively. "+" indicate that impurity scattering is a pairbreaker and "-" is that impurity scattering is not a pairbreaker. There is a qualitative difference between the potential scattering in s-wave superconductors and any other case. Potential scattering impurities are not pairbreakers in s-wave case due to Anderson theorem. This is an exceptional case. For any other case any impurity scattering will suppress superconductivity. Obviously the details depend on scattering strength and other details. At high enough concentrations both magnetic and nonmagnetic impurities will suppress superconductivity regardless of symmetry.

This figure "fig1.jpeg" is available in "jpeg" format from:

This figure "fig2.jpeg" is available in "jpeg" format from:

This figure "fig3.jpeg" is available in "jpeg" format from:

This figure "fig4.jpeg" is available in "jpeg" format from:

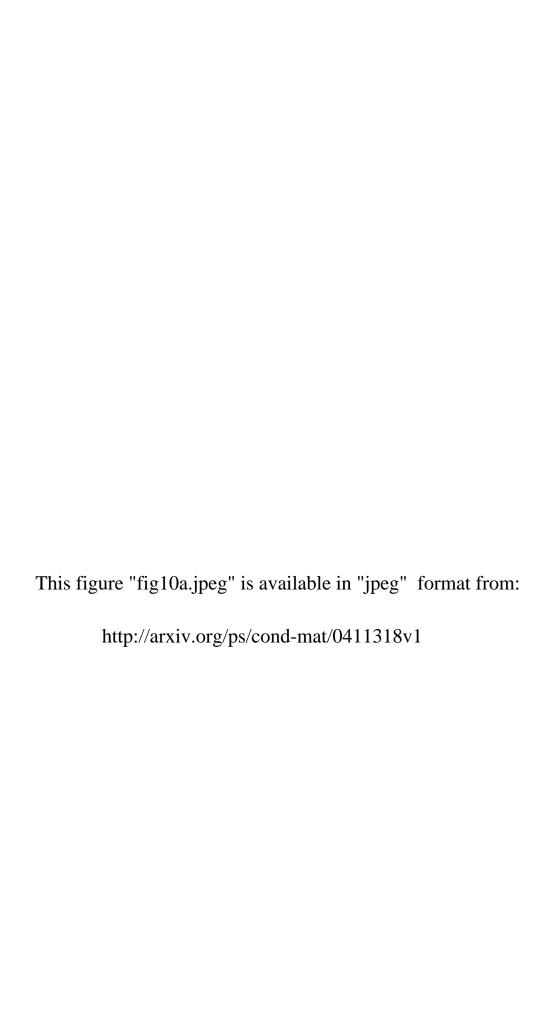
This figure "fig5.jpeg" is available in "jpeg" format from:

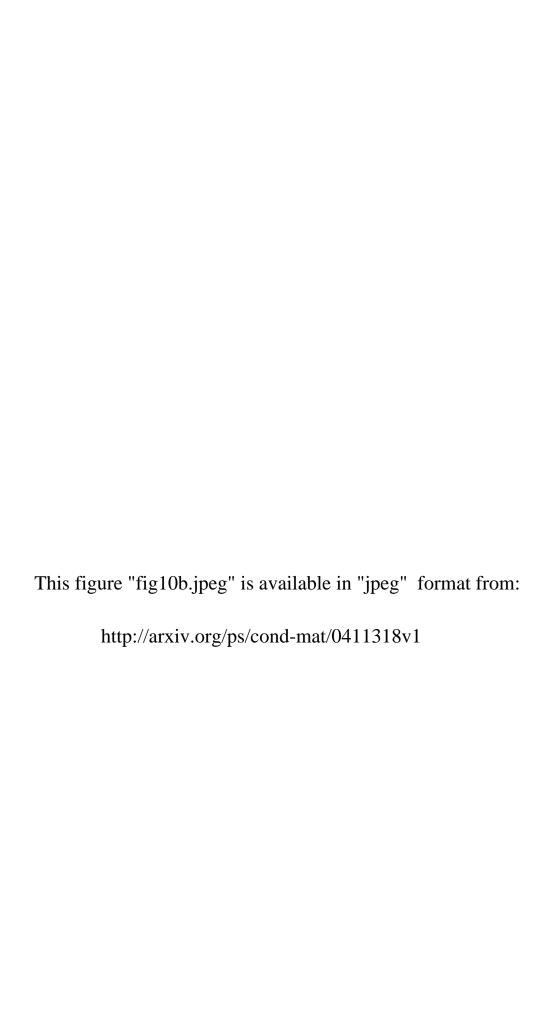
This figure "fig6.jpeg" is available in "jpeg" format from:

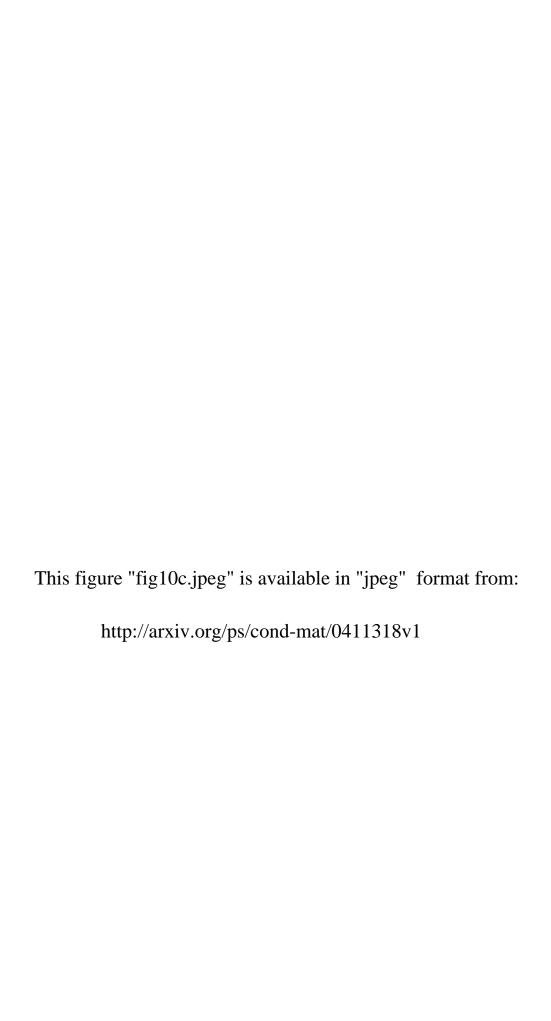
This figure "fig7.jpeg" is available in "jpeg" format from:

This figure "fig8.jpeg" is available in "jpeg" format from:

This figure "fig9.jpeg" is available in "jpeg" format from:







This figure "fig11.jpeg" is available in "jpeg" format from:

This figure "fig12.jpeg" is available in "jpeg" format from:

This figure "fig13.jpeg" is available in "jpeg" format from:

This figure "fig14.jpeg" is available in "jpeg" format from:

This figure "fig15.jpeg" is available in "jpeg" format from:

This figure "fig16.jpeg" is available in "jpeg" format from:

http://arxiv.org/ps/cond-mat/0411318v1

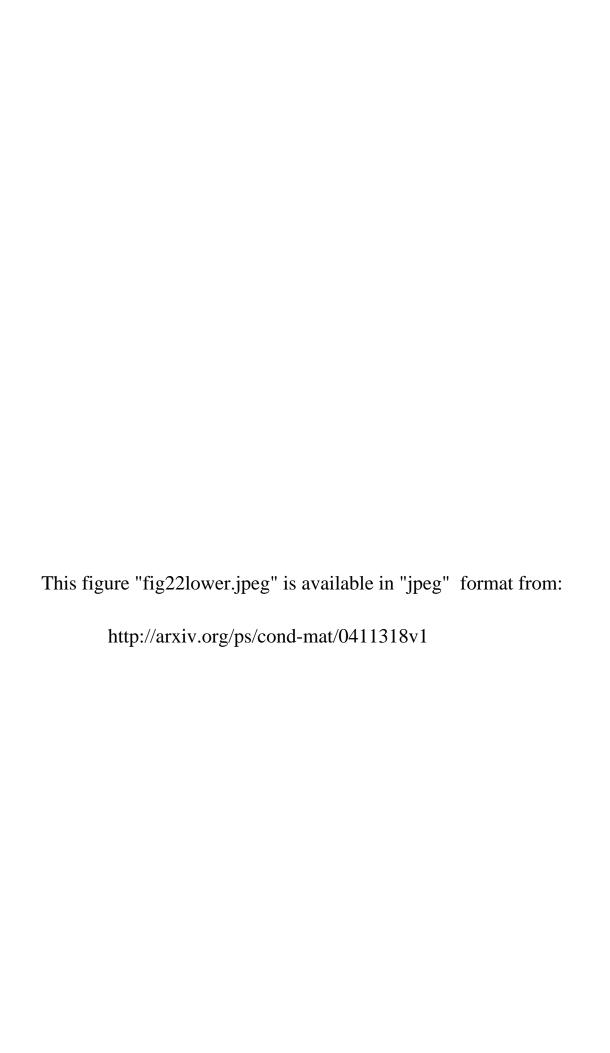
This figure "fig17.jpeg" is available in "jpeg" format from:

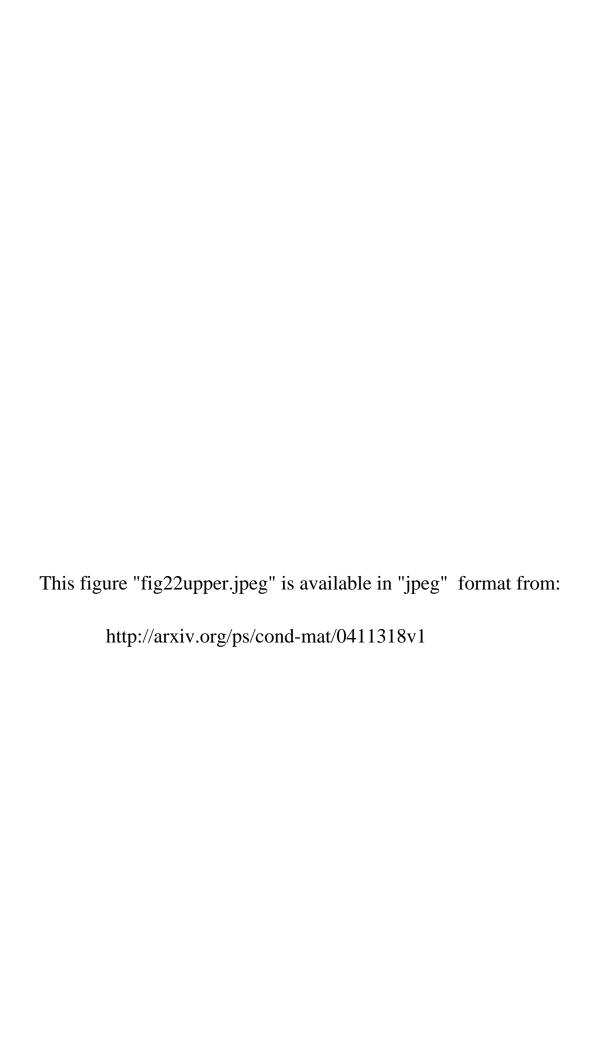
This figure "fig18.jpeg" is available in "jpeg" format from:

This figure "fig19.jpeg" is available in "jpeg" format from:

This figure "fig20.jpeg" is available in "jpeg" format from:

This figure "fig21.jpeg" is available in "jpeg" format from:





This figure "fig23.jpeg" is available in "jpeg" format from:

This figure "fig24.jpeg" is available in "jpeg" format from:

This figure "fig25.jpeg" is available in "jpeg" format from:

This figure "fig26.jpeg" is available in "jpeg" format from:

This figure "fig27.jpeg" is available in "jpeg" format from:

This figure "fig28.jpeg" is available in "jpeg" format from:

This figure "fig29.jpeg" is available in "jpeg" format from:

This figure "fig30.jpeg" is available in "jpeg" format from:

This figure "fig31.jpeg" is available in "jpeg" format from:

This figure "fig32.jpeg" is available in "jpeg" format from:

This figure "fig33.jpeg" is available in "jpeg" format from:

This figure "fig34.jpeg" is available in "jpeg" format from:

This figure "fig35.jpeg" is available in "jpeg" format from:

This figure "fig36.jpeg" is available in "jpeg" format from:

This figure "fig37.jpeg" is available in "jpeg" format from:

This figure "fig38.jpeg" is available in "jpeg" format from:

This figure "fig39.jpeg" is available in "jpeg" format from:

This figure "fig40.jpeg" is available in "jpeg" format from:

This figure "fig41.jpeg" is available in "jpeg" format from: